

ENVIRONMENTAL RESEARCH, MONITORING AND EVALUATION: RESULTS OF THE STREAM PROJECT

David Juříčka and Václav Pecina (eds.)

Mendel University in Brno

David Juříčka and Václav Pecina (eds.)

Environmental Research, Monitoring and Evaluation:

Results of the STREAM Project

May 2024



Authors

David Juříčka

Hydropedology

david.juricka@mendelu.cz

Mendel University in Brno, Zemědělská 1, 613 00, Brno, Czech Republic

Martin Valtera

Soil Science

martin.valtera@mendelu.cz

Mendel University in Brno, Zemědělská 1, 613 00, Brno, Czech Republic

Burenjargal Otgonsuren

Soil biology (Mycorrhiza)

burenjargal.o@muls.edu.mn

Mongolian University of Life Sciences, Ulaanbaatar 17024, Mongolia

Pavel Peška

Pedoanthracology

xpeska2@mendelu.cz

Mendel University in Brno, Zemědělská 1, 613 00, Brno, Czech Republic

Jan Novák

Pedoanthracology

prourou@gmail.com

Charles University, Opletalova 38, 110 00 Staré Město, Praha, Czech Republic

Jan Šebesta

Botany

jan.sebesta@mendelu.cz

Mendel University in Brno, Zemědělská 1, 613 00, Brno, Czech Republic

Vladimír Hula

Entomology

vladimir.hula@mendelu.cz

Mendel University in Brno, Zemědělská 1, 613 00, Brno, Czech Republic

Editors

David Juříčka

Hydropedology

david.juricka@mendelu.cz

Mendel University in Brno, Zemědělská 1, 613 00, Brno, Czech Republic

Václav Pecina

Forest Ecology and Management

vaclav.pecina@mendelu.cz

Mendel University in Brno, Zemědělská 1, 613 00, Brno, Czech Republic

Reviewer

Antonín Kusbach

Forest Ecology and Classification

antonin.kusbach@mendelu.cz

Mendel University in Brno, Zemědělská 1, 613 00, Brno, Czech Republic

Project

This report was prepared by experts from Mendel University in Brno as part of the Sustainable Resilient Ecosystem and Agriculture Management in Mongolia (STREAM) project. The STREAM project, co-financed by the European Union and the German Federal Ministry for Economic Cooperation and Development, is being implemented by the Mongolian Ministry of Environment and Tourism with the support of the Deutsche Gesellschaft für Internationale Zusammenarbeit (GIZ) and the Food and Agriculture Organization of the United Nations (FAO).



Mendel University in Brno heads a consortium of twelve educational and research institutions that collaborate on the forestry component of the project led by the GIZ.

More information about the project: <https://www.giz.de/en/worldwide/128246.html>

Contents

1 LONG-TERM MONITORING OF SELECTED CLIMATIC AND SOIL CONDITIONS	14
1.1 Introduction	14
1.2 Methods	16
Monitoring design	17
Rainfall evaluation	21
Air temperature, soil temperature and soil moisture monitoring	21
Soil sample analyses.....	23
Soil hydro limit.....	24
Remote sensing climate conditions evaluation	24
1.3 Rainfall evaluation	25
Annual and total rainfall.....	25
Monthly rainfall.....	26
Daily amount of rainfall for the whole observed period	28
Comparation of site monitoring and ERA5 data	30
1.4 Air temperature evaluation.....	35
1.5 Soil temperature evaluation.....	37
1.6 Soil moisture evaluation.....	46
Summary of soil moisture evaluation.....	51
1.7 Drought risk.....	52
1.8 Management recommendations.....	55
1.9 References	56
2 SOIL AND MYCORRHIZA SURVEY	61
2.1 Introduction	61
2.2 Methods	62
Soil survey.....	62
Mycorrhiza survey.....	63
2.3 Results	65
Evaluation of soil properties at the demonstration plots	65
Mycorrhiza community	66
Soil descriptions and classification	69

2.4	Summary and recommendations	79
2.5	Acknowledgment	79
2.6	References	80
3	PEDOANTHRACOLOGICAL SURVEY: REFLECTION OF HISTORICAL FOREST DEVELOPMENT.....	82
3.1	Introduction	82
3.2	Methods.....	83
	Amount of anthracomass.....	87
	Radiocarbon dating	88
3.3	Results	88
	Tunkhel.....	88
	Javkhlant.....	89
	Bugant	89
	Binder	90
	Bayan-Adarga.....	92
3.4	Summary	93
3.5	Management recommendations.....	94
3.6	References	95
4	BOTANICAL SURVEY.....	98
4.1	Introduction	98
4.2	Methods.....	99
4.3	Results	100
	Tunkhel.....	100
	Javkhlant.....	101
	Bugant	101
	Umnudelger.....	102
	Binder	102
	Bayan-Adarga.....	102
4.4	References	103
5	LEPIDOPTERA EVALUATION: A REFLECTION OF BIODIVERSITY	105
5.1	Introduction	105
5.2	Methods.....	106
	Butterflies	106
	Moths.....	106

5.3	Results and discussion.....	107
5.4	References	109

List of figures

Figure 1. Forests in Mongolia in the context of permafrost occurrence.	15
Figure 2. Location of the STREAM demonstration plots.	17
Figure 3. STREAM demonstration plots in Khentii aimag.	19
Figure 4. STREAM demonstration plots in Selenge aimag.	20
Figure 5. a = Pronamic Pro rain gauge (EMS Brno, 2024), b = rain gauge placement at the Tunkhel demonstration plot E1.	21
Figure 6. TOMST TMS4 sensor description.	22
Figure 7. Visualization of installation and placement of the TOMST TMS4 sensors in the field.	23
Figure 8. Total amounts of rainfall for the monitored period and their sum.	25
Figure 9. Monthly rainfall totals.	26
Figure 10. Daily amount of rainfall at demonstration plots in Khentii aimag.	28
Figure 11. Daily amount of rainfall at demonstration plots in Selenge aimag.	29
Figure 12. Site rainfall measuring and ERA 5 satellite precipitation data in Khentii aimag. .	31
Figure 13. Site rainfall measuring and ERA 5 satellite precipitation data in Selenge aimag. .	32
Figure 14. Difference (mm) between site monitoring and ERA 5 data for Khentii aimag. The negative values mean that ERA 5 shows a higher amount of precipitation than site monitoring; the positive values mean that site monitoring shows a higher amount of precipitation than ERA data.	33
Figure 15. Difference (mm) between site monitoring and ERA 5 data for Selenge aimag. The negative values mean that ERA 5 shows a higher amount of precipitation than site monitoring; the positive values mean that site measuring shows a higher amount of precipitation than ERA data.	34
Figure 16. Monthly air temperatures.	35
Figure 17. Soil temperatures at depths of 10, 30 and 60 cm and at demonstration plots in Khentii aimag.	38
Figure 18. Soil temperatures at depths of 10, 30 and 60 cm and at demonstration plots in Selenge aimag.	39
Figure 19. Soil temperatures at a depth of 10 cm and difference between the enclosure (E7) and the control plot (CE7) at Javkhlant.	40
Figure 20. Developed herb layer in the enclosure at Javkhlant.	41

Figure 21. Soil temperature at 10 cm depth and difference between the exclosure in the sparse forest (E1) and the burned forest without canopy cover (E2) at Tunkhel.	42
Figure 22. Soil temperature at 10 cm depth and difference between the exclosure (E1) and the control plot (CE1) at Bayan-Adarga.	43
Figure 23. Soil temperature at 10 cm depth and difference between the exclosure (E1) and the control plot (CE1) at Binder.	44
Figure 24. Soil temperature at 10 cm depth and difference between the exclosure (E2) and the control plot (CE2) at Umnudelger.	45
Figure 25. Soil moisture at the sites at Khentii aimag.	47
Figure 25. Soil moisture at the sites at Khentii aimag.	49
Figure 26. Soil moisture at the sites in Selenge aimag (without Bugant). Clearcut = post-fire unstocked area in the forest.	50
Figure 27. Volumetric water content at the Bugant site.	51
Figure 28. Dry period at the sites at Khentii aimag.	53
Figure 29. Dry period at the sites at Selenge aimag.	54
Figure 30. Location of the demonstration plots, on background of the georeferenced soil map according to FAO - WRB (Batkishig, 2009).	63
Figure 31. Grid sampling design.	64
Figure 32. Mycorrhiza sampling. a = larch forest at Umnudelger, b = pine forest at Binder. .	64
Figure 33. Ectomycorrhizal morphotypes on <i>Pinus sylvestris</i> of pine forest at Binder, Khentii. a = branched (yellowish-brown), b = coralloid (brown), c = unbranched (black, hairy tips), d = unbranched (black), e = unbranched (yellow), f = unbranched, black (hairy tips).	67
Figure 34. Ectomycorrhizal morphotypes on <i>Pinus sylvestris</i> of pine forest at Bayan-Adarga, Khentii. a = unbranched (brown), b = dichotomously branched (yellow), c = branched (brown and black), dichotomously branched (yellowish-brown), e-f = Tuberculate ectomycorrhiza.	68
Figure 35. Phaeozem at Tunkhel.	69
Figure 36. Phaeozem at Tunkhel.	70
Figure 37. Phaeozem at Umnudelger.	71
Figure 38. Phaeozem at Umnudelger.	72
Figure 39. Phaeozem at Javkhlant.	73
Figure 40. Arenozem at Javkhlant.	74
Figure 41. Cambizem at Binder.	75
Figure 42. Arenozem at Binder.	76
Figure 43. Arenozem at Bayan-Adarga.	77

Figure 44. Arenozem at Bayan-Adarga.	78
Figure 45. Charcoal accumulated in soil.	82
Figure 46. Cross section of <i>Ulmus pumilla</i> charcoal piece.	83
Figure 47. Charcoal separation using the wet sieving method.	84
Figure 48. Result of primary separation of the collected soil sample.	84
Figure 49. Drying of samples collected at Bayan Adarga.	85
Figure 50. Cross section of <i>Pinus sylvestris</i> charcoal.	86
Figure 51. Cross section of <i>Populus tremula</i> charcoal.	86
Figure 52. Pedoanthracological sampling at Bugant.	87
Figure 53. Results of the pedoanthracological analysis from the Tunkhel site.	88
Figure 54. Results of the pedoanthracological analysis from Javkhlant.	89
Figure 55. Results of the pedoanthracological analysis from Bugant.	90
Figure 56. Results of the pedoanthracological analysis from Binder (forest).	91
Figure 57. Results of the pedoanthracological analysis from Binder (steppe).	92
Figure 58. Results of the pedoanthracological analysis from the Bayan-Adarga site.	93
Figure 59. Light trap in operation.	107
Figure 60. Typical non-forest habitat within forest. Such places host very valuable fauna. .	108
Figure 61. <i>Lycaena helle</i> is an example of butterfly, which is almost extinct in Europe due to the destruction of its habitat, but which is still quite common in Mongolia.	109

List of tables

Table 1. Total amounts of rainfall for the monitored period and their sum.	25
Table 2. Monthly rainfall (mm) characteristics in demonstration plots. N/A = not available (no rain). Orange = dry period with a limited amount of rainfall; Tot ERA 5 = monthly precipitation (rainfall/snowfall) provided by the remote sensing ERA5 product (9 km resolution); Diff tot = difference between site monitoring and ERA5 data (the negative values mean that ERA 5 shows a higher amount of precipitation than site monitoring; the positive values mean that site monitoring shows a higher amount of precipitation than ERA data).	27
Table 3. Monthly air temperatures.	36
Table 4. Main characteristics of the 0–30 cm mineral topsoil layer (mean ± standard deviation)	66
Table 5. Soil profile in a forest at the Tunkhel site (17.06.2022).	69
Table 6. Soil profile in an unstocked forest at the Tunkhel site (28.06.2022).	70
Table 7. Soil profile in a forest at the Umnudelger site (29.06.2023).	71
Table 8. Soil profile on a steppe at the Umnudelger site (03.07.2022).	71
Table 9. Soil profile in a forest at the Bugant site (26.06.2022).	73
Table 10. Soil profile on a steppe at the Javkhlant site (21.06.2022).	74
Table 11. Soil profile in a forest at the Binder site (01.07.2023).	74
Table 12. Soil profile on a forest-steppe at the Binder site (06.07.2022).	76
Table 13. Soil profile in a forest at the Bayan-Adarga site (02.07.2023).	77
Table 14. Soil profile on a forest-steppe at the Bayan-Adarga site (08 .07.2022).	78

**LONG-TERM MONITORING
OF SELECTED CLIMATIC
AND SOIL CONDITIONS**

1 LONG-TERM MONITORING OF SELECTED CLIMATIC AND SOIL CONDITIONS

David Juříčka¹

¹ *Mendel University in Brno, Zemědělská 1, 613 00, Brno, Czech Republic*

1.1 Introduction

Mongolia is a landlocked country characterized by the extreme arid to semi-arid continental climate with temperatures reaching up to -50 °C in winter and 40 °C in summer. The warmest month of the year is July with an average temperature of between 15 and 22 °C. Annual precipitation is relatively low, from less than 50 mm in the Gobi Desert area to 400 mm in the forest-rich north (Batima & Dagvadorj, 2000). Rainfall occurs mainly from June to August preceded by a dry period from November to March (Natsagdorj, 2000). However almost 90% of precipitation is lost by evapotranspiration annually (Batima & Dagvadorj, 2000).

Precipitations together with the natural annual melting of the permafrost active layer (Klinge et al., 2021; Sharkhuu, 2003) are fundamental factors for forest development and distribution in Mongolia. Permafrost, the ground frozen at least two years continuously, covers at least 67% of the Mongolian territory (Tumurbaatar & Mijiddorj, 2006). The forests in Mongolia (Figure 1) grow almost exclusively on sites supplied by the supra-permafrost water from the natural annual melting of the dynamic topmost layer (active layer) of permafrost (Gravis et al., 1974). This water is the main source of water for vegetation during the dry period before the rain season in Mongolia (Sharkhuu, 2003; Sugimoto et al., 2002). Forests growing in permafrost regions are extremely sensitive ecosystems responding to even small-scale disturbances (Klinge et al., 2020). The late successional stages of forests in permafrost regions are strictly linked with the natural annual freeze/melt cycle of the permafrost active layer (Bohannon, 2008; Genxu et al., 2012; Kokelj et al., 2010). Permafrost and vegetation are in close interaction. Changes of vegetation structures caused by logging or forest fires can significantly affect the freeze/melt cycle of the permafrost active layer and lead to permafrost degradation (Runyan & D’Odorico, 2012). Permafrost degradation causes significant changes in soil moisture which significantly affect the vegetation structure. Then, the spiral of mutual degradation (forest vs. permafrost) is deepening. Degradation of permafrost can change the hydrologic processes

(Walker et al., 2003) and ground water systems at regional scale with the critical impact on ecosystems and the environment (Chang et al., 2015; Luo, 2012; Yao et al., 2013).

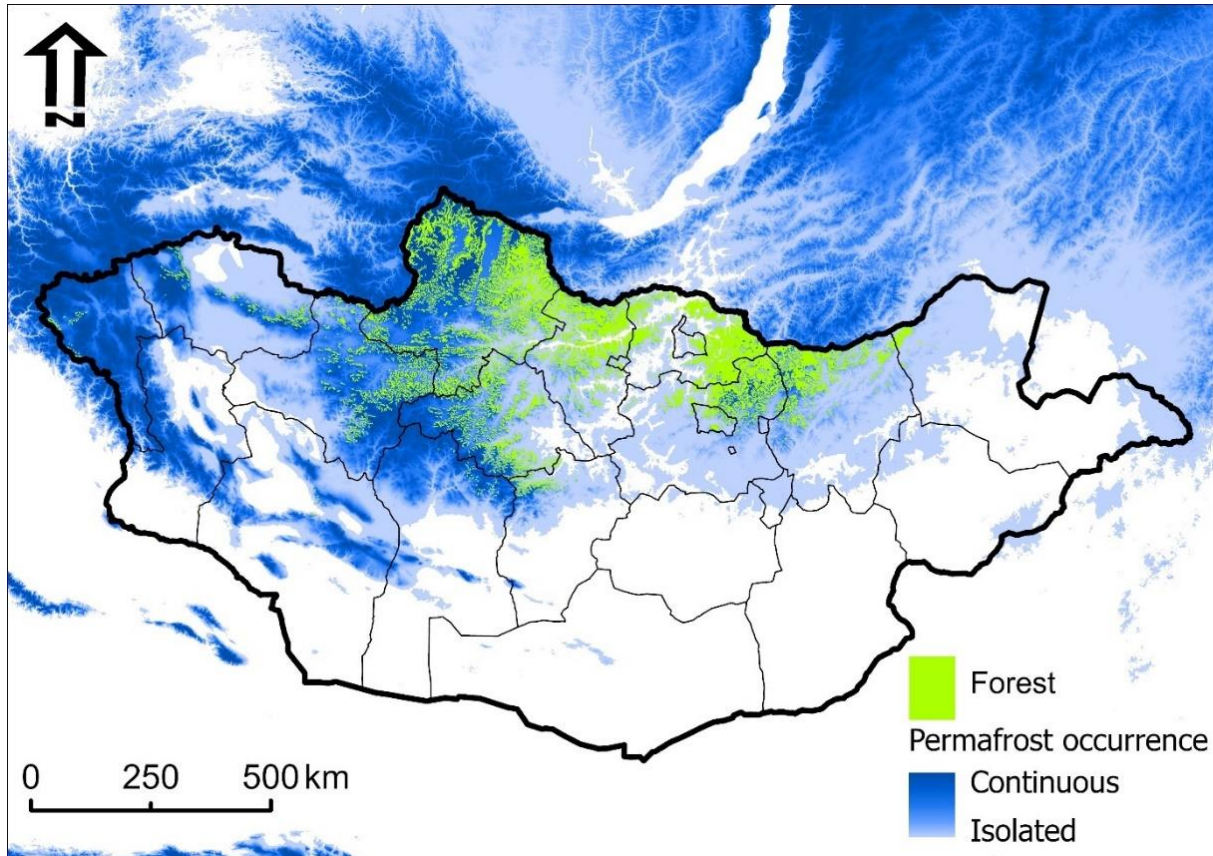


Figure 1. *Forests in Mongolia in the context of permafrost occurrence.*

Facing the ongoing climate change in Mongolia (Shukla et al., 2019), the long-term monitoring of environmental and soil moisture and temperature conditions is an essential part of sustainable forest management. Long-term monitoring allows to predict the future development of environmental conditions and helps to adapt forest management to the changing environment.

Environmental conditions in Mongolia are changing dramatically: i) the frequency of dust storms is significantly increasing (Natsagdorj et al., 2003), ii) the average annual temperature is increasing gradually by 2.1 °C over the last 70 years (Oyuntuya et al., 2015), iii) the average temperature will increase by 1–2 °C in Central Asia by 2030–2050 (Lioubimtseva et al., 2005), iv) annual precipitation decreased (Khishigjargal et al., 2013), and v) the character of precipitation has changed from “silk” to “hard” rain when the rain falls in small amounts during heavy events (Marin, 2010). Another scenario also predicts a decrease in precipitation directly

for the Khentii region (Sato et al. 2007). Climate change strongly negatively affected permafrost and the thickness of its active layer. Ongoing permafrost degradation could lead to its total elimination with the catastrophic impact on the environment and society (Juříčka et al., 2020; Smith & Riseborough, 2002).

Knowledge of environmental conditions including local climate and soil moisture and temperature fluctuations is an essential part of sustainable forest management. Exact data allow to select the most suitable tree species composition adapted to local environmental conditions and determine the most suitable period (based on long-term monitoring) for planting to reduce the damage and mortality of seedlings by drought. A detailed knowledge of site climatic and soil conditions is crucial to establishing a resilient and valuable forest.

Facing the climate change, the forest management excluding the scientific approach in Mongolia is an irresponsible hazard with a threat of strong wide-ranging negative impacts to landscape and society.

This report provides a detailed evaluation of rainfall, air temperature, soil temperature and soil moisture at the STREAM demonstration plots for the period of 2022–2023. The data were also used for forest management recommendations (output Sustainable forest management measures realized within the STREAM project) and educational graphical abstracts (e.g. Mountain permafrost degradation).

Two years of monitoring is not enough to provide long-term perspectives; however, it provides a basic understanding of local environmental conditions. Long-term monitoring is necessary. Mendel University in Brno (MENDELU) together with the consortium partners ensure the continuation of the monitoring and data collection and analysis in the future.

1.2 Methods

Long-term, continuous, and stable monitoring of soil and climate conditions has been taking place at six STREAM project sites in Khentii and Selenge aimags since 2022 (Figure 2).

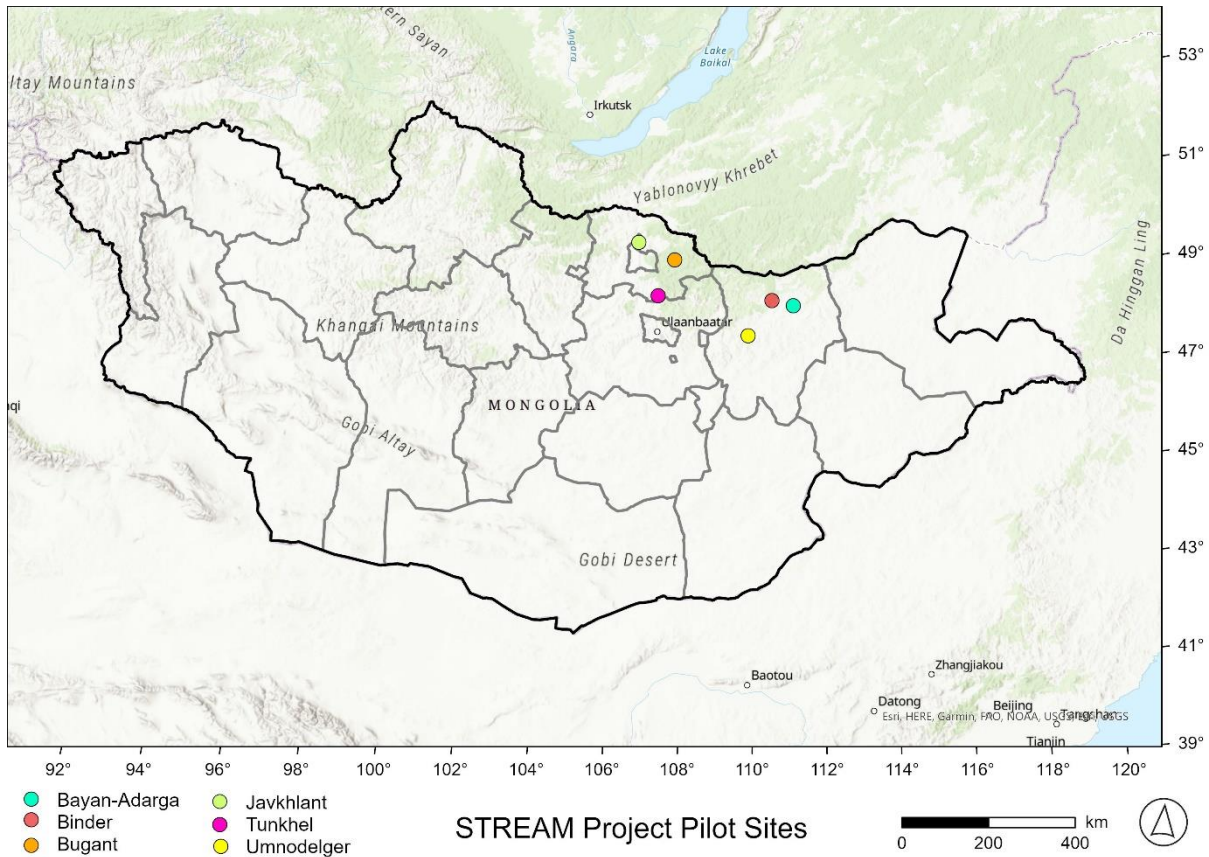


Figure 2. Location of the STREAM demonstration plots.

Monitoring design

In Khentii aimag, the monitoring takes place in Bayan-Adarga, Binder and Umnudelger (Figure 3). Three sets of TOMST TMS4 probes were established at the Bayan-Adarga site. Two sets of probes were placed in the unstocked forest near the forest edge into the centre of the enclosure E1 ($X=48.53677$, $Y=111.112375$) and into the centre of the control plot CE1 ($X=48.537035$, $Y=111.112638$). One set of probes was placed in the forest ($X=48.537267$, $Y=111.114162$). One rain gauge was placed into the E1 plot.

Three sets of TOMST TMS4 probes were established at the Binder site. Two sets of probes were placed in the unstocked forest near the forest edge into the centre of the enclosure E1 ($X=48.646873$, $Y=110.447881$) and into the centre of the control plot CE1 ($X=48.64667$, $Y=110.448103$). One set of probes was placed in the forest ($X=48.645809$, $Y=110.447215$). One rain gauge was placed into the E1 plot.

Three sets of TOMST TMS4 probes were established at the Umnudelger site. Two sets of probes were placed on the steppe near the forest edge into the centre of the enclosure E2 ($X=47.906173$,

Y=109.72514) and into the centre of the control plot CE2 (X= 47.906001, Y=109.724875). One set of probes was placed in the forest (X=47.905528, Y=109.725367). One rain gauge was placed into the E2 plot.

In Selenge aimag, the monitoring takes place at Bugant, Javkhlant and Tunkhel sites. One set of TOMST TMS4 probes (air temperature, soil temperature and soil moisture) was placed in the forest into the centre of the T1 plot (X=49.430748, Y=107.345183, Figure 4) at the Bugant site. One rain gauge was placed in the west part of the I2 plot (X=49.430844, Y=107.346017).

Two sets of TOMST TMS4 probes were established on the steppe at the Javkhlant site. One set was placed into the centre of the exclosure E7 (x=49.751758, Y=106.171462) and another one into the centre of the control plot CE7 (X= 49.75152, Y=106.170978). One rain gauge was placed into the E7 plot.

Four sets of TOMST TMS4 probes were established in the forest and in the unstocked forest at the Tunkhel site. Two sets of TOMST TMS 4 probes were placed in the forest into the centre of the exclosure E1 (x=48.668612, Y=106.877057) and into the centre of the control plot CE1 (X=48.668874, Y=106.876998); another two sets of probes were established in the burned forest area (unstocked forest) into the exclosure E2 (X=48.668049, Y=106.877368) and into the control plot CE2 (X=48.66811, Y=106.877631). One rain gauge was placed in the forest into the I2 plot.

The sensors were installed at the demonstration plots until July 2022. The reference forest stands at Binder, Bayan-Adarga and Umnudelger were established with sensors in 2023. The data were downloaded in September 2023. The data from demonstration plots presented in this report were evaluated for the period from 1st July to 31st August.

A more detailed description of the mentioned plots can be found in the output Sustainable forest management measures realized within the STREAM project.

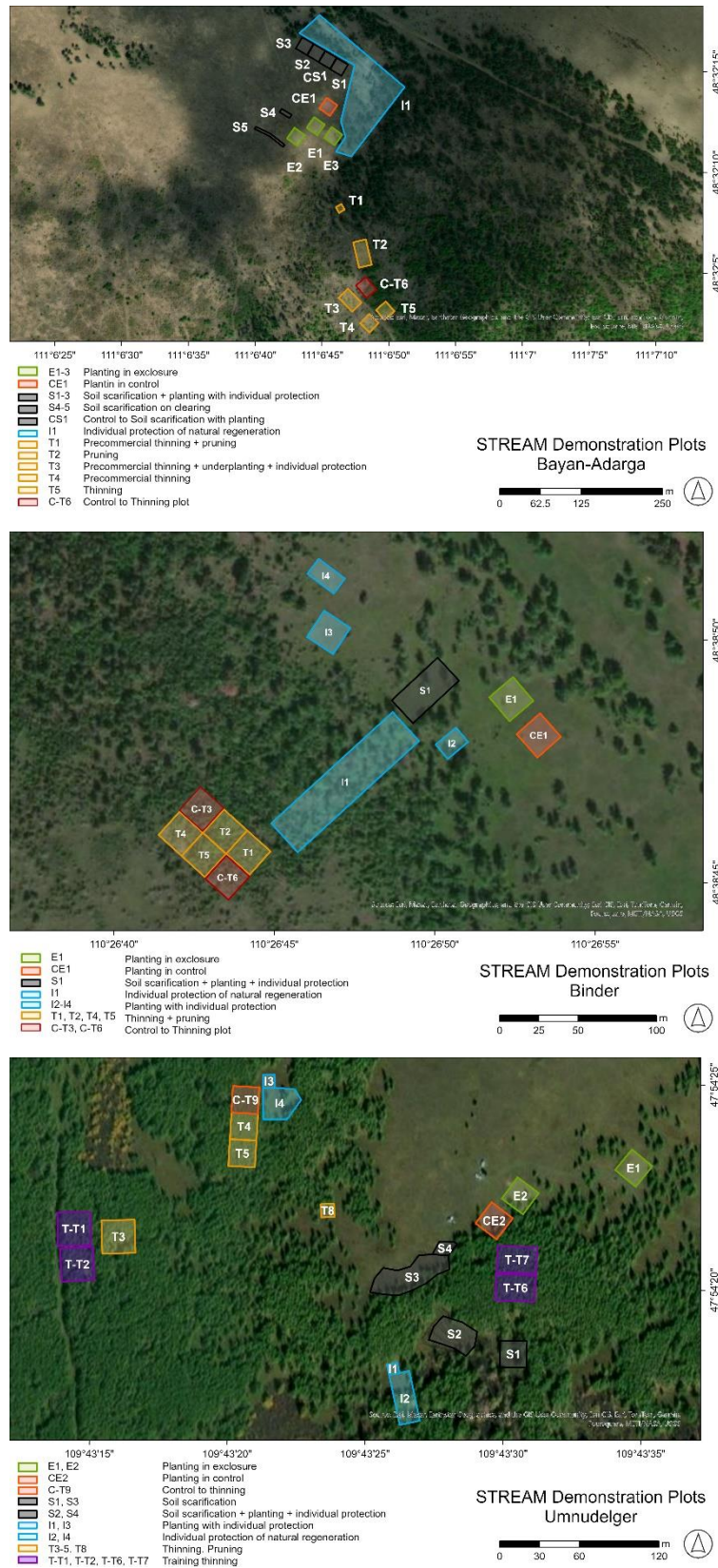


Figure 3. STREAM demonstration plots in Khentii aimag.

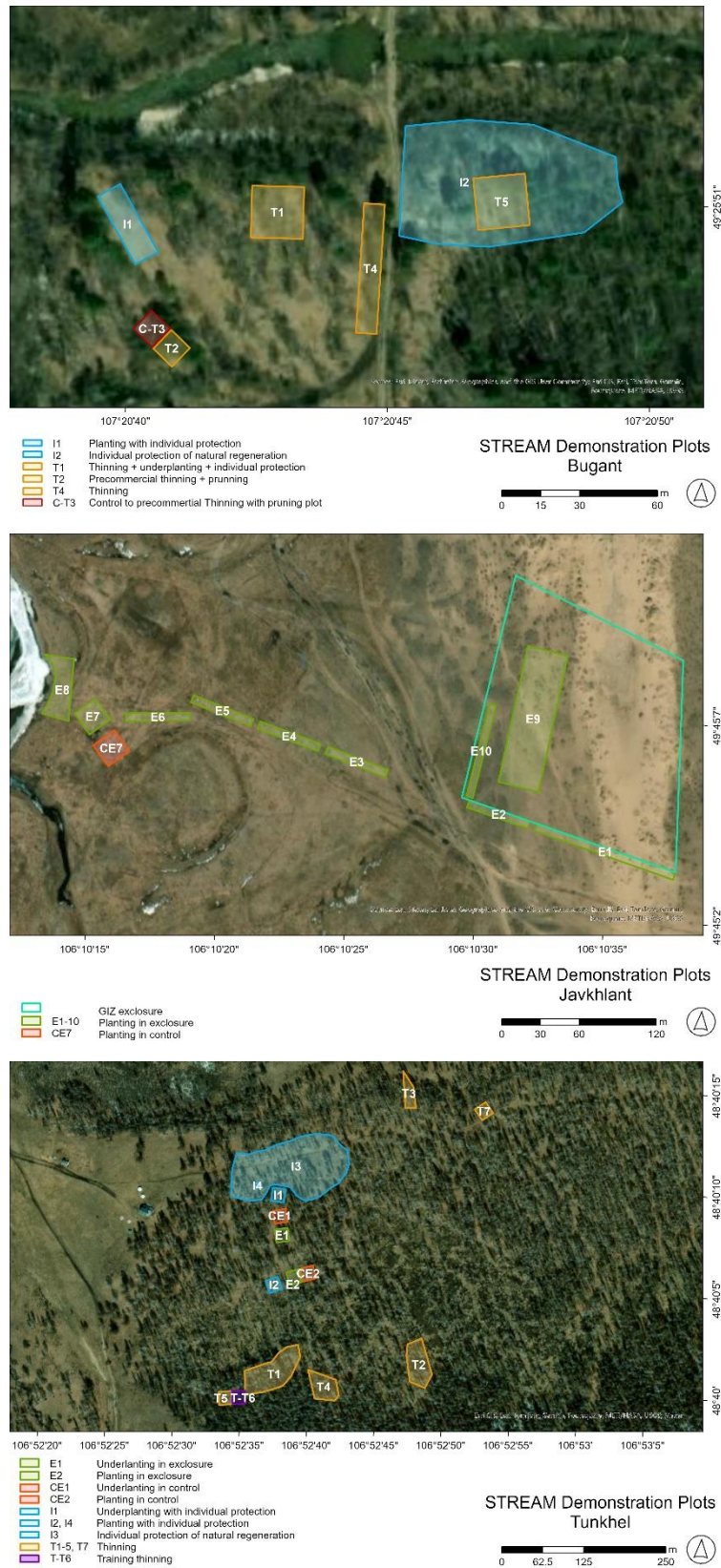


Figure 4. STREAM demonstration plots in Selenge aimag.

Rainfall evaluation

Rainfall was measured with the professional rain gauge Pronamic Pro (Figure 5a) in conjunction with the datalogger Minikin Eri provided by company Environmental Measuring Systems s.r.o. (EMS Brno, 2024). The rain gauge measures mainly rainfall events. Snowfall and other types of precipitation (e.g. dew, hoar frost) are not detected. The rain gauges were placed into the exclosures (except Bugant) to be protected from animal damage (Figure 5b). The resolution of the rain gauge is 0.2 mm; the memory capacity 18 000 records; the rainfall capacity 3 000 mm; the collecting area 200 cm²; the battery lifetime is more than 5 years; the protection rating IP68; the operating temperature -40–60 °C; the operating humidity is 0–100% (EMS Brno, 2024).



Figure 5. *a = Pronamic Pro rain gauge (EMS Brno, 2024), b = rain gauge placement at the Tunkhel demonstration plot E1.*

Air temperature, soil temperature and soil moisture monitoring

TOMST TMS4 sensors were used for air temperature, soil temperature and soil moisture monitoring at the STREAM demonstration plots. TOMST sensors are composed of two separated sensors connected by a cable (Figure 6). On one side of the TMS4 probe, there is a soil sensor (moisture and temperature; “green spoon” with black point). On the opposite side of the probe, there is an air sensor (temperature). The lengths of the cables between the soil and the air sensors are 1.5 and 2 m.

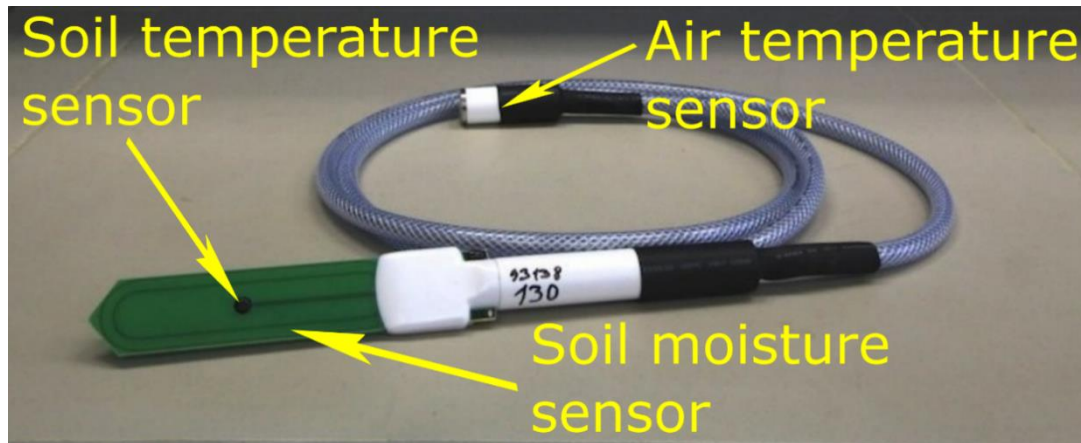


Figure 6. *TOMST TMS4 sensor description.*

The TMS4 probes were established in sets of three. The soil sensors were placed 10, 30 and 60 cm under the ground (Figure 7). Measuring in the selected soil depths allows to evaluate the hypodermic flows and rainwater infiltration (Hemr et al., 2023). The probes were connected to a wooden pole. The topmost air sensor was covered with a solar radiation shield to protect it against the direct sunlight. The data from the topmost-placed air sensor are used for air temperature evaluation. The sensors measure at 15 min intervals.

The temperature sensor is composed of 3x MAXIM/DALLAS Semiconductor DS7505U+, with a resolution of 0.0625 °C and with an accuracy of ± 0.5 °C. The range of measurement is -40 to 60 °C. The datalogger works even at temperatures ranging from -60–85°C, however, it can have a negative impact on the lifespan of battery. The lithium battery (3,6 V; 2600 mAh) inside the sensor allows measuring up to 10 years continuously. The soil moisture sensor works on the principle of time domain transmission (TDT). The TDT method is largely independent of temperature and salinity where the measurement error does not exceed 1%. The probes placed outside the exclosures were protected by a fence against animal damage.

Each individual soil moisture sensor was precisely calibrated according to specific local soil properties. For that purpose, soil samples were taken from each soil layer where the sensors were placed. The raw unitless data from the soil sensors were converted to cm^3/cm^3 and then to the volumetric water content (%) following the original TOMST calibration protocol. The input data were soil bulk density, soil texture (clay, dust, and sand), and the raw unitless data from the measuring of demineralized water and air.

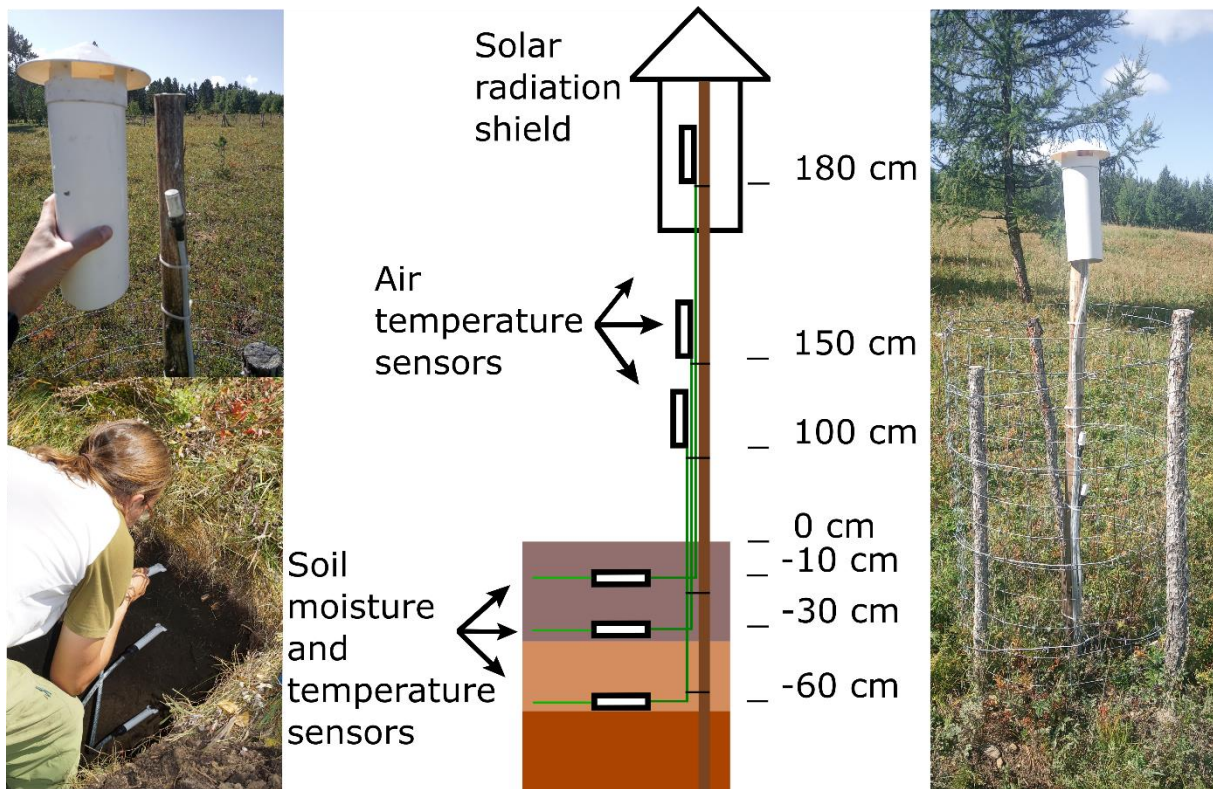


Figure 7. Visualization of installation and placement of the TOMST TMS4 sensors in the field.

Soil sample analyses

Three undisturbed soil samples were taken from each layer where the soil moisture sensors were placed to cover the heterogeneity of the soil environment. Then, the samples were mixed to one composite soil sample of the respective layer. Undisturbed soil samples were taken using Kopecky's ring of exact volume 100 cm^3 . A total of 135 composite soil samples were taken.

The composite soil samples taken in 2022 and 2023 were dried at a room temperature in the laboratory of National University of Mongolia (NUM). The soil samples taken in 2022 were sieved using a 2 mm sieve in the laboratory of NUM. The samples taken in 2023 were sieved in the laboratory of MENDELU. The dried soil samples were taken to the Czech Republic and analysed in the laboratory of MENDELU (the transport permit was issued by Mongolian University of Life Sciences).

The sieved soil samples were dried at $105 \text{ }^\circ\text{C}$ to determine bulk density. Then, the sieved and dried samples were used for texture analysis. Before this analyses, soil organic matter was removed using H_2O_2 and carbonates were removed using HCl according to ISO 11277. FAO soil fractions, namely coarse sand ($2000\text{--}630 \text{ }\mu\text{m}$), middle sand ($630\text{--}200 \text{ }\mu\text{m}$), fine sand ($200\text{--}63 \text{ }\mu\text{m}$), silt ($63\text{--}2 \text{ }\mu\text{m}$) and clay ($<2 \text{ }\mu\text{m}$), were determined using Mastersizer 3000®.

Soil hydro limit

To identify drought risk, soil moisture was assessed in relation to wilting point (WP) soil hydro limit. WP defines the minimum amount of water in soil that the plant requires not to wilt. WP range was set to 10–15% of soil moisture for coarse textured soils and to 26–32% of soil moisture for fine textured soils (Rai et al., 2017). Because of the high variability of organic matter content in the soils at the sites, the upper level of WP range was defined as high drought risk (HDR), i.e. the limited amount of water in the soil just partly usable by plants when plants are under high drought stress. The bottom level of WP range shows water content when water is not available enough for plants.

Remote sensing climate conditions evaluation

Air temperature and precipitation were evaluated additionally by the remote sensing method using the ERA5 output with a resolution of one pixel being nine kilometres. ERA5 provides the data of accumulated liquid and frozen water, including rain and snow, that falls to the Earth's surface. It is the sum of large-scale precipitation (that precipitation which is generated by large-scale weather patterns, such as troughs and cold fronts) and convective precipitation (generated by convection which occurs when air at lower levels in the atmosphere is warmer and less dense than the air above, so it rises). Precipitation variables do not include fog, dew or the precipitation that evaporates in the atmosphere before it lands on the Earth's surface. This variable is accumulated from the beginning of the forecast time to the end of the forecast step. The units of precipitation are depth in meters. It is the depth water would have if it was spread evenly over the grid box. Care should be taken when comparing model variables with observations, because observations are often local to a particular point in space and time, rather than representing averages over a model grid box and model time step.

1.3 Rainfall evaluation

Annual and total rainfall

The total amount of rainfall was higher at all the sites in 2023 than in the previous year (Figure 8). The rainfall events in 2023 were extremely high and caused heavy floods (OCHA, 2023). The highest total amount of rainfall (752 mm) with 280 mm in 2022 and 472 mm in 2023 was recorded in Bugant (Table 1). The lowest total amount of rainfall (400 mm) of 153 mm in 2022 and 247 mm in 2023 was recorded in Bayan-Adarga. The lowest annual amount of rainfall was recorded in Umnudelger (237 mm) in 2023. The differences in the total amount of rainfall between Bayan-Adarga, Binder, Bugant, Javkhlant, Tunkhel and Umnudelger were 6–44 mm and 9–126 mm in 2022 and 2023, respectively.

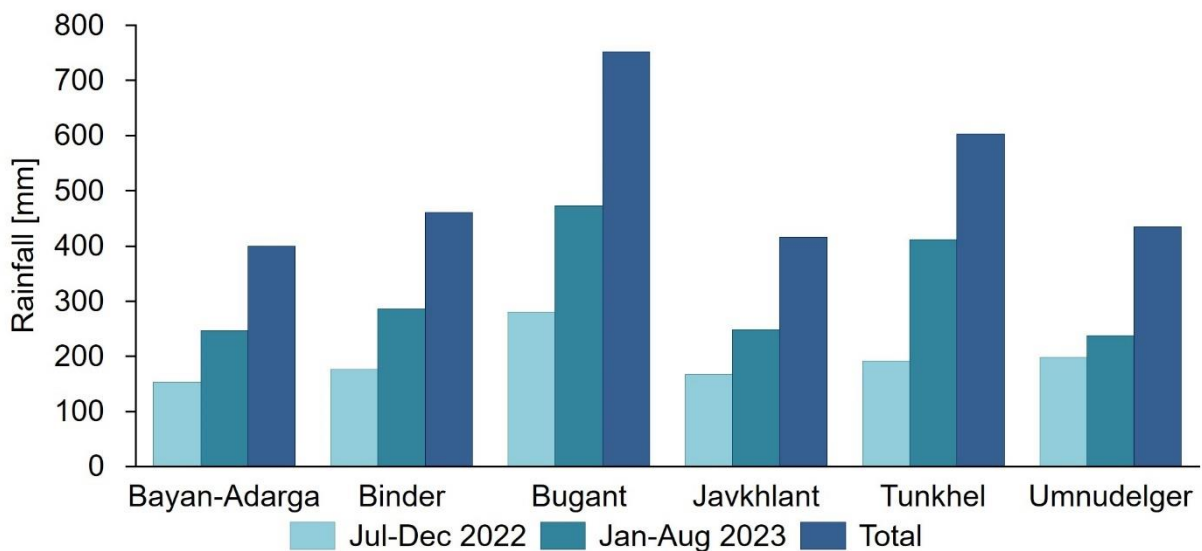


Figure 8. Total amounts of rainfall for the monitored period and their sum.

Table 1. Total amounts of rainfall for the monitored period and their sum.

	Bayan-Adarga	Binder	Bugant	Javkhlant	Tunkhel	Umnudelger
Jul-Dec 2022	153	176	280	167	192	198
Jan-Aug 2023	246	285	472	248	412	237
Total	400	461	753	416	603	435

Monthly rainfall

The extreme events and annual peak of rainfall were recorded in July 2023 (except Bayan-Adarga) (Figure 9). The highest monthly total amount of rainfall (259 mm; Table 2) and the maximum amount of rainfall in 24 hours (52 mm; Table 2) were recorded in Tunkhel in July 2023. The mean monthly amount of rainfall (monthly total/day in month) was ranging from 3.5 mm in Bayan-Adarga to 8.4 mm in Bugant (Table 2).

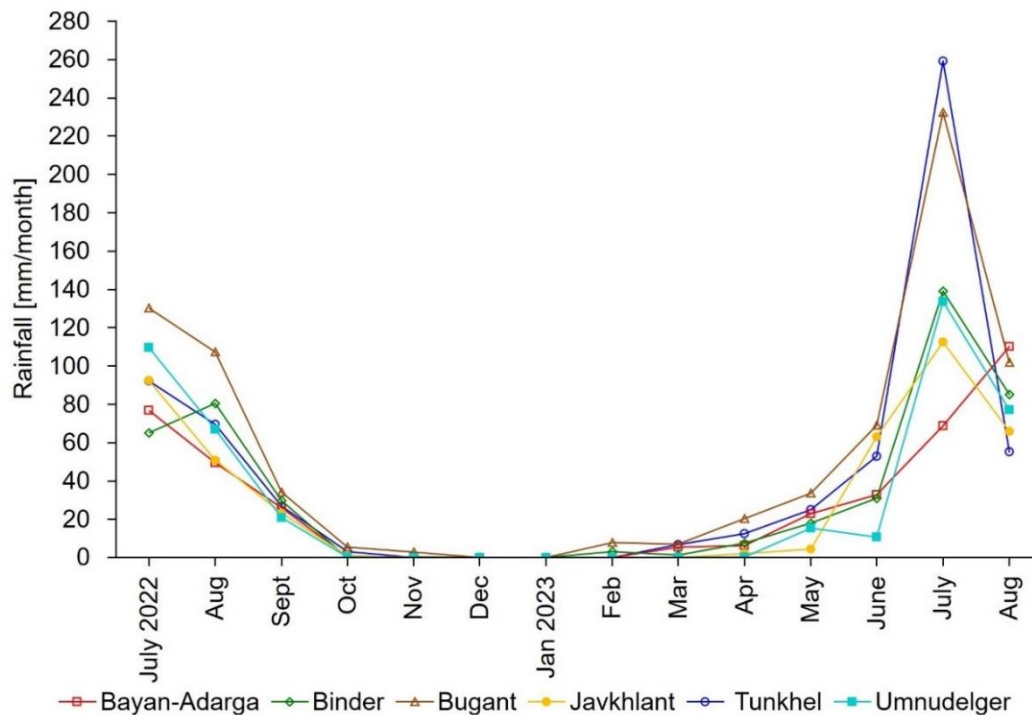


Figure 9. Monthly rainfall totals.

The dry period (Natsagdorj, 2000) was identified at all the sites (Table 1, Table 2). For this report, the author defined the dry period as the continuous time without or with only a limited amount of rainfall (daily rainfall event of less than 14 mm, Juřička et al., 2022; <20 mm/month). It was defined on the basis of the response of soil moisture at a depth of 10 cm to rainfall (recorded on the plots). The snow precipitation impact is not included. The snow is starting to melt when the soil is still frozen which significantly limits soil wetting. Dry periods were found from October (<5.6 mm/month) to March (<7.2 mm/month) at all sites (7 months; Table 2). The longest dry period was found in Umnudelger from October to June (9 months).

Snow cover was evaluated by the ERA 5 remote sensing product for the period from December 2022 to March 2023 (average monthly air temperatures below zero; Table 2). The amount of

snow precipitation for the period was from 22 mm at Umnudelger to 57 mm at Bugant. The evaluation is addressed in chapter 3.4.

Table 2. Monthly rainfall (mm) characteristics in demonstration plots. N/A = not available (no rain). Orange = dry period with a limited amount of rainfall; Tot ERA 5 = monthly precipitation (rainfall/snowfall) provided by the remote sensing ERA5 product (9 km resolution); Diff tot = difference between site monitoring and ERA5 data (the negative values mean that ERA 5 shows a higher amount of precipitation than site monitoring; the positive values mean that site monitoring shows a higher amount of precipitation than ERA data).

		2022					2023								
		July	Aug	Sept	Oct	Nov	Dec	Jan	Feb	Mar	Apr	May	June	July	Aug
Bayan-Adarga	Mean	2.5	1.6	0.9	0.0	0.0	N/A	N/A	N/A	0.2	0.2	0.7	1.1	2.2	3.6
	Max	16.6	8.4	9.2	0.4	0.2	N/A	N/A	N/A	4.8	4.4	5.8	19.4	16.4	30.2
	Tot	76.8	49.6	26.0	0.6	0.2	N/A	N/A	N/A	5.4	6.2	23.0	32.8	68.8	110.2
	Tot ERA5	103.0	65.0	36.0	19.0	7.0	10.0	2.0	1.0	15.0	11.0	25.0	28.0	94.0	108.0
	Diff tot	-26.2	-15.4	-10.0	-18.4	-6.8	-10.0	-2.0	-1.0	-9.6	-4.8	-2.0	4.8	-25.2	2.2
Biner	Mean	2.1	2.6	1.0	0.0	0.0	N/A	N/A	0.1	0.0	0.3	0.6	1.0	4.5	2.7
	Max	23.6	20.6	16.6	0.0	0.2	N/A	N/A	3.2	1.0	6.0	7.2	12.4	28.4	27.2
	Tot	65.2	80.6	29.8	0.0	0.2	N/A	N/A	3.2	1.2	7.6	18.0	31.0	139.2	85.2
	Tot ERA5	129.0	70.0	34.0	20.0	9.0	11.0	2.0	1.0	14.0	13.0	29.0	43.0	102.0	110.0
	Diff tot	-63.8	10.6	-4.2	-20.0	-8.8	-11.0	-2.0	-1.0	-12.8	-5.4	-11.0	-12.0	37.2	-24.8
Bugant	Mean	4.2	3.5	1.1	0.2	0.1	N/A	N/A	0.3	0.2	0.7	1.1	2.3	7.5	3.3
	Max	22.2	23.2	11.6	1.8	1.6	N/A	N/A	7.2	1.6	5.2	11.6	15.6	44.4	24.0
	Tot	130.2	107.4	34.2	5.6	2.8	N/A	N/A	7.8	7.2	20.4	33.6	69.0	232.4	102.0
	Tot ERA5	114.0	78.0	80.0	17.0	13.0	18.0	9.0	4.0	26.0	28.0	51.0	65.0	158.0	130.0
	Diff tot	16.2	29.4	-45.8	-11.4	-10.2	-18.0	-9.0	-1.0	-18.8	-7.6	-17.4	4.0	74.4	-28.0
Javkhiant	Mean	3.0	1.6	0.8	0.0	N/A	N/A	N/A	N/A	N/A	0.1	0.1	2.1	3.6	7.3
	Max	16.4	9.0	6.2	0.8	N/A	N/A	N/A	N/A	N/A	1.8	3.0	17.8	34.2	18.4
	Tot	92.4	50.8	23.2	1.0	N/A	N/A	N/A	N/A	N/A	2.0	4.6	63.0	112.6	66.0
	Tot ERA5	70.0	52.0	52.0	6.0	6.0	13.0	7.0	2.0	15.0	17.0	26.0	52.0	123.0	63.0
	Diff tot	22.4	-1.2	-28.8	-5.0	6.0	-13.0	-7.0	-2.0	-15.0	-15.0	-21.4	11.0	-10.4	3.0
Tunkhel	Mean	3.0	2.2	0.9	0.1	N/A	N/A	N/A	N/A	0.2	0.4	0.8	1.8	8.4	1.8
	Max	32.8	15.0	7.6	1.9	N/A	N/A	N/A	N/A	3.2	2.2	5.8	12.0	52.0	24.0
	Tot	92.3	69.5	26.7	3.1	N/A	N/A	N/A	N/A	6.9	12.6	25.0	52.9	259.1	55.3
	Tot ERA5	107.0	101.0	41.0	14.0	12.0	13.0	6.0	2.0	15.0	24.0	63.0	64.0	162.0	120.0
	Diff tot	-14.7	-31.5	-14.3	-10.9	-12.0	-13.0	-6.0	-2.0	-8.1	-11.4	-38.0	-11.1	97.1	-64.7
Umnudelger	Mean	3.5	2.2	0.7	0.0	N/A	N/A	N/A	N/A	N/A	0.0	0.5	0.4	4.3	2.5
	Max	19.4	23.6	12.6	0.2	N/A	N/A	N/A	N/A	N/A	0.2	9.4	6.0	26.2	23.8
	Tot	109.8	67.0	20.8	0.2	N/A	N/A	N/A	N/A	N/A	0.2	15.4	10.8	133.6	77.0
	Tot ERA5	84.0	86.0	22.0	29.0	10.0	9.0	3.0	1.0	9.0	16.0	36.0	26.0	115.0	66.0
	Diff tot	25.8	-19.0	-1.2	-28.8	-10.0	-9.0	-3.0	-1.0	-9.0	-15.8	-20.6	-15.2	18.6	11.0

Daily amount of rainfall for the whole observed period

A detailed overview of daily rainfall events is shown in Figure 10 and Figure 11.

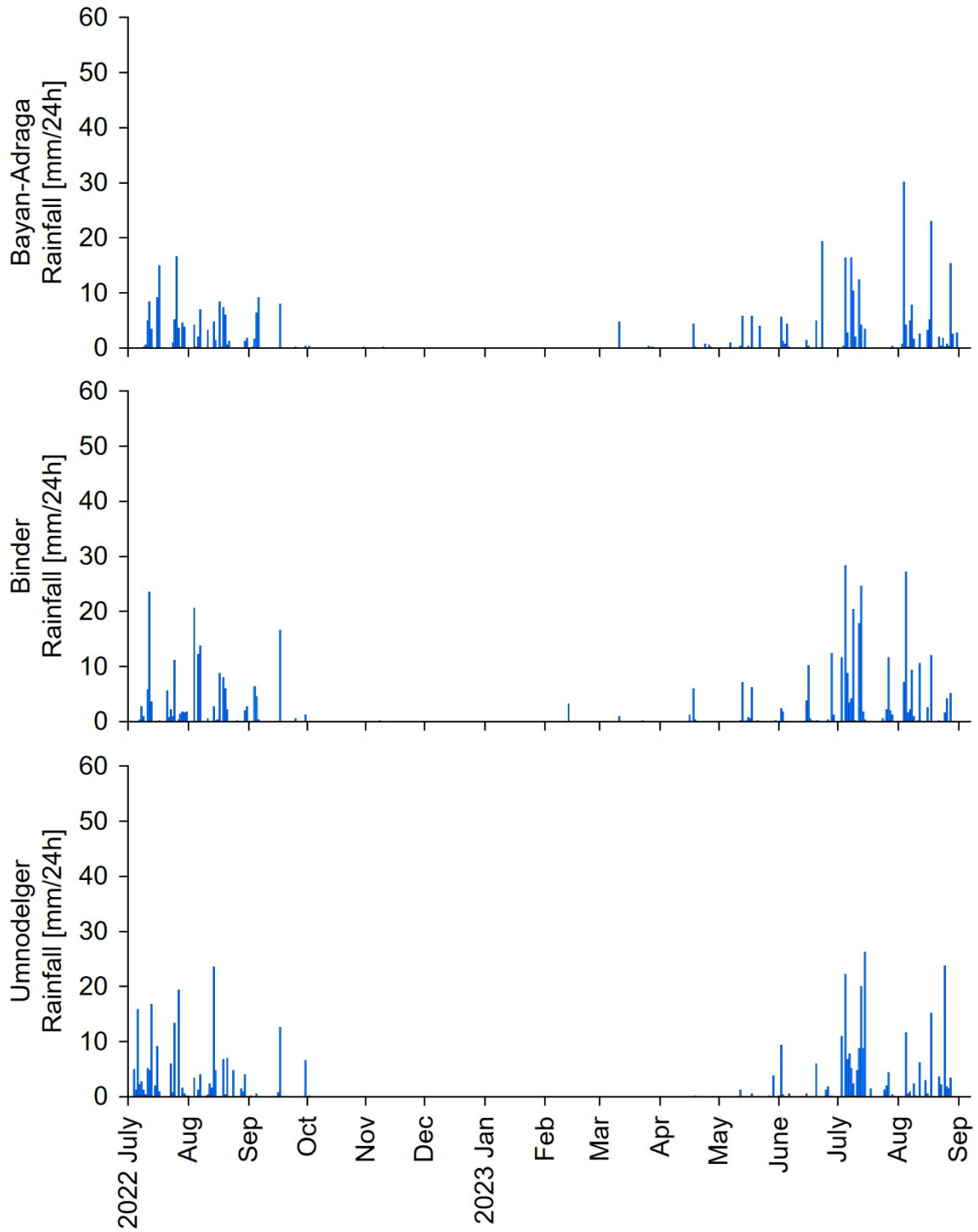


Figure 10. Daily amount of rainfall at demonstration plots in Khentii aimag.

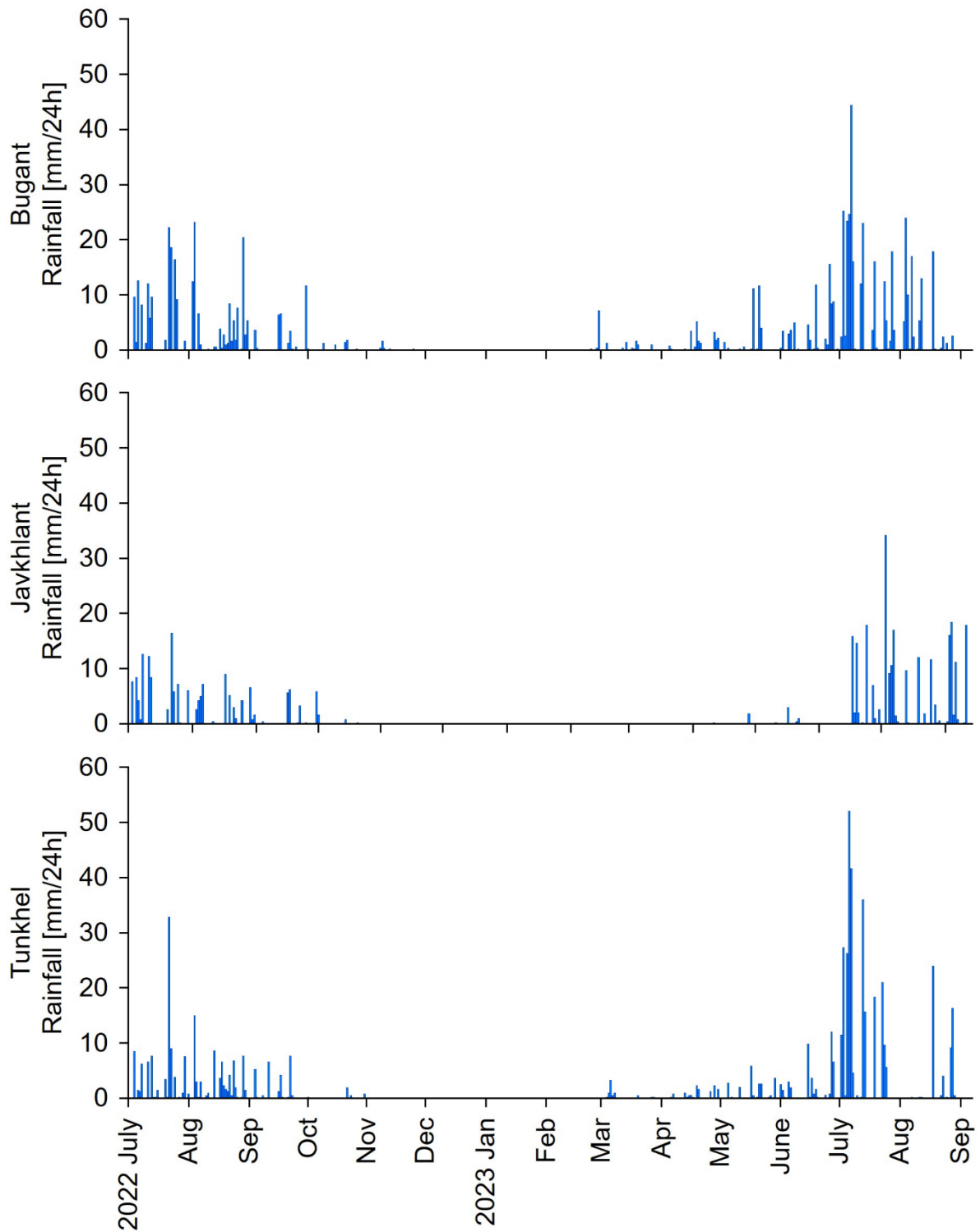


Figure 11. Daily amount of rainfall at demonstration plots in Selenge aimag.

Comparison of site monitoring and ERA5 data

Precipitation (rainfall/snowfall) was additionally evaluated by the ERA5 remote sensing output (Figure 12, Figure 13). The main reason was to evaluate the potential of remote sensing for site environmental conditions evaluation in forestry practice in Mongolia. High site-related heterogeneity between ERA5 and site monitoring results was found (Figure 14, Figure 15). ERA5 overestimates annual rainfall significantly. The precipitations measured by ERA5 (excluding the snowfall from December to March) were found to be higher by 96, 101, 39, 105 and 55 mm than the site monitoring results at Bayan-Adarga, Binder, Javkhlant, Tunkhel and Umnudelger, respectively. The lowest difference between the data from ERA5 and site monitoring was found in Bugant (13 mm). Because of low resolution, the remote sensing methods are not able to provide reliable site-specific data. On the other hand, based on the long-term time series, remote sensing has the potential to predict trends of environmental conditions development. To show exact site-specific values, regular site monitoring is still irreplaceable.

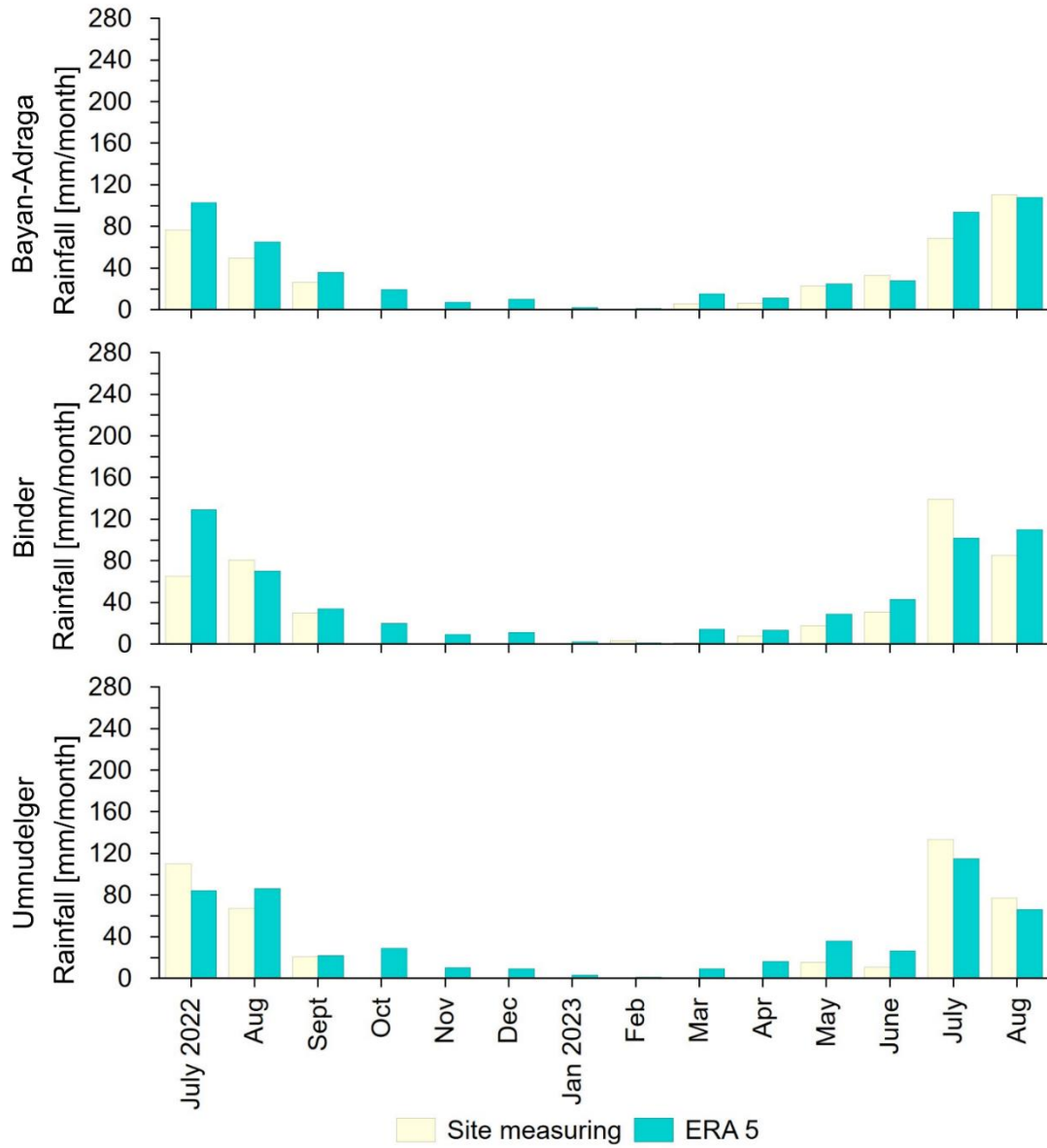


Figure 12. Site rainfall measuring and ERA 5 satellite precipitation data in Khentii aimag.

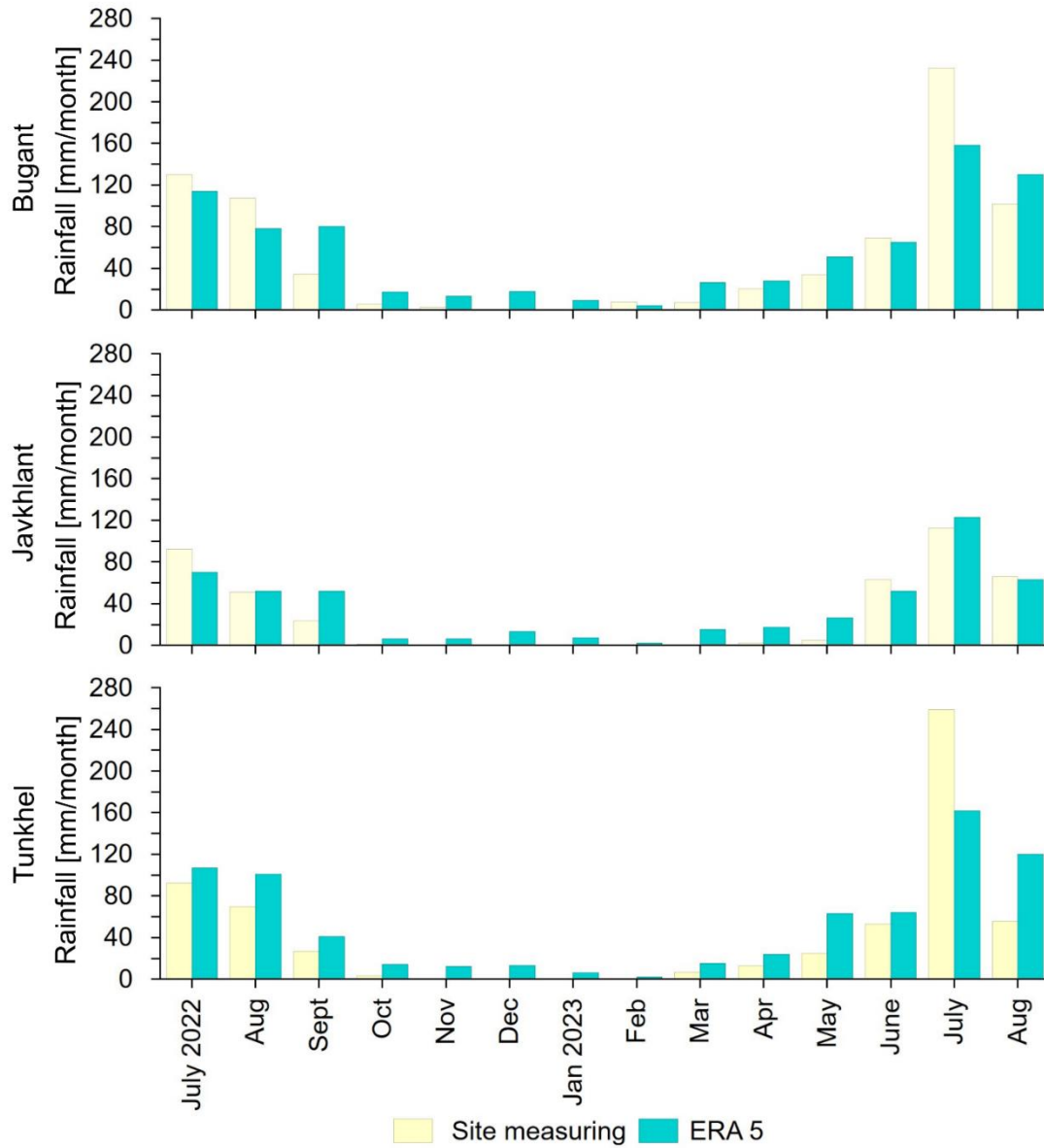


Figure 13. Site rainfall measuring and ERA 5 satellite precipitation data in Selenge aimag.

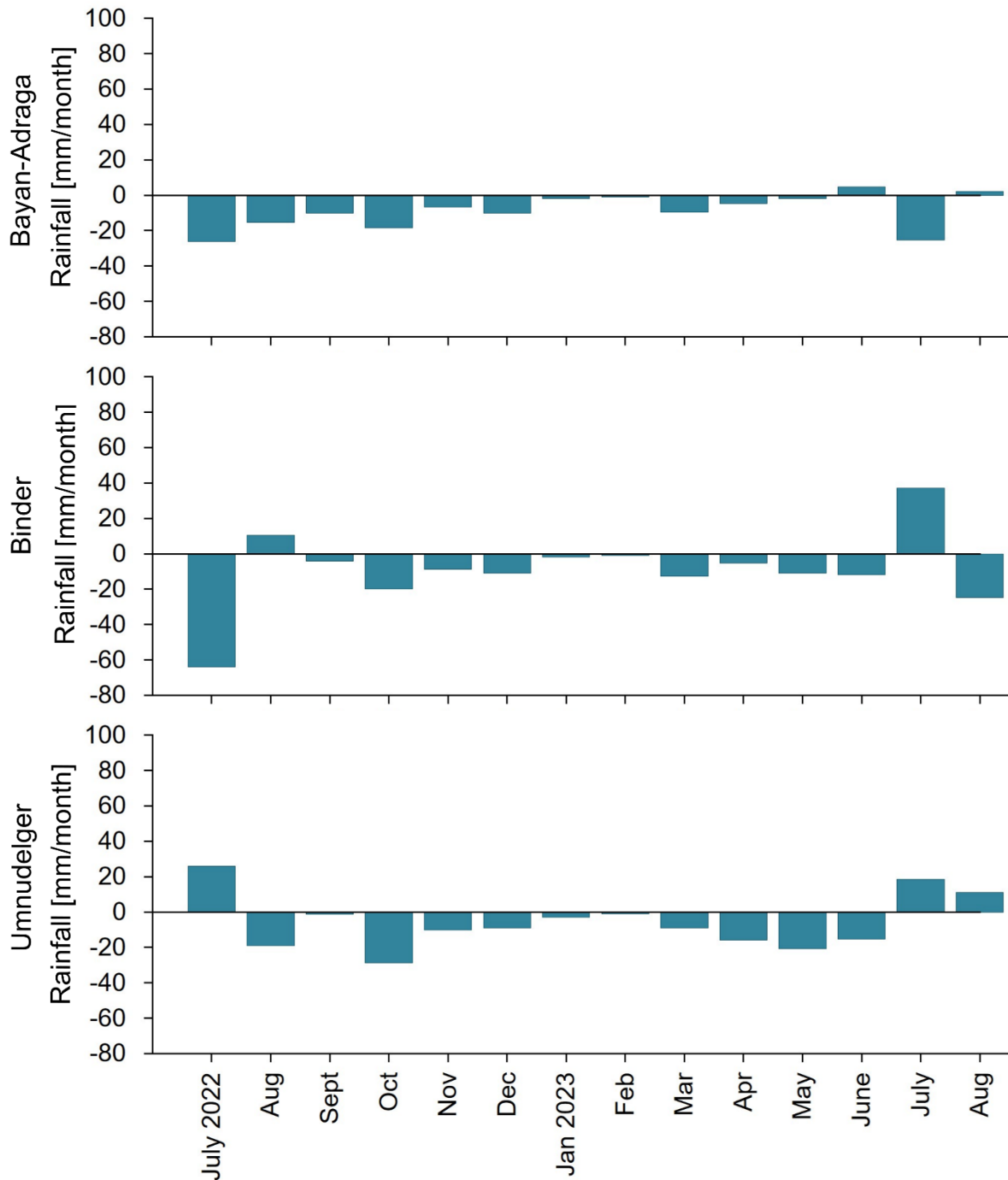


Figure 14. *Difference (mm) between site monitoring and ERA 5 data for Khentii aimag. The negative values mean that ERA 5 shows a higher amount of precipitation than site monitoring; the positive values mean that site monitoring shows a higher amount of precipitation than ERA data.*

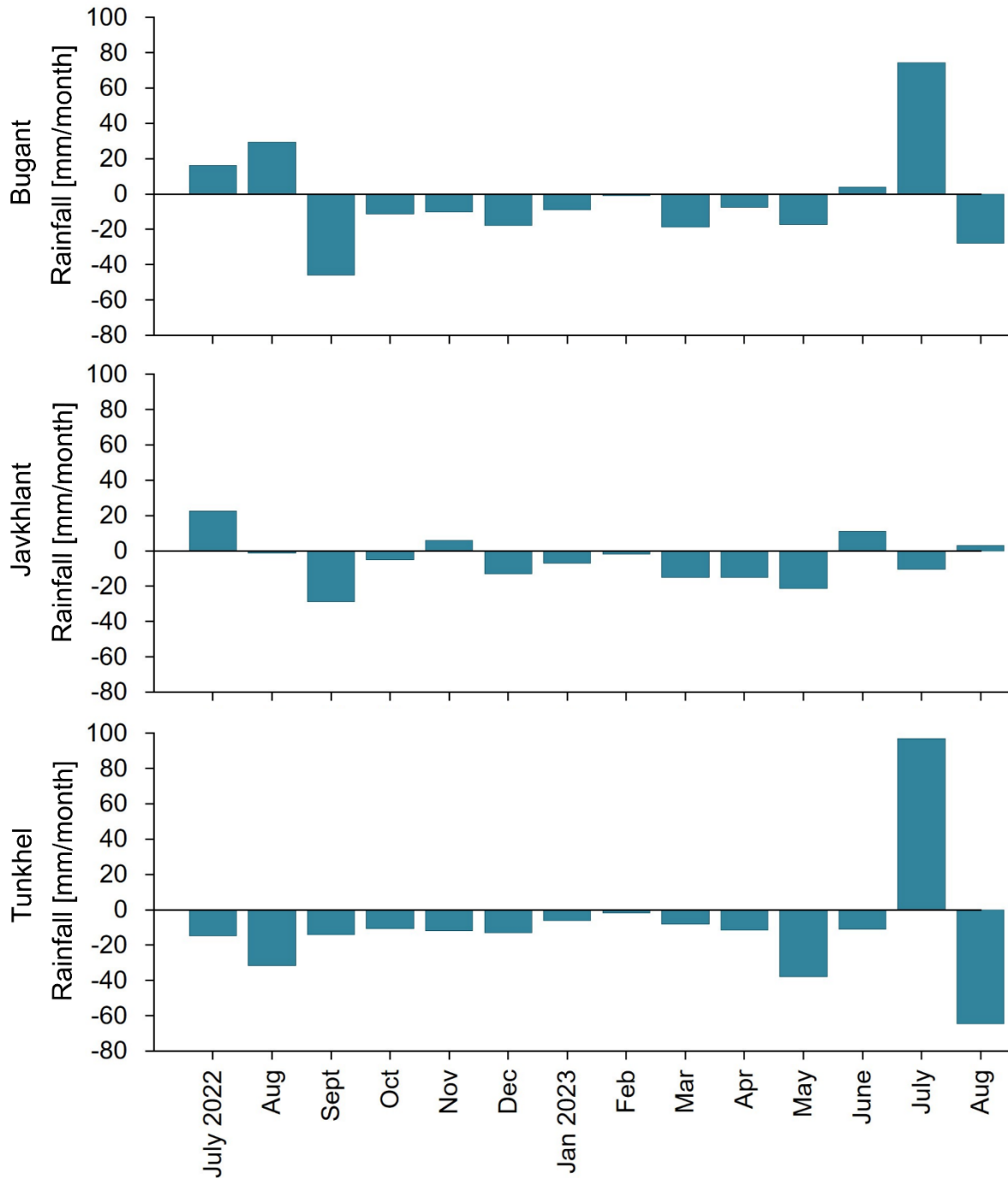


Figure 15. Difference (mm) between site monitoring and ERA 5 data for Selenge aimag. The negative values mean that ERA 5 shows a higher amount of precipitation than site monitoring; the positive values mean that site measuring shows a higher amount of precipitation than ERA data.

1.4 Air temperature evaluation

The highest monthly air temperatures were recorded from June to July 2023 (Figure 16, Table 3). Mean monthly air temperatures dropped below 0 °C at most of the sites in October and remained there until April. The highest (18.9 °C) and the lowest (-24 °C) mean monthly air temperatures were recorded in Javkhlant. The highest air temperature was recorded in Javkhlant in July 2022 (37.6 °C) and the lowest air temperature was recorded in Bugant in January 2023 (-45.4 °C). Temperatures below -40 °C were also recorded in Javkhlant and Tunkhel.

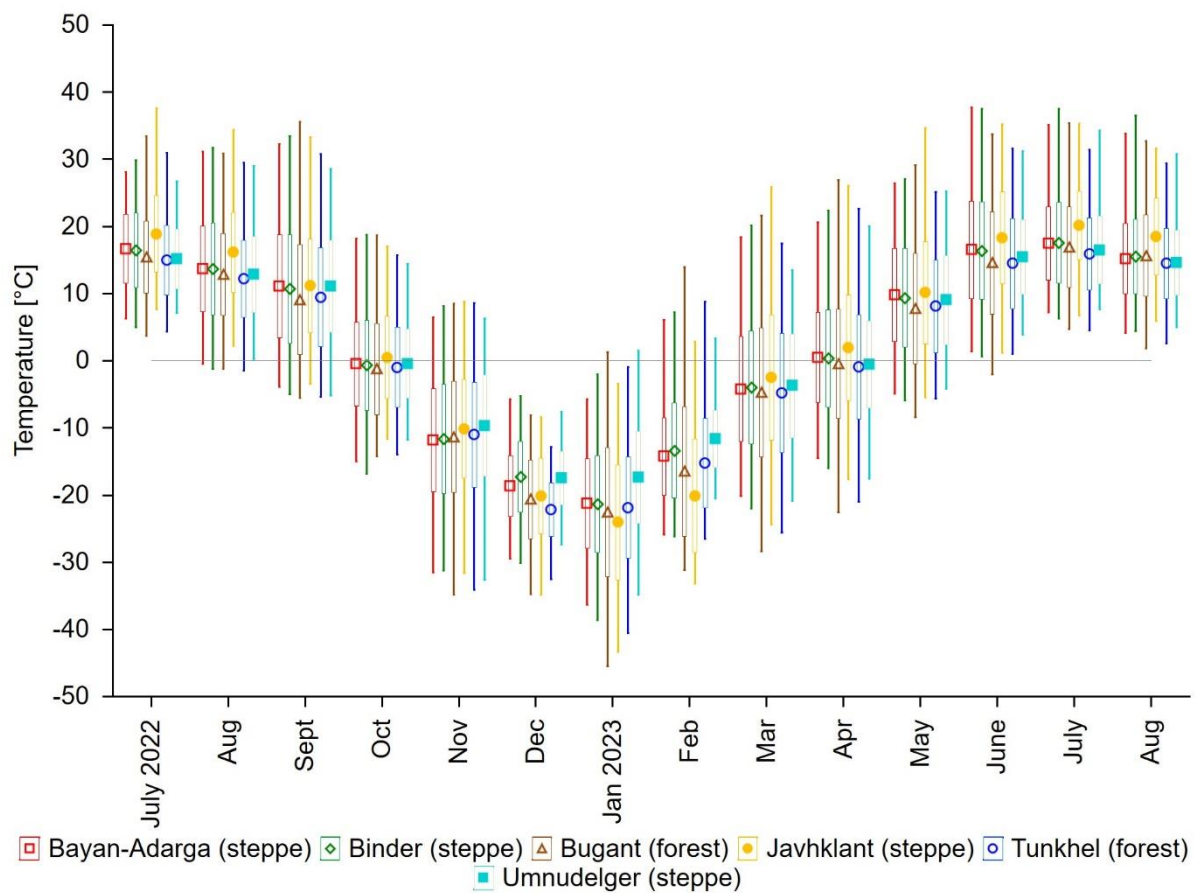


Figure 16. Monthly air temperatures.

Table 3. Monthly air temperatures.

		Bayan-Adarga	Binder	Bugant	Javkhlant	Tunkhel	Umnudelger
July 2022	Mean	16.7	16.5	15.4	18.9	15.0	15.1
	Min	6.3	5.0	3.7	7.6	4.4	7.1
	Max	28.1	29.9	33.4	37.6	31.0	26.8
Aug 2022	Mean	13.7	13.7	12.9	16.2	12.2	12.9
	Min	-0.5	-1.2	-1.2	2.3	-1.4	0.3
	Max	31.1	31.8	30.9	34.4	29.5	29.0
Sept 2022	Mean	11.1	10.7	9.1	11.2	9.4	11.1
	Min	-3.9	-5.0	-5.5	-3.4	-5.3	-5.2
	Max	32.3	33.5	35.6	33.3	30.8	28.6
Oct 2022	Mean	-0.5	-0.7	-1.2	0.5	-1.0	-0.4
	Min	-15.0	-16.8	-14.2	-11.7	-14.0	-11.8
	Max	18.3	18.8	18.6	17.0	15.8	14.4
Nov 2022	Mean	-11.8	-11.6	-11.3	-10.1	-11.0	-9.7
	Min	-31.5	-31.2	-34.9	-31.6	-34.1	-32.6
	Max	6.5	8.1	8.5	8.8	8.6	6.3
Dec 2022	Mean	-18.7	-17.3	-20.6	-20.2	-22.2	-17.5
	Min	-29.4	-30.1	-34.8	-34.9	-32.5	-27.4
	Max	-5.7	-5.3	-8.1	-8.4	-12.9	-7.6
Jan 2023	Mean	-21.3	-21.3	-22.6	-24.0	-21.9	-17.4
	Min	-36.3	-38.6	-45.4	-43.3	-40.6	-34.8
	Max	-5.8	-2.0	1.3	-3.4	-0.9	1.5
Feb 2023	Mean	-14.3	-13.4	-16.5	-20.1	-15.2	-11.6
	Min	-25.9	-26.2	-31.1	-33.1	-26.5	-20.5
	Max	6.1	7.3	13.9	2.9	8.8	3.4
Feb 2023	Mean	-4.2	-4.0	-4.7	-2.5	-4.8	-3.7
	Min	-20.1	-22.0	-28.4	-24.4	-25.6	-20.9
	Max	18.4	20.1	21.6	25.9	17.5	13.5
Apr 2023	Mean	0.5	0.3	-0.5	2.0	-0.9	-0.6
	Min	-14.5	-15.9	-22.5	-17.6	-21.0	-17.6
	Max	20.6	22.4	26.9	26.1	22.6	20.1
May 2023	Mean	9.8	9.4	7.8	10.2	8.1	9.0
	Min	-4.9	-5.9	-8.4	-5.4	-5.6	-4.1
	Max	26.4	27.1	29.1	34.6	25.1	25.3
June 2023	Mean	16.5	16.4	14.6	18.3	14.5	15.4
	Min	1.4	0.7	-2.0	1.2	1.1	3.9
	Max	37.8	37.5	33.8	35.3	31.6	31.3
July 2023	Mean	17.5	17.6	16.9	20.2	15.9	16.5
	Min	7.3	6.3	4.8	6.8	4.5	7.6
	Max	35.1	37.5	35.4	35.3	31.4	34.3
Aug 2023	Mean	15.2	15.5	15.6	18.5	14.5	14.6
	Min	4.1	4.4	1.8	5.9	2.6	5.0
	Max	33.9	36.5	32.8	31.6	29.4	30.8

1.5 Soil temperature evaluation

The main purpose of the soil temperature monitoring at the demonstration plots was to evaluate the effects of the implemented management measures on the soil environment. It is assumed that soil temperature at plots protected from grazing by fencing could be lower in summer and higher in winter in comparison with the reference plots. The difference between grazed and ungrazed areas can be clearly visible as the herb layer is highly developed after exclusion of grazing pressure. Dense herb layer protects the soil from over-heating in summer and deep freezing in winter. In addition, it helps to decrease water loss by evaporation in summer and could reduce damage to the root system of seedlings by frost in winter. An evaluation of soil temperature could also be helpful for understanding the natural processes at the sites. Melting and freezing of soils can be critical for defining the growing season.

In general, knowledge of a long-term soil temperature regime can support the legal setting of suitable periods for logging, timber transport and planting operations in forests. This is critical for maintaining the health of the soil as well as the quality of the road network. The short period of monitoring does not allow for the prediction of long-term trends necessary for specific adjustments, but it can contribute to the initial orientation about the issue.

The soil freezes between November and December and starts melting in April (Figure 17, Figure 18). The peak of soil temperatures was observed from July to August in the summer and from January to February in the winter.

Probably the most visible difference in soil temperatures between an enclosure and its reference plot was observed in Javkhlant (Figure 19). Soil temperature was found to be higher in the enclosure at the beginning of the monitoring period. Then, in early June, the soil temperature started to decrease in the enclosure since the herb layer was being developed (Figure 20). The highest difference between the soil temperature in the enclosure and the control plot was almost 4 °C in summer. Then, in winter, the soil temperature was higher in the enclosure from early January. Soil temperature in the reference plot was higher from early June again. The protecting effect of the herb layer is clearly visible (Figure 19). The developed vegetation cover reduced the heating of the soil in summer and protected the soil from freezing in winter.

A similar natural phenomenon was observed in Tunkhel due to the presence of trees. Soil temperature at 10 cm depth was higher in summer and lower in winter in the burned forest (unstocked area without canopy cover) in comparison with the sparse forest. The protecting effect of the tree cover is clearly visible (Figure 21).

In Bayan-Adarga, Binder and Umnudelger, the protecting effect of the herb layer has not been clearly visible yet (Figure 22, Figure 23, Figure 24). It can be expected that the plant communities and the herb layer were not fully restored after the long-term disturbances. In addition, it has not yet been possible to expect the effect of planted seedlings; their significant impact on the surrounding environment can be expected in a few years. Long-term monitoring is necessary to clearly evaluate the effect of management measures in Bayan-Adarga, Binder and Umnudelger.

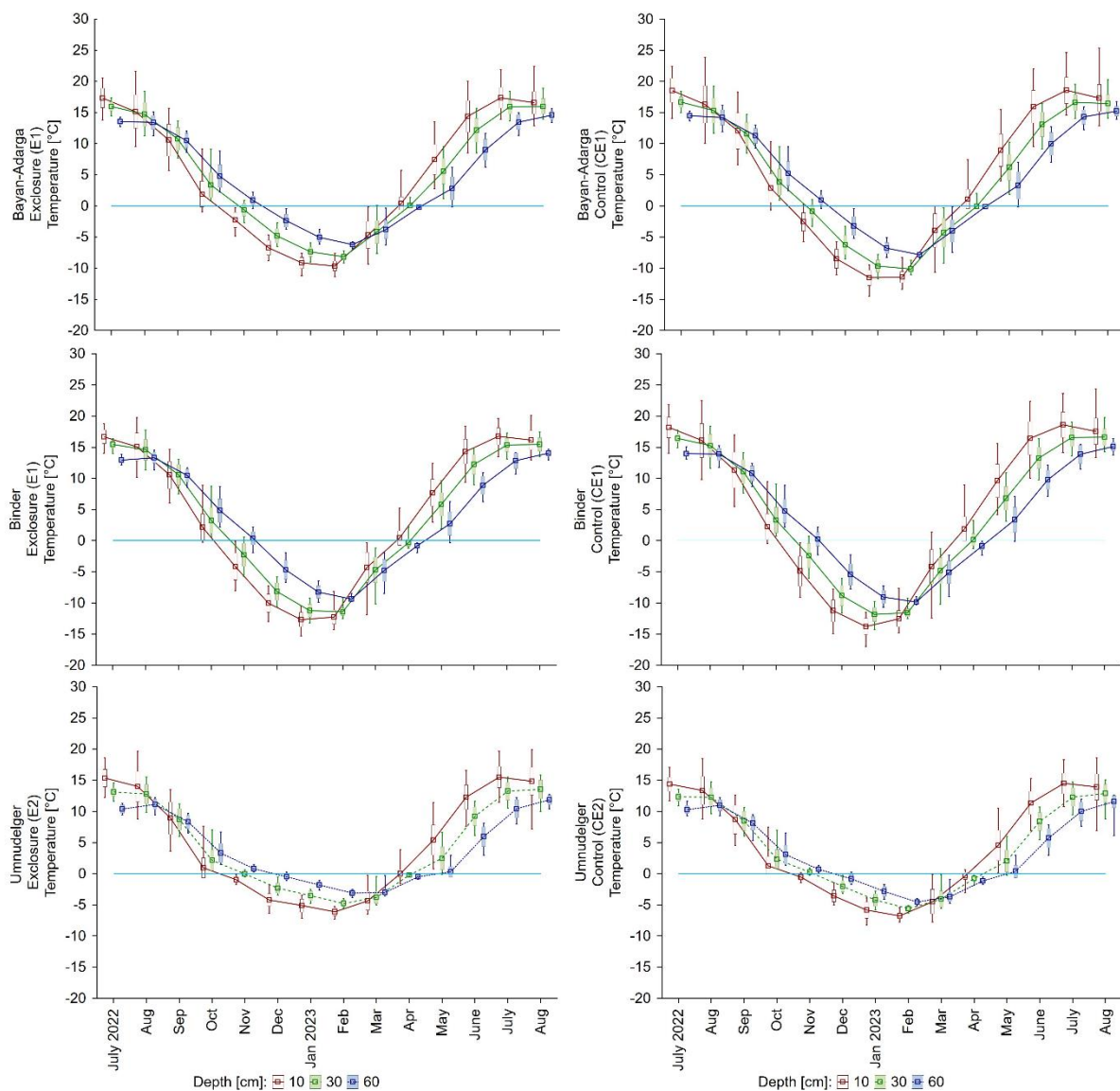


Figure 17. Soil temperatures at depths of 10, 30 and 60 cm and at demonstration plots in *Khentii aimag*.

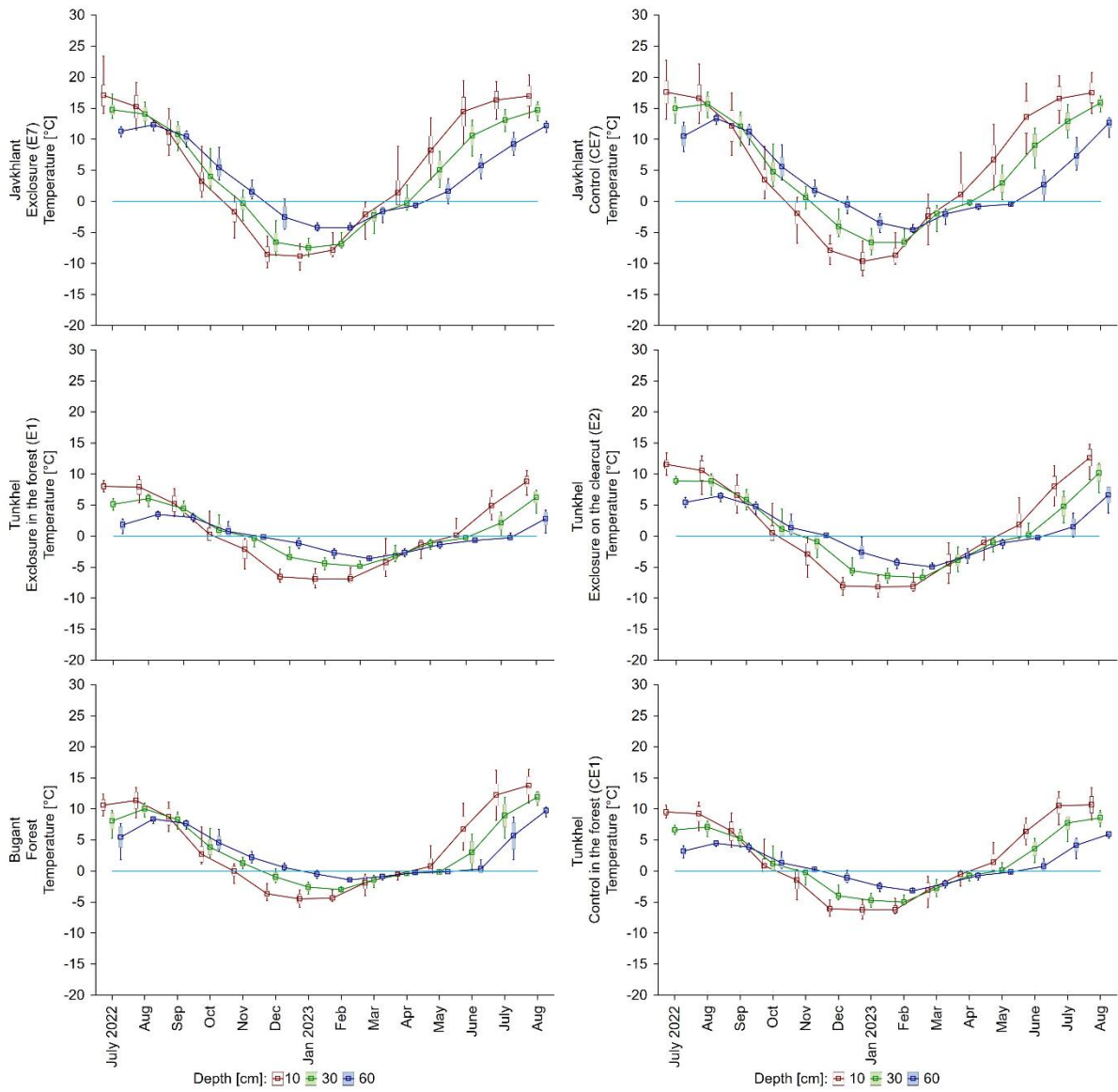


Figure 18. Soil temperatures at depths of 10, 30 and 60 cm and at demonstration plots in Selenge aimag.

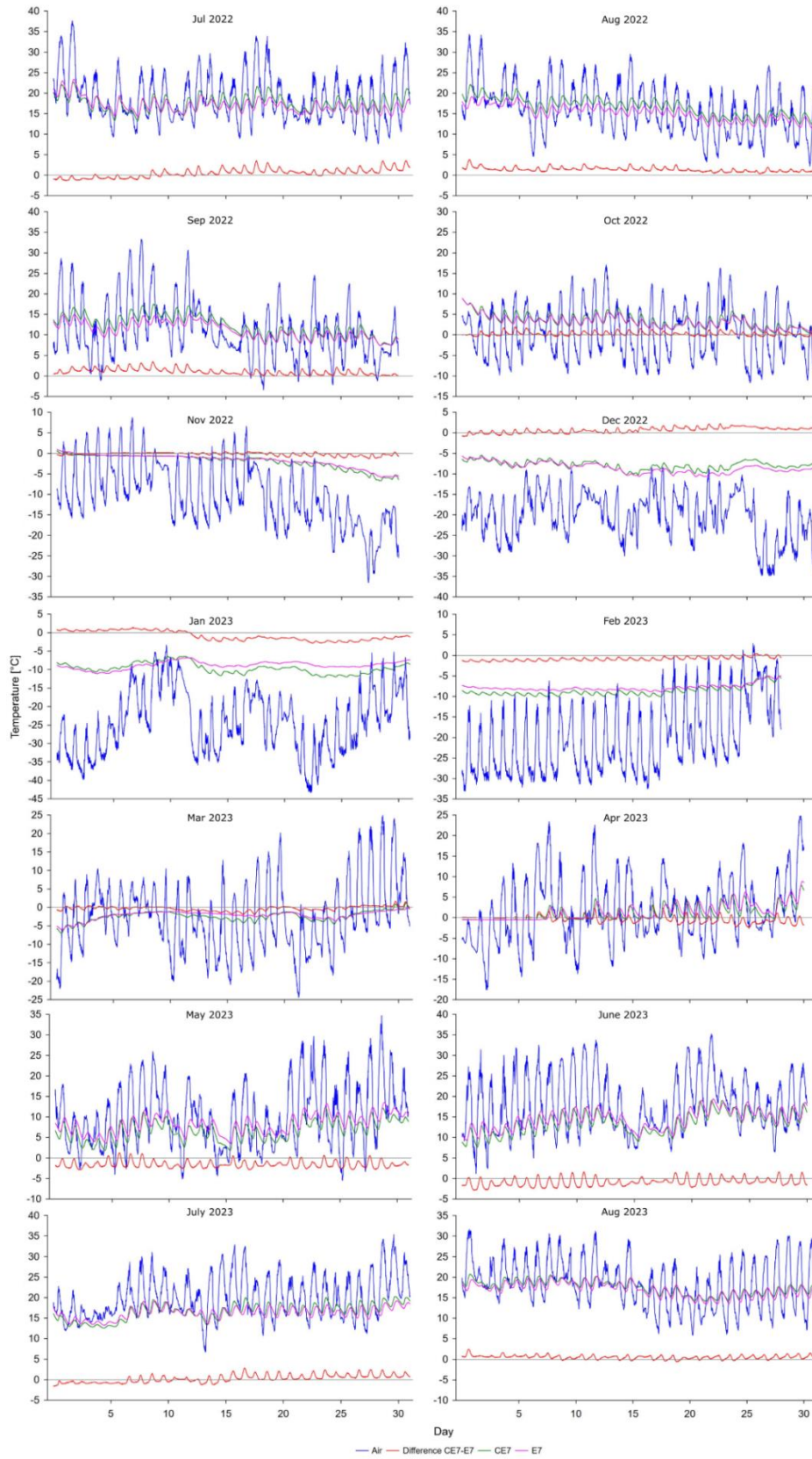


Figure 19. Soil temperatures at a depth of 10 cm and difference between the enclosure (E7) and the control plot (CE7) at Javkhlant.



Figure 20. *Developed herb layer in the exclosure at Javkhlant.*

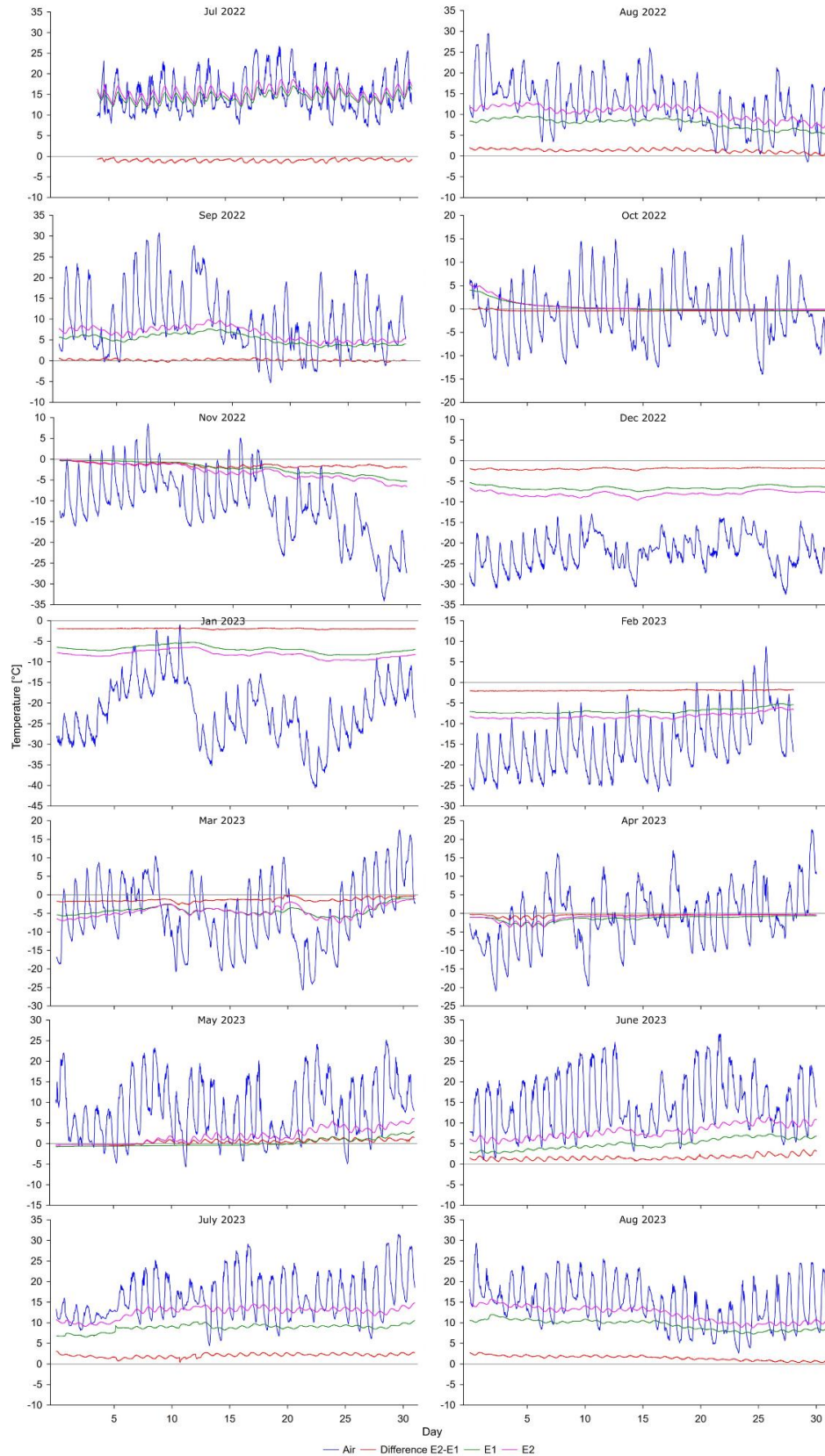


Figure 21. Soil temperature at 10 cm depth and difference between the exclosure in the sparse forest (E1) and the burned forest without canopy cover (E2) at Tunkhel.

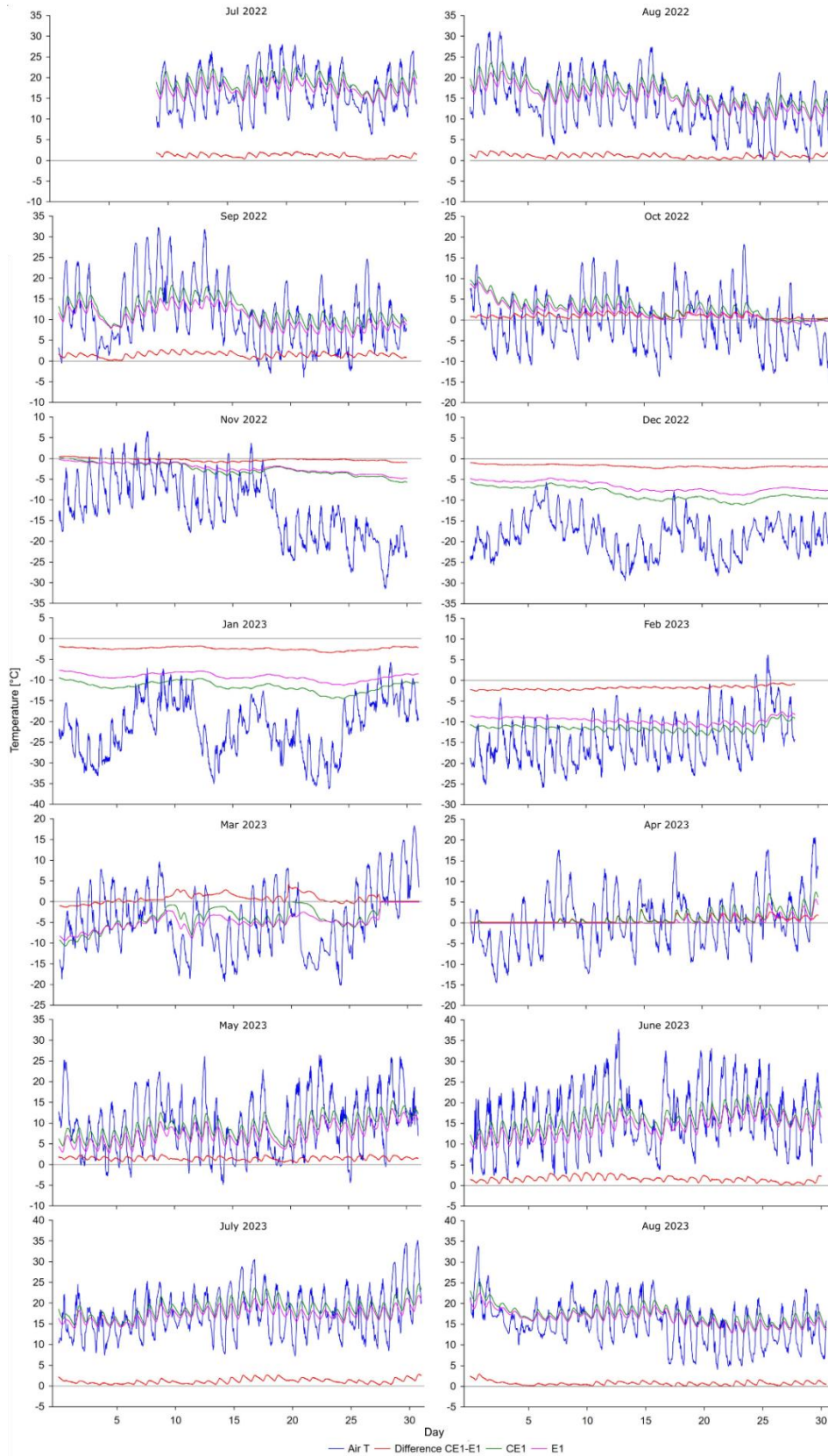


Figure 22. Soil temperature at 10 cm depth and difference between the exclosure (E1) and the control plot (CE1) at Bayan-Adarga.

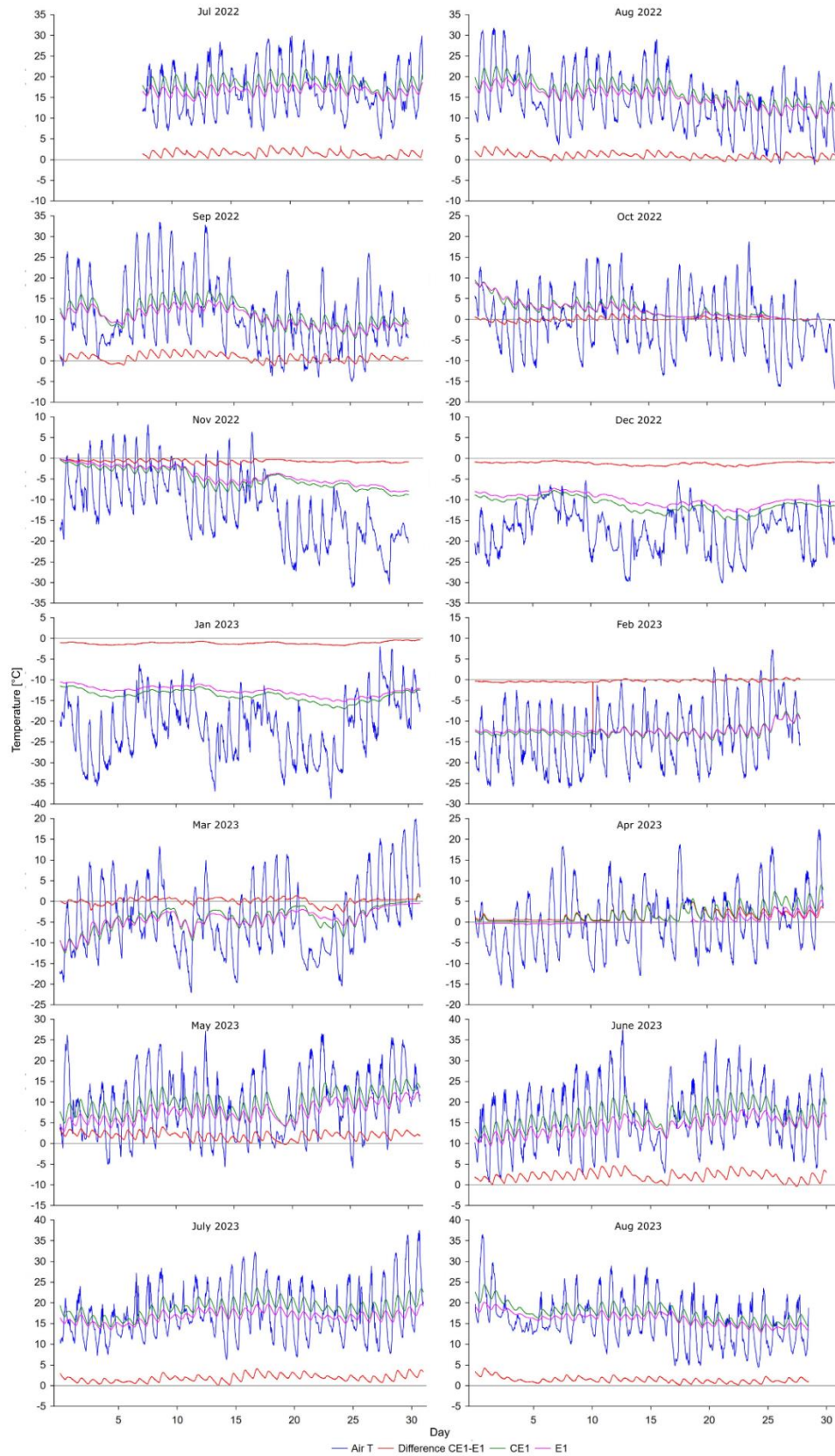


Figure 23. Soil temperature at 10 cm depth and difference between the exclosure (E1) and the control plot (CE1) at Binder.

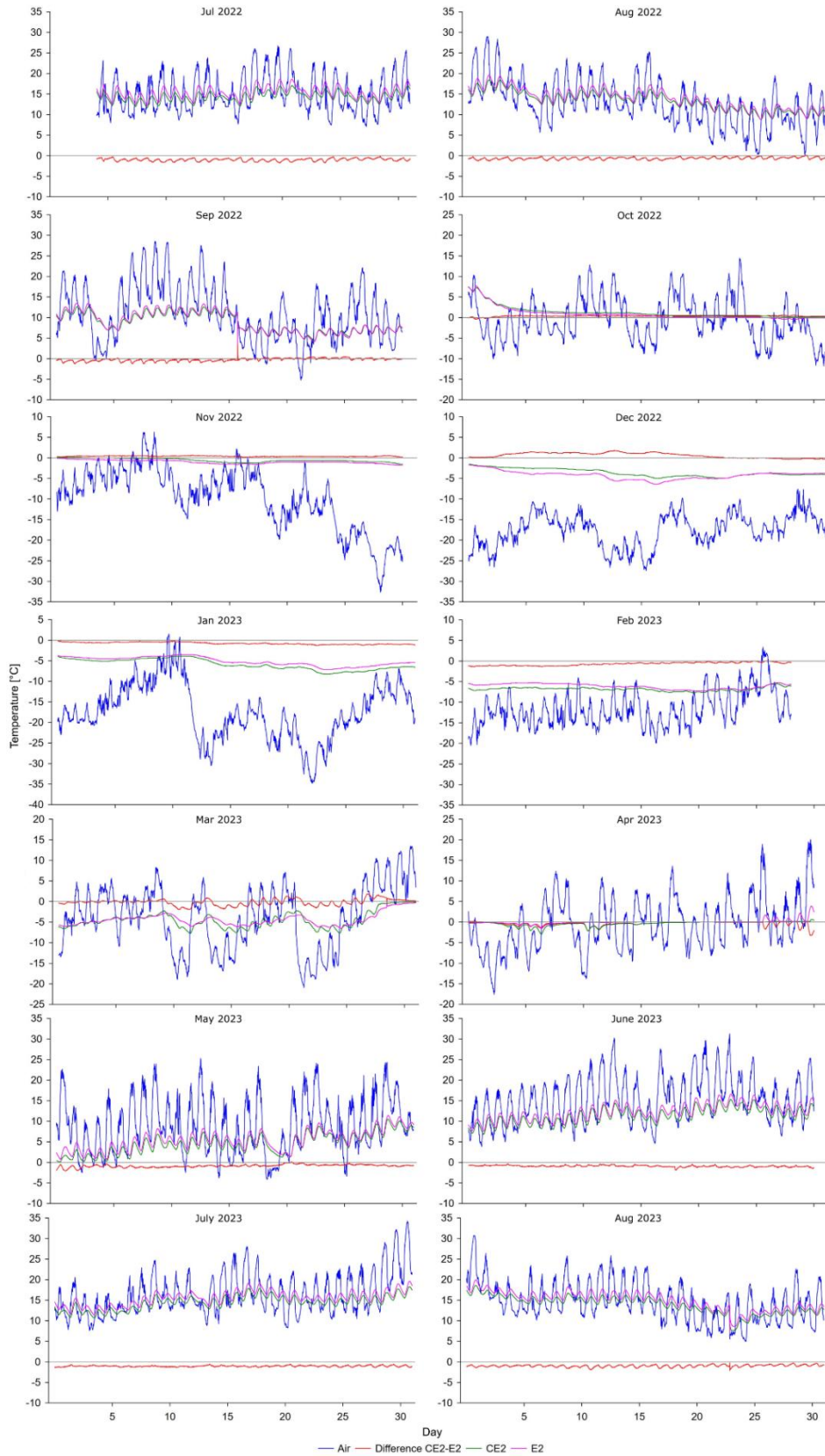


Figure 24. Soil temperature at 10 cm depth and difference between the exclosure (E2) and the control plot (CE2) at Umnudelger.

1.6 Soil moisture evaluation

Soil moisture is one of the most important factors affecting the distribution, composition, and vitality of forests in Mongolia. Unfortunately, there is a critical lack of information about the distribution, dynamics, and volume of soil moisture in Mongolia. Deeper knowledge of this issue is essential for setting and practising of sustainable forest management in specific areas and ecosystems of Mongolia. Information about the moisture conditions of a habitat is critical for evaluating the potential for growing specific tree species, setting up forest regeneration methods, supporting biodiversity and predicting the natural development of the forest regarding climate change and the related adjustment of forest management. Related important issue is tree planting timing when the information on distribution and volume of soil moisture could help to schedule regional dates of field work into safe periods and thus contribute to decreasing seedling mortality rate caused by drought.

Depending on the site, soil moisture in the surface soil layer (0–60 cm) can be composed of the infiltrated rainwater together with the water originating from the melting of the permafrost active layer. Although the distribution of forest in Mongolia is generally associated with permafrost, there are still significant gaps in the understanding of linkages and interactions.

Soil moisture recorded at the sites was put in the context of WP soil hydro limit. The upper level of WP is for the purpose of this report defined as high drought risk i.e. the amount of water is only limitedly available to plants and plants are under the drought stress. The bottom level shows the soil water content when not enough water is available for plants (Figure 25, Figure 27, Figure 28).

In the exclosure (E1) at Bayan-Adarga, soil moisture volume at 10, 30 and 60 cm depths was below WP in early June at the beginning of the monitoring period in 2022 (Figure 25). The same situation was recognized in June and August 2023. Soil moisture at 10 cm depth is strongly dependent on rainfall and was very close to the point of high drought risk (HDR) several times between the rainfall periods. The moisture content at 30 and 60 cm depths was very low, fluctuating between HRD and WP almost for the whole monitoring period according to rainfall periods. However, soil moisture in the exclosure was at 30 cm depth generally higher than at 60 cm depth. The highest soil moisture was recorded at 10 cm depth. In the control plot, soil moisture at 10 and 30 cm depths had a similar course as in the exclosure. Soil moisture at 60 cm depth in the control plot was significantly higher than in the exclosure. It was close to HRD but

not lower. It seems that this deepest soil layer could be independent of direct infiltration from the surface and could be supplied by the hypodermic flow from the upper part of the valley. In general, soil moisture at 0–60 cm depth at the Bayan-Adarga site is strongly dependent on rainfalls.

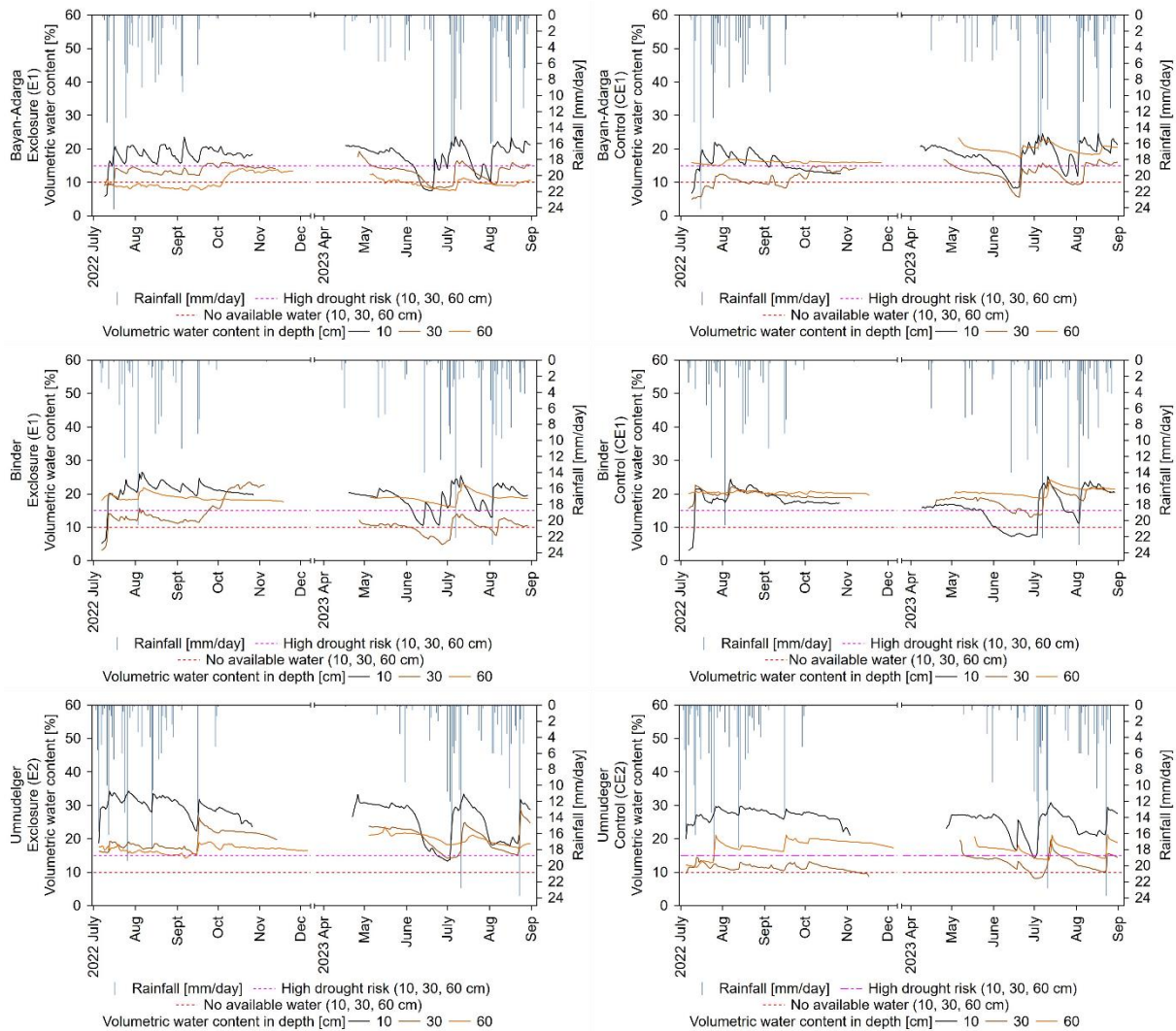


Figure 25. Soil moisture at the sites at *Khentii aimag*.

At the Binder site, both in the exclosure and control plots, soil moisture at 10 cm depth was strictly dependent on rainfall. Soil moisture at 30 and 60 cm depths shows response to rainfall especially after heavy rainfall events (Figure 25). Soil moisture at 10 cm depth reached WP in July 2022. Then, soil moisture at 10 cm depth was mostly above HDR for the rest of the year

and was very close to WP several times in 2023. Soil moisture at 30 cm depth was fluctuating mostly between HRD and WP in the enclosure and was above HRD at the control plot. Soil moisture at 60 cm depth was observed above HRD and higher or on the similar level as at 10 cm depth both in the enclosure and the reference plot. The deepest layer also showed a limited response to rainfall and indicated that soil moisture at 60 cm depth is mostly dependent on the capillary rise from the ground water table.

At the Umnudelger site, soil moisture at 10, 30 and 60 cm depths was strictly dependent on rainfall. Soil moisture at 10 cm depth was generally higher than in Bayan-Adarga and Binder and never reached WP (Figure 25). However, the dramatic decrease of soil moisture at 10 cm depth observed in June and partly in August 2023 was very close to HRD both in the enclosure and the reference plots. Soil moisture at 30 and 60 cm depths in the enclosure was mostly above HRD. In the control plot, soil moisture at 30 cm depth was fluctuating between HRD and WP and soil moisture at 60 cm depth was observed mostly above HRD.

At the Javkhlant site, soil moisture at 10, 30 and 60 cm depths was generally higher than in Bayan-Adarga, Binder and Umnudelger. Soil moisture there was just partly dependent on rainfall. A significant response of soil moisture to rainfall was observed just in the case of heavy rainfall events in 2023 which resulted in floods (Figure 27). A very weak response to regular rainfall events was observed at 10 cm and even weaker at 30 cm depths in 2022 at the beginning of the rainfall season in July. This indicated that the soil moisture is driven mainly by the capillarity coming from the ground water table. The plots are close to the river and about two meters above the river level which means the presence of a shallow ground water aquifer close to the soil surface. It also explains the high soil moisture content at all the depths above the HDR level.

At the Tunkhel site, soil moisture at 10, 30 and 60 cm depths was driven mainly by the capillary rise just the same as at the Javkhlant site (Figure 27). However, in Tunkhel, the source of soil water is predominantly the active layer of permafrost. A significant response of soil moisture to rainfall was observed just in the case of heavy rainfall events in 2023 which resulted in floods. The very weak response to regular rainfall events was observed at 10 cm depth and even weaker at 30 cm depth in 2022 at the beginning of the rainfall season in July. The highest soil moisture from all the sites (almost 60% after the heavy rainfall events in July 2023) was recorded here. Soil moisture content was highly variable between the plots. Soil moisture at 10, 30 and 60 cm

depths was mostly above HDR except the enclosure in the sparse forest. Soil moisture there at 10 and 60 cm depths was fluctuating between HDR and WP.

The Bugant site was well supplied by soil moisture (Figure 28). Soil moisture there at 10, 30 and 60 cm depths seems to be just partly dependent on rainfall. The weak response of soil moisture to heavy rainfall events is visible especially at 10 cm depth. The significant source of water is probably the capillary rise from a shallow ground water aquifer. Soil moisture content is at all depths above the HDR level.

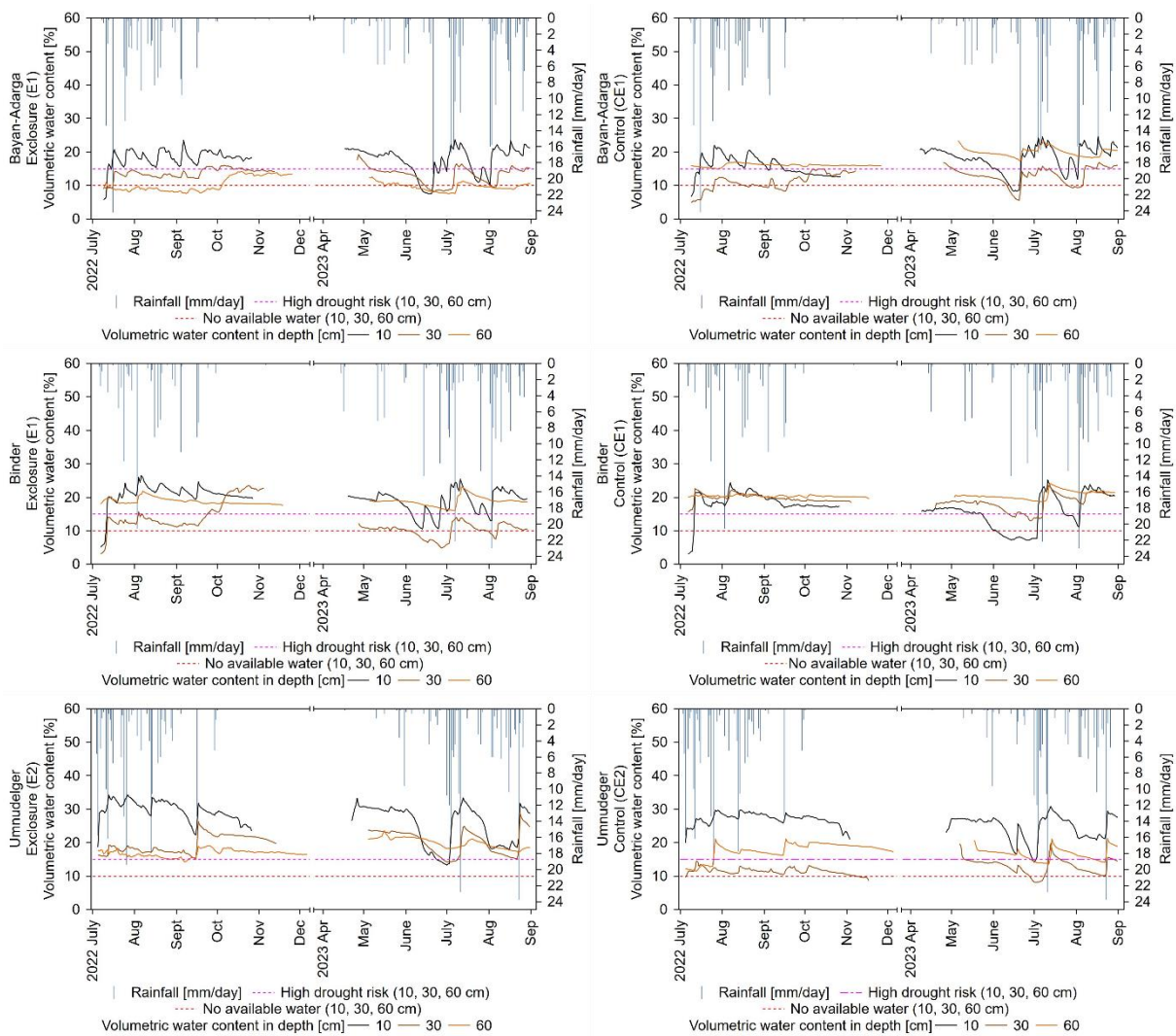


Figure 26. Soil moisture at the sites at Khentii aimag.

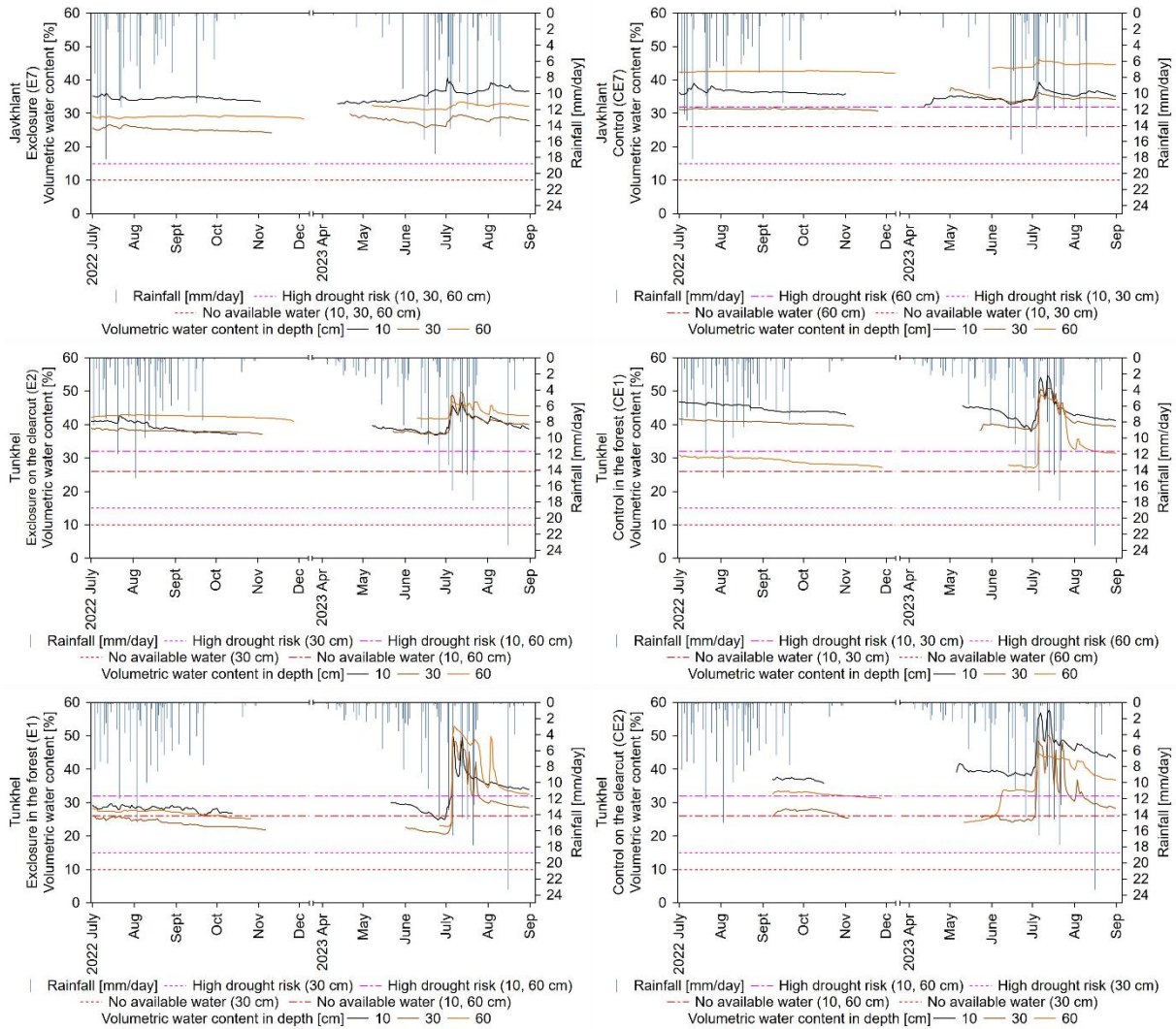


Figure 27. Soil moisture at the sites in Selenge aimag (without Bugant). Clearcut = post-fire unstocked area in the forest.

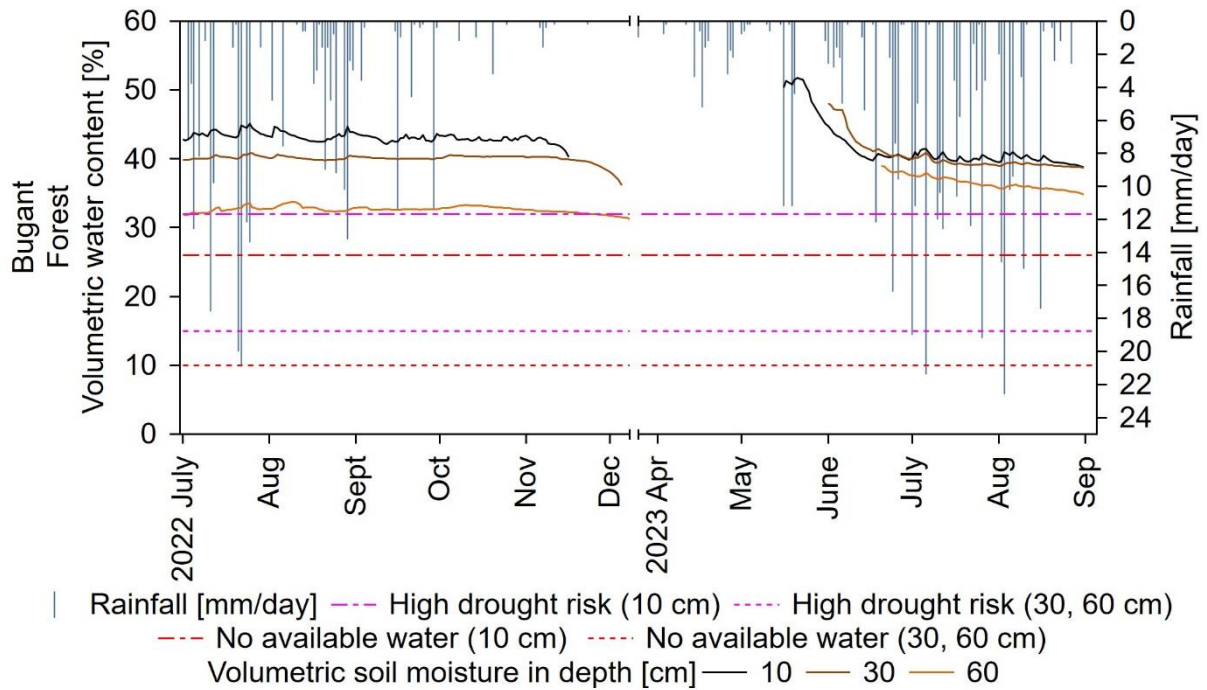


Figure 28. Volumetric water content at the Bugant site.

Summary of soil moisture evaluation

Long-term monitoring shows that soil moisture at the sites in Khentii aimag (Bayan-Adarga, Binder, Umnudelger) is strictly dependent on rainfall. Soil moisture at the sites in Selenge aimag (Bugant, Javkhlant, Tunkhel) is in the case of common annual rainfall influenced mainly by groundwater income. At the sites which are strictly dependent on rainfall, the soil moisture content is lower than at the sites with mainly groundwater-affected soil moisture. At the sites strictly dependent on rainfall, the soil moisture content more often reaches the wilting point where the soil moisture is not available enough for plants. Soil moisture at the Tunkhel site is supplied mainly by natural annual permafrost active layer melting. In Javkhlant, as the site is close to the river, the soil moisture is supplied mainly by the capillary rise from shallow ground water aquifers. However, it should be considered that this only applies to the area near the river and conditions will be different further into the steppe. At the Bugant site, soil moisture is supplied mainly by groundwater from natural annual permafrost active layer melting in the upper part of the valley.

1.7 Drought risk

The drought period was put into the context of air temperature (Figure 29, Figure 30) and site soil moisture origin (rainfall vs. groundwater) to identify the drought sensitivity of the sites. The drought sensitivity was determined as a combination of increasing air temperature in early summer with a limited amount of rainfall resulting in a lack of soil moisture. Basically, the increasing air temperature (> 30 °C in May and June) accelerated evapotranspiration but there is no rainfall to cover soil moisture deficit. Soil moisture content at drought-sensitive sites is decreasing rapidly in May and June reaching the wilting point. The sites highly sensitive to drought are these where soil moisture is strictly dependent on rainfall (Bayan-Adarga, Binder and Umnudelger). The sites with soil moisture supplied mainly by groundwater (Javkhlant, Bugant and Tunkhel) have higher soil moisture and the local ecosystems have the potential to survive drought periods. These sites are less sensitive to annual climate and rainfall fluctuations.

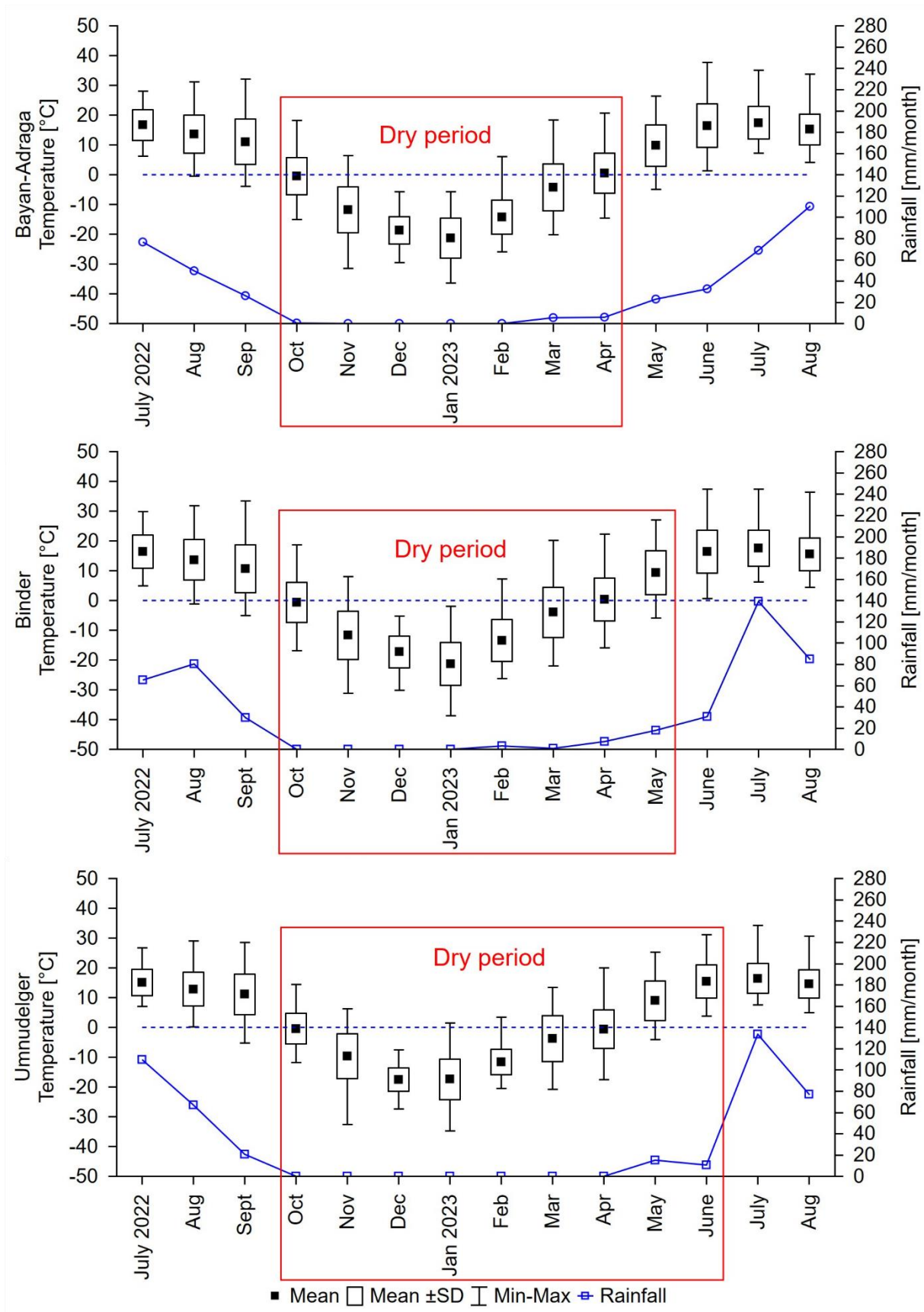


Figure 29. Dry period at the sites at Khentii aimag.

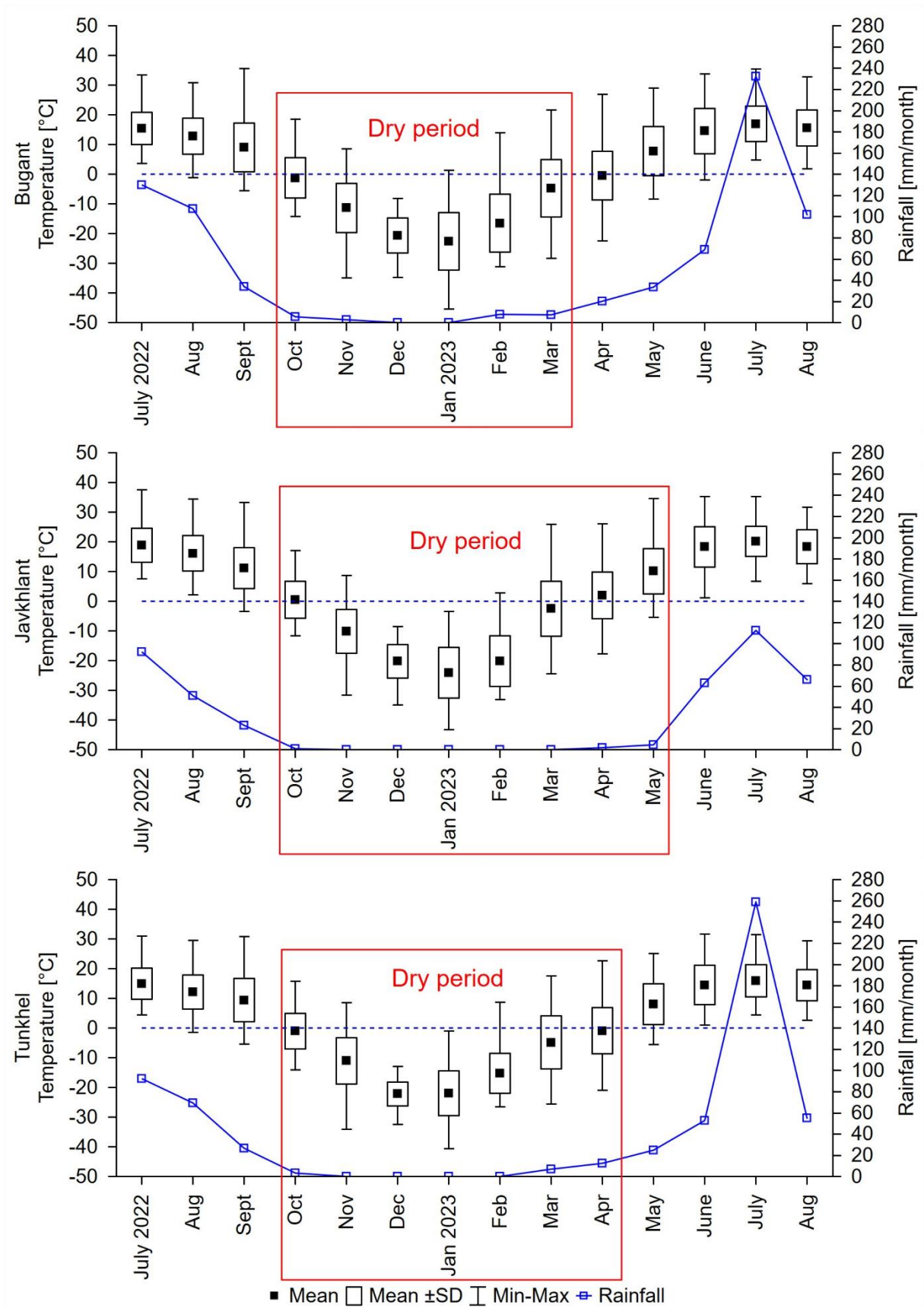


Figure 30. Dry period at the sites at Selenge aimag.

1.8 Management recommendations

The re/afforestation at the sites sensitive to drought is extremely challenging. According to locals, the spring of 2023 was extremely dry in the Khentii area. The data also confirmed this. Especially in May and June when the soil moisture was critically low and air temperature went up, there was a serious threat of seedlings wilting. The high mortality of seedlings planted in the Khentii province within the STREAM project corresponds to these critical conditions. Local observation and experience will allow a better understanding of the natural dynamics of the environment. However, long-term scientific monitoring and evaluation is needed for the adaptation of local ecosystems and the maintenance of forests in the landscape in times of climate change in the long term. On the basis of these measurements, it is only possible to predict whether the investments made in reforestation in these extreme locations are reasonable and truly sustainable. It is necessary to restore forests in places where they grow naturally to mitigate the effects of climate change. However, one of the most critical challenges for the direction of forestry activities in Mongolia is to answer the question of whether it will be possible to sustainably grow forests in those places due to the limited ecological niches of tree species within the horizon of the next 10 years. This question cannot be answered without scientific evaluation, and all the funds spent on forest restoration can thus be devalued.

Facing the ongoing climate change in Mongolia, it is extremely important to identify environmental limits of the ecosystems. Excluding a scientific approach from landscape management planning is dangerous with possible serious negative impacts on biodiversity, society, and national economy and such an approach goes against the principles of sustainability and the Global Goals. To achieve sustainable and effective forest management, it is necessary to recognize: i) common regional-specific dry period, ii) main source of water (rainfall vs. groundwater) at site level and then identify iii) site drought sensitivity. If the site is drought-sensitive, it is appropriate to use for tree planting supporting additives (e.g., hydrogel) or alternative approaches (e.g., container seedlings) to increase the survival rate of seedlings and success of reforestation. In addition, only reforestation can be strictly recommended, afforestation in places where the forest has not grown in the last few centuries is unsustainable in most cases. The reason is the expected further deterioration of the conditions for forest growth.

Forest expansion over the current stands or reforestation of large unstocked areas should respect the natural forest cycle especially at the sites strictly dependent on rainfall. Extreme

environmental conditions often accompanied by livestock grazing and browsing could be challenging for the growth of climax tree species (Siberian larch, Scots pine). However, future forest stands can be established by fast growing pioneer tree species (birch, aspen) which will prepare suitable conditions for larch and pine.

In the case of areas dependent mainly on rainfalls (drought-sensitive sites), it is important to manage the site extensively to increase the forest resilience. Forest management should be based on balancing the ecological and production functions of the forest with an emphasis on ecological ones in the case of worsening environmental conditions. The commercial use of drought-sensitive sites must be secondary. On the other hand, the sites which are well-donated by groundwater from permafrost natural melting are potentially suitable for sustainable forest management and commercial use.

1.9 References

- Batima, P., & Dagvadorj, D. (2000). Climate change and its impacts in Mongolia. *Natl Agency Meteorol Hydrol Environ Monit JEMR Publ Ulaanbaatar, Mong* 227p.
- Bohannon, J. (2008). Climate change: The big thaw reaches Mongolia's Pristine North. *Science*, 319(5863), 567–568. <https://doi.org/10.1126/science.319.5863.567>
- Chang, J., Wang, G. X., Li, C. J., & Mao, T. X. (2015). Seasonal dynamics of suprapermafrost groundwater and its response to the freeing-thawing processes of soil in the permafrost region of Qinghai-Tibet Plateau. *Science China Earth Sciences*, 58(5), 727–738. <https://doi.org/10.1007/s11430-014-5009-y>
- EMS Brno. (2024). *Precipitation gauge*. EMS Brno. <http://www.emsbrno.cz/p.axd/en/Precipitation.gauge.html>
- Genxu, W., Guangsheng, L., Chunjie, L., & Yan, Y. (2012). The variability of soil thermal and hydrological dynamics with vegetation cover in a permafrost region. *Agricultural and Forest Meteorology*, 162–163, 44–57. <https://doi.org/10.1016/j.agrformet.2012.04.006>
- Gravis, G. F., Zabolotnik, S. I., Sukhodrovxky, V. L., Gavrilova, M. K., & Lisun, A. M. (1974). *Geocryological conditions in the People's Republic of Mongolia* (P. I. Melnikov, Ed.; Nauka Publ).
- Hemr, O., Vichta, T., Brychtová, M., Kupec, P., Žižlavská, N., Tomášová, G., & Deutscher, J. (2023). Stemflow infiltration hotspots near-tree stems along a soil depth gradient in a mixed oak–beech forest. *European Journal of Forest Research*, 142(6), 1385–1400. <https://doi.org/10.1007/s10342-023-01592-7>
- IUSS Working Group WRB. (2015). *World Reference Base for Soil Resources 2014*. FAO.

- IUSS Working Group WRB. (2022). *World Reference Base for Soil Resources: International soil classification system for naming soils and creating legends for soil maps*. International Union of Soil Sciences .
- Juříčka, D., Novotná, J., Houška, J., Pařílková, J., Hladký, J., Pecina, V., Cihlářová, H., Burnog, M., Elbl, J., Rosická, Z., Brtnický, M., & Kynický, J. (2020). Large-scale permafrost degradation as a primary factor in *Larix sibirica* forest dieback in the Khentii massif, northern Mongolia. *Journal of Forestry Research*, *31*(1), 197–208. <https://doi.org/10.1007/s11676-018-0866-4>
- Juříčka, D., Valtera, M., Deutscher, J., Vichta, T., Pecina, V., Patočka, Z., Chalupová, N., Tomášová, G., Jačka, L., & Pařílková, J. (2022). The role of pit-mound microrelief in the redistribution of rainwater in forest soils: a natural legacy facilitating groundwater recharge? *European Journal of Forest Research*, *141*(2), 321–345. <https://doi.org/10.1007/s10342-022-01439-7>
- Khishigjargal, M., Dulamsuren, C., Lkhagvadorj, D., Leuschner, C., & Hauck, M. (2013). Contrasting responses of seedling and sapling densities to livestock density in the Mongolian forest-steppe. *Plant Ecology*, *214*(11), 1391–1403. <https://doi.org/10.1007/s11258-013-0259-x>
- Klinge, M., Dulamsuren, C., Schneider, F., Erasmi, S., Hauck, M., Bayarsaikhan, U., & Sauer, D. (2020). Modelled potential forest area in the forest-steppe of central Mongolia is about three times of actual forest area. *Biogeosciences Discussions, March*, 1–37. <https://doi.org/10.5194/bg-2020-13>
- Klinge, M., Schneider, F., Dulamsuren, C., Arndt, K., Bayarsaikhan, U., & Sauer, D. (2021). Interrelations between relief, vegetation, disturbances, and permafrost in the forest-steppe of central Mongolia. *Earth Surface Processes and Landforms*, *46*(9), 1766–1782. <https://doi.org/10.1002/esp.5116>
- Kokelj, S. V., Riseborough, D., Coutts, R., & Kanigan, J. C. N. (2010). Permafrost and terrain conditions at northern drilling-mud sumps: Impacts of vegetation and climate change and the management implications. *Cold Regions Science and Technology*, *64*(1), 46–56. <https://doi.org/10.1016/j.coldregions.2010.04.009>
- Lioubimtseva, E., Cole, R., Adams, J. M., & Kapustin, G. (2005). Impacts of climate and land-cover changes in arid lands of Central Asia. *Journal of Arid Environments*, *62*(2), 285–308. <https://doi.org/10.1016/j.jaridenv.2004.11.005>
- Luo, D. (2012). *Degradation of permafrost and cold-environments on the interior and eastern Qinghai Plateau. May 2020*.
- Marin, A. (2010). Riders under storms: Contributions of nomadic herders' observations to analysing climate change in Mongolia. *Global Environmental Change*, *20*(1), 162–176. <https://doi.org/10.1016/j.gloenvcha.2009.10.004>
- Natsagdorj, L. (2000). Climate change. In P. Batima & D. Dagvadorj (Eds.), *Climate Change and its Impacts in Mongolia*. JEMR Publishing.

- Natsagdorj, L., Jugder, D., & Chung, Y. S. (2003). Analysis of dust storms observed in Mongolia during 1937–1999. *Atmospheric Environment*, 37(9–10), 1401–1411. [https://doi.org/10.1016/S1352-2310\(02\)01023-3](https://doi.org/10.1016/S1352-2310(02)01023-3)
- OCHA. (2023, July 1). *Mongolia: Floods - Jul 2023*. <https://reliefweb.int/disaster/fl-2023-000111-mng>
- Oyuntuya, S., Dorj, B., Shurentsetseg, B., & Bayarjargal, E. (2015). Agrometeorological information for the adaptation to climate change. In N. B. Badmaev & C. B. Khutakova (Eds.), *Soils of steppe and forest steppe ecosystems of inner asia and problems of their sustainable utilization*. (pp. 135–140).
- Rai, R. K., Singh, V. P., & Upadhyay, A. (2017). Soil Analysis. In *Planning and Evaluation of Irrigation Projects* (pp. 505–523). Elsevier. <https://doi.org/10.1016/B978-0-12-811748-4.00017-0>
- Rowley, M. C., Grand, S., & Verrecchia, É. P. (2018). Calcium-mediated stabilisation of soil organic carbon. *Biogeochemistry*, 137(1–2), 27–49. <https://doi.org/10.1007/s10533-017-0410-1>
- Runyan, C. W., & D’Odorico, P. (2012). Ecohydrological feedbacks between permafrost and vegetation dynamics. *Advances in Water Resources*, 49, 1–12. <https://doi.org/10.1016/j.advwatres.2012.07.016>
- Sharkhuu, N. (2003). Recent Changes in the Permafrost of Mongolia. *Proceedings of the Eighth International Conference on Permafrost*, 2, 1029–1034.
- Shukla, P. R., Skeg, J., Buendia, E. C., Masson-Delmotte, V., Pörtner, H.-O., Roberts, D. C., Zhai, P., Slade, R., Connors, S., & van Diemen, S. (2019). *Climate Change and Land: an IPCC special report on climate change, desertification, land degradation, sustainable land management, food security, and greenhouse gas fluxes in terrestrial ecosystems*.
- Smith, M. W., & Riseborough, D. W. (2002). Climate and the limits of permafrost: a zonal analysis. *Permafrost and Periglacial Processes*, 13(1), 1–15. <https://doi.org/10.1002/ppp.410>
- Sugimoto, A., Yanagisawa, N., Naito, D., Fujita, N., & Maximov, T. C. (2002). Importance of permafrost as a source of water for plants in east Siberian taiga. *Ecological Research*, 17(4), 493–503. <https://doi.org/10.1046/j.1440-1703.2002.00506.x>
- Tshikolovets V., Yakovlev R., & Bálint Z. (2009). *The butterflies of Mongolia*. Tshikolovets publishing.
- Tumurbaatar, B., & Mijiddorj, B. (2006). Permafrost and permafrost thaw in Mongolia. In J. Gelhaus & B. Boldvig (Eds.), *The geology, biodiversity and ecology of Lake Hovsgol (Mongolia)*. (pp. 41–48). Backhuys Publishers.
- Walker, D. A., Jia, G. J., Epstein, H. E., Reynolds, M. K., Chapin, I. S., Copass, C., Hinzman, L. D., Knudson, J. A., Maier, H. A., Michaelson, G. J., Nelson, F., Ping, C. L., Romanovsky, V. E., & Shiklomanov, N. (2003). Vegetation-soil-thaw-depth relationships along a low-arctic bioclimate gradient, Alaska: Synthesis of information from the ATLAS

studies. *Permafrost and Periglacial Processes*, 14(2), 103–123.
<https://doi.org/10.1002/ppp.452>

Yao, T. D., Qin, D. H., Shen, Y. P., Zaho, L., Wang, N. L., & Lu, A. X. (2013). Cryospheric changes and their impacts on regional water cycle and ecological conditions in the Qinghai-Tibetan Plateau. *Chin J Nat*, 35(3), 179–186. <https://doi.org/10.3969/j.issn.0253-9608.2013.03.004>

SOIL AND MYCORRHIZA SURVEY

2 SOIL AND MYCORRHIZA SURVEY

Martin Valtera¹ and Burenjargal Otgonsuren²

¹ *Mendel University in Brno, Zemědělská 1, 613 00, Brno, Czech Republic*

² *Mongolian University of Life Sciences, Ulaanbaatar 17024, Mongolia*

2.1 Introduction

Soils are the largest terrestrial pool of organic carbon (OC). Unlike inorganic carbon (IC), such as carbonate rocks, organic carbon pools are highly sensitive to land management and can either increase or decrease in time depending on the climatic conditions and land use changes. The turnover time of OC in a soil typically ranges from years to millennia. The long-term stability of OC in a soil is supported through several mechanisms, such as the *association with minerals* (especially clay and silt particles, with the high specific surface area), *bonding with metal ions* (including Al, Fe, or Ca), and the *occlusion in soil aggregates* (e.g. earthworm casts). The dominant mechanisms behind soil OC (SOC) stabilization can be easily indicated from soil mineralogy, texture, and pH (Rowley et al., 2018).

Soil classification is used for the international communication about soils and is defined on soil properties that are related to soil forming process and, in many cases, highly significant for the use of soils and land management. The information on soil classification can be used to compile national or global soil databases, as well as for the inventory and monitoring of soil resources, such as those provided and historically published by the Food and Agriculture Organization of the United Nations (IUSS Working Group WRB, 2015) and currently by the International Soil Reference and Information Centre (IUSS Working Group WRB, 2022).

An important part of environmental monitoring connected to soil environment is Mycorrhiza survey. Mycorrhiza is a symbiotic relationship between tree (or other plants) roots and fungi and is a one of the most essential factors influencing tree growth. Fungi provide trees with nutrients and water, which in the harsh environment of Mongolia are some of the most limiting factors for the growth and distribution of forest. There is a lack of information on mycorrhiza in Mongolia. Knowledge about mycorrhiza can help us understand how trees adapt to Mongolia's extreme natural conditions and to find the most suitable measures for sustainable

forest management. To our knowledge, only the STREAM scientific group has carried out studies on mycorrhizas in the related project areas of Mongolia so far.

The aim of this report was to provide basic information about the soil properties in the STREAM project demonstration plots and to develop basic management recommendations with an emphasis on soil protection, carbon sequestration, and the sustainable productivity of the forest, steppe, and forest-steppe ecotone.

2.2 Methods

Soil survey

A soil survey was conducted at six STREAM project demonstration sites (Figure 31). At each of the sites, standard soil profiles were excavated, described, and classified according to the international standards (IUSS Working Group WRB 2022). From each soil profile, a set of soil samples was collected at the three fixed depths: 10 cm, 30 cm, and 60 cm from mineral soil surface to verify the field descriptions and classifications by laboratory analyses. The soil profiles were mostly identical with those used for soil moisture and temperature monitoring (see chapter 1).

To evaluate soil properties across demonstration plots, composite samples of the organic layer and of the 0–30 cm mineral soil were collected in 3 to 6 demonstration plots per site (3 forest plots and 3 steppe or unstocked forest plots, if present). Each composite sample consisted of three subsamples per plot collected at three sampling points with a spacing of approx. 10 m from each other. The surface organic layer was collected using a knife and gloves within a plastic tube of 15.2 cm or 18.9 cm diameter. The mineral soil was sampled using a core auger of 5.0 cm diameter. Each sample was placed into a sealed plastic bag and stored in a cooling box during transport. In the laboratory, the soil samples were separated on a 2-mm mesh sieve into the fine-earth (< 2 mm) and the coarse fraction (i.e., rocks, roots, and undecomposed wood or charcoal). Total carbon and nitrogen contents of the composite organic and mineral samples were determined (Vario MACRO Cube, Elementar, Germany) on the basis of the 105 °C dry weight. Soil pH was determined using a glass electrode in a 1:5 (volume fraction) suspension in deionized water.

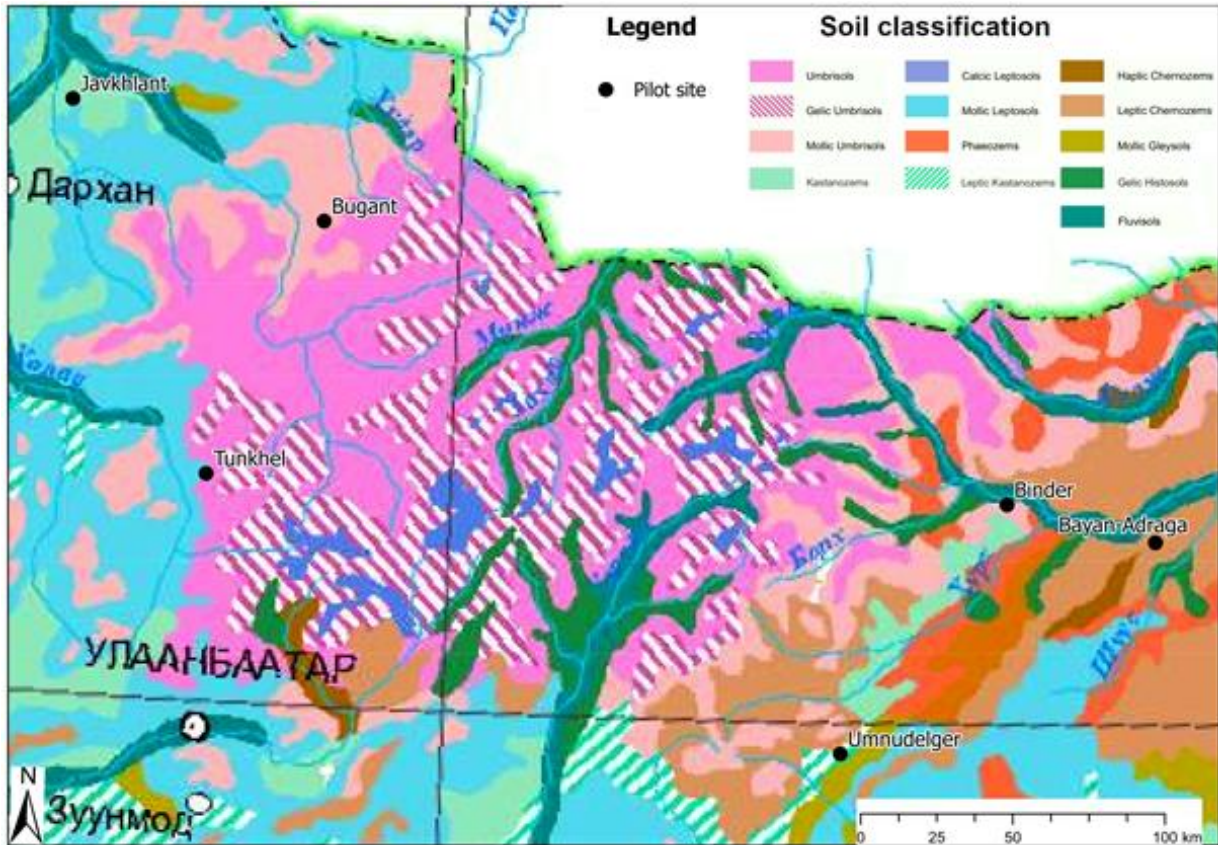


Figure 31. Location of the demonstration plots, on background of the georeferenced soil map according to FAO - WRB (Batkhishig, 2009).

Mycorrhiza survey

The mycorrhiza sampling was performed at six STREAM demonstration sites in June, July and September 2023. The samples were taken according to grid system (30×30 m) following the SPUN protocol (Figure 32). Nine core soil samples containing roots were taken from the depth of 10 cm. The roots were separated from the soil and placed in individual plastic bags (Figure 33). The soil matter from each of nine core samples was mixed and one composite soil sample was prepared for analysis of DNA. The soil samples were kept cool in the cool box using freezing bags. For DNA analysis, the soil samples were air dried and sieved to 2 mm and then a 50 g sample was frozen at -20 °C.

The roots were washed and placed on Petri dishes filled with clean tap water and stored at 4 °C. All ectomycorrhizal root tips that were turgescient and vital in appearance were divided into morphotypes following the method of Agerer (1997), using a ZEISS (Stemi 2000CS) dissecting microscope connected to an AxioCam ERc5s camera. A minimum of 100 ectomycorrhizal root

tips for each core sample were analyzed and determined. Final identification to genus or species level (if possible) was carried out by molecular sequencing and identification. The samples were then stored at $-20\text{ }^{\circ}\text{C}$ until DNA extraction.

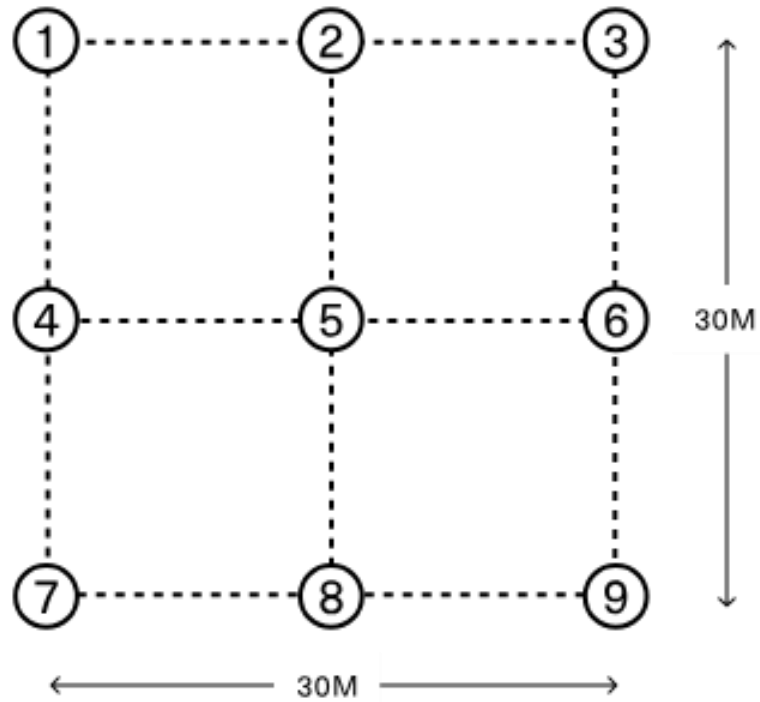


Figure 32. *Grid sampling design.*



Figure 33. *Mycorrhiza sampling. a = larch forest at Umnudelger, b = pine forest at Binder.*

2.3 Results

Evaluation of soil properties at the demonstration plots

Soils in the demonstration plots were classified into a few reference soil groups, mostly Phaeozems (Tunkhel, Umnudelger, Bugant, Javkhlant) and Cambisols (Binder) or Arenosols (Javkhlant, Binder, Bayan-Adarga), which mostly did not fit the expected soil classification from the available maps (c.f. Figure 31 and Table 4). Unlike Umbrisols, the soil pH was mostly slightly acidic or near neutral, with the exception of the Javkhlant site, where the soils were alkaline ($\text{pH}_{\text{water}} > 8.5$).

Phaeozems had the thick and dark mineral topsoil (i.e., Mollic horizon), which is rich in organic carbon (see chapter 2.4). Except the Javkhlant site, the soils had mostly loamy texture, with a relatively higher proportion of silt and clay particles, which enhanced the capacity of a soil to store organic carbon. Therefore, particularly high topsoil organic carbon stocks were found at the Tunkhel, Umnudelger, and Bugant sites. In contrast, Arenozems and the soils with high contents of sand particles (Javkhlant, Binder, and Bayan-Adarga) had relatively lower mineral-topsoil carbon stocks (Table 2), likely due to the lower ability of sand particles to bond with organic matter.

The lower OC:N (carbon to nitrogen ratio) at the Javkhlant site reflects a relatively higher availability of soil nitrogen, likely due to the intensive grazing by livestock. In contrast, higher OC:N at the Bugant, Binder, and Bayan-Adarga sites indicates a relatively lower availability of soil nitrogen in these soils, likely due to the higher proportion of Scots pine.

Soils at the Umnudelger site were mostly skeletal, with the high proportion of rock fragments. Soils at the other sites had mostly low (Binder, Tunkhel) to very low (Bugant, Javkhlant) contents of rock fragments, particularly in the topsoil layer, except the forest plots (I1 and I2) at the Binder site, where the rock contents ranged from 5 to 32% (by weight) due to the significant input of slope sediments in the upper part of a soil profile.

Table 4. *Main characteristics of the 0–30 cm mineral topsoil layer (mean ± standard deviation)*

Site ^a	RSG ^b	Texture ^c	OC stock (t/ha)	OC % (dg/kg)	OC:N	pH	Rocks % (dg/kg)
TU	PH	Loamic	122 ± 9	7.2 ± 0.9	11.9 ± 0.7	6.2 ± 0.5	4.2 ± 3.4
UM	PH	Loamic	83 ± 8	4.1 ± 0.6	11.6 ± 0.4	5.7 ± 0.3	20.9 ± 4.7
BU	PH	Loamic	79 ± 9	4.2 ± 0.6	14.6 ± 1.9	5.4 ± 0.1	0.5 ± 0.2
JA	PH/A R	Arenic	48 ± 18	1.6 ± 0.7	9.8 ± 0.5	8.7 ± 0.1	0.9 ± 0.1
BI	CA/A R	Loamic/ Arenic	39 ± 6	1.4 ± 0.3	15.3 ± 2.5	6.3 ± 0.5	8.2 ± 12.2
BA	AR	Arenic	37 ± 6	1.1 ± 0.2	14.7 ± 2.1	5.9 ± 0.2	1.2 ± 1.1

^a STREAM demonstration plots: TU = Tunkhel, UM = Umnudelger, BU = Bugant, JA = Javkhlant, BI = Binder, and BA = Bayan-Adarga

^b a reference soil group: AR= Arenozem, CM = Cambizem, PH = Phaeozem

^c a texture-class qualifier according to WRB (IUSS Working Group WRB 2022)

Mycorrhiza community

The mycorrhiza community from Binder and Bayan-Adarga were analyzed and various types of morphotypes were found (Figure 34, Figure 35). The most frequent were black and brown coloured ectomycorrhizas. Black melanised ectomycorrhizas are associated with harsh environments (Trappe, 1964) and are known to be highly drought tolerant (Herzog et al., 2013). This suggests that Binder and Bayan-Adarga are naturally dry sites which is in accordance with the results of monitoring and assessment of precipitation and soil moisture (see chapter 1) and the overall species composition of vegetation (see chapter 4) and the character of local ecosystems.

This finding should be taken into account in forest management measures and site use considering the high sensitivity of such ecosystems to large-scale changes. Dry sites have a limited potential for profitable and sustainable commercial use without responsible expert forestry supervision and management.

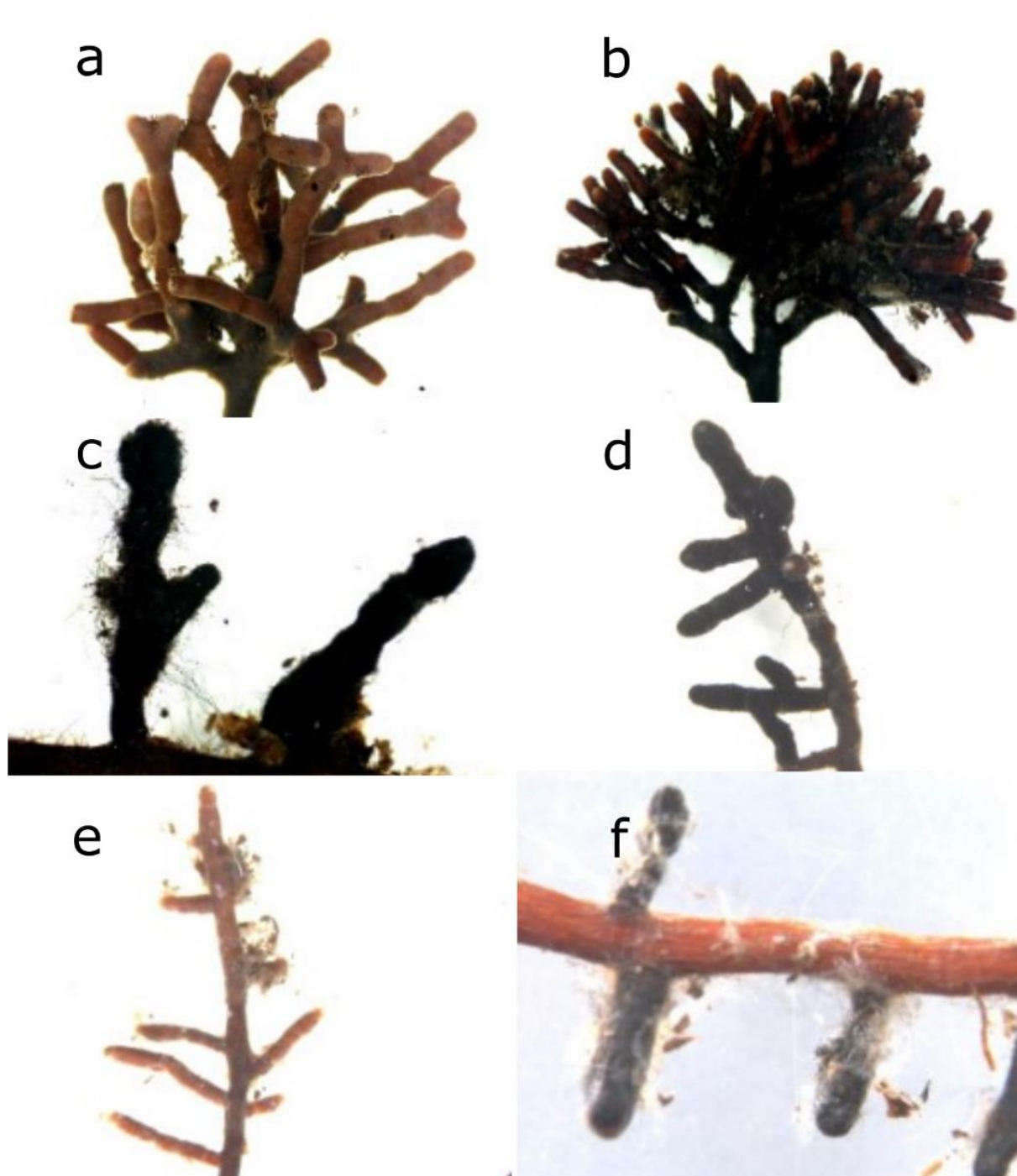


Figure 34. *Ectomycorrhizal morphotypes on Pinus sylvestris of pine forest at Binder, Khentii.*
a = branched (yellowish-brown), b = coralloid (brown), c = unbranched (black, hairy tips), d = unbranched (black), e = unbranched (yellow), f = unbranched, black (hairy tips).

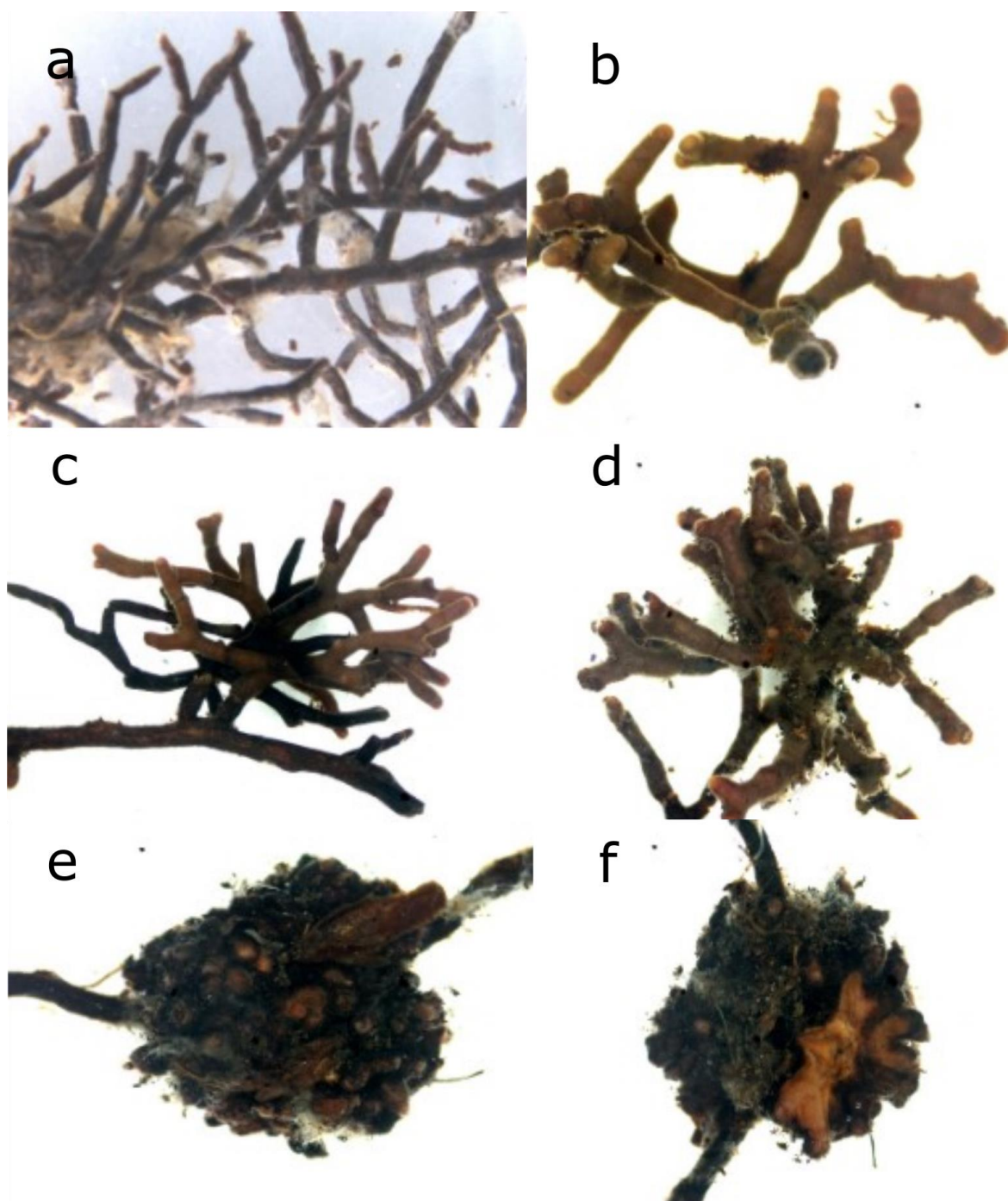


Figure 35. *Ectomycorrhizal morphotypes on Pinus sylvestris of pine forest at Bayan-Adarga, Khentii. a = unbranched (brown), b = dichotomously branched (yellow), c = branched (brown and black), dichotomously branched (yellowish-brown), e-f = Tuberculate ectomycorrhiza.*

Soil descriptions and classification

Table 5. *Soil profile in a forest at the Tunkhel site (17.06.2022).*

Plot	RSG	Prefix	Suffix	Exposition	Slope	Position
E1	PH	cm	lo	N	sloping	MS
Horizon code	Upper lim. (cm)	Lower lim. (cm)	Texture class	Munsell colour	Rock frags.	Notes
O	8	0			none	
Ah	0	22			none	Mollic
AB	22	32	L		none	
Bw	32	42	L		very few	Cambic
Bwf	42	62+	L		few	frozen



Figure 36. *Phaeozem at Tunkhel.*

Table 6. Soil profile in an unstocked forest at the Tunkhel site (28.06.2022).

Plot	RSG	Prefix	Suffix	Exposition	Slope	Position
E2	PH	cm	lo	N	sloping	MS
Horizon code	Upper lim. (cm)	Lower lim. (cm)	Texture class	Munsell colour	Rock frags.	Notes
O	6	0			none	
Ah	0	44		10YR3/1	very few	Mollic
Bw	44	60	CL	10YR4/2	few	
AB	60	70	CL	10YR3/3	few	
C	70	95+	SCL		common	



Figure 37. Phaeozem at Tunkhel.

Table 7. Soil profile in a forest at the Umnudelger site (29.06.2023).

Plot	RSG	Prefix	Suffix	Exposition	Slope	Position
E2	PH	cm	lo	N	sloping	MS
Horizon code	Upper lim. (cm)	Lower lim. (cm)	Texture class	Munsell colour	Rock frags.	Notes
O	1.5	0				
Ah	0	30	L	10YR3/4	common	Mollic
A/B	30	40	L		many	
Bw	40	70+	L	10YR4/4	abundant	Cambic



Figure 38. Phaeozem at Umnudelger.

Table 8. Soil profile on a steppe at the Umnudelger site (03.07.2022).

Plot	RSG	Prefix	Suffix	Exposition	Slope	Position
T-T7	PH	cm, sk	lo	N	Sloping	MS
Horizon code	Upper lim. (cm)	Lower lim. (cm)	Texture class	Munsell colour	Rock frags.	Notes
O	3.5	0				
Ah	0	30	L	10YR2/2	20%	Mollic
AB	30	40	L	10YR2/3	25%	
Bw	40	70+	L	10YR4/4	30%	Cambic



Figure 39. Phaeozem at Umnudelger.

Table 9. Soil profile in a forest at the Bugant site (26.06.2022).

Plot	RSG	Prefix	Suffix	Exposition	Slope	Position
CE7	PH	st, fv	ar, tu	W	flat	BO
Horizon code	Upper lim. (cm)	Lower lim. (cm)	Texture class	Munsell colour	Rock frags.	Notes
O	0	0				
Ah	0	28	SL	10YR3/3	SL	Mollic
B@	28	50	LS		SL	
ABb@	50	70	L		SL	
Bg@	70	85	LS			
Cg	85	90+	LS			



Figure 40. Phaeozem at Javkhlant.

Table 10. Soil profile on a steppe at the Javkhlant site (21.06.2022).

Plot	RSG	Prefix	Suffix	Exposition	Slope	Position
T1	PH	fv	lo	N	level	TS
Horizon code	Upper lim. (cm)	Lower lim. (cm)	Texture class	Munsell colour	Rock frags.	Notes
O	10	0			none	
Ah	0	32		10YR2/3		Mollic
Bw1	32	38				Fluvic
ABb	38	45				Fluvic
Bw2	45	72		CL		Cambic
Bf	72	83+		CL		ice



Figure 41. Arenozem at Javkhlant.

Table 11. *Soil profile in a forest at the Binder site (01.07.2023).*

Plot	RSG	Prefix	Suffix	Exposition	Slope	Position
CE1	AR	eu	oh	NE	sloping	TS
Horizon code	Upper lim. (cm)	Lower lim. (cm)	Texture class	Munsell colour	Rock frags.	Notes
O	0.5	0				
Ah	0	2		10YR4/2	none	
B1	2	50	LS	10YR4/3		
B2	50	68	LS	10YR4/4		
B/C	68	95+	S	2.5Y5/3		



Figure 42. *Cambizem at Binder.*

Table 12. Soil profile on a forest-steppe at the Binder site (06.07.2022).

Plot	RSG	Prefix	Suffix	Exposition	Slope	Position
T1	CM	eu	lo, oh	NE	sloping	LS
Horizon code	Upper lim. (cm)	Lower lim. (cm)	Texture class	Munsell colour	Rock frags.	Notes
O	2	0				
A	0	8	SL		none	
A/B	8	15	SL		rare	charcoal
B	15	40	SL	10YR3/4	rare	Cambic
BC	40	70+	LS	10YR4/3	none	



Figure 43. Arenozem at Binder.

Table 13. Soil profile in a forest at the Bayan-Adarga site (02.07.2023).

Plot	RSG	Prefix	Suffix	Exposition	Slope	Position
I1	AR	eu	oh	NW	level	BO
Horizon code	Upper lim. (cm)	Lower lim. (cm)	Texture class	Munsell colour	Rock frags.	Notes
O	2	0				
A	0	20	LS	10YR3/3		
AB	20	40	LS	10YR3/4		
B	40	48	MS	7.5YR4/4	none	
BC	48	73	MS	7.5YR5/4		
C	73	90+	MS	7.5YR6/4		



Figure 44. Arenosol at Bayan-Adarga.

Table 14. Soil profile on a forest-steppe at the Bayan-Adarga site (08.07.2022).

Plot	RSG	Prefix	Suffix	Exposition	Slope	Position
CE1	AR	eu	oh	NW	level	BO
Horizon code	Upper lim. (cm)	Lower lim. (cm)	Texture class	Munsell colour	Rock frags.	Notes
O	2	0				
H/A	0	3		10YR3/2		
A	3	30	LS	10YR3/3		
B	30	55	LS	7.5YR5/4	none	
C	55	80+	MS	10YR6/4		



Figure 45. Arenosol at Bayan-Adarga.

2.4 Summary and recommendations

Sandy soils in the arid and semi-arid lands have been traditionally used for extensive (nomadic) grazing. However, the low coherence of soil particles, low nutrient storage capacity, and high sensitivity to erosion make these soils highly prone to degradation. Uncontrolled grazing can easily destabilize the soil cover, reverting the loose sand back to shifting dunes (IUSS Working Group WRB, 2015), such as those at the Javkhlant site. If water is not a limit to tree growth, forestry is the most promising conservation management for sandy soils, with a strong emphasis on the increasing need for soil protection and water conservation, as well as other ecosystem services required in a modern society (wood production, biodiversity, and recreation). *Pinus sylvestris* is the tree species well adapted to low mineral nutrition and low water-holding capacity of the soils. Any admixture of broadleaves with the rich and easily degradable litter such as *Populus tremula* can enhance nutrient cycling at the site and serve as the important soil amelioration species in production forests, such as those at the Binder and Bayan-Adarga sites.

Phaeozems represent soils of relatively wet, tall-grass steppe and forest regions. The soils are much like Chernozems and Kastanozems, but less rich in secondary carbonates. Phaeozems have the dark topsoil rich in organic matter and, unlike Umbrisols, provide a higher nutritional value (base saturation $\geq 50\%$ in the upper metre of the soil), which favours the overall high fertility and productivity of these soils (IUSS Working Group WRB, 2015). However, the topsoil layer can be seriously endangered by wind erosion when dry, and by water erosion during periods of seasonal wetting. Therefore, sustainable management of these soils should aim to protect the fertile topsoil layer from degradation and avoid harvesting in the wet vegetation season to prevent the risk of soil compaction by wheel vehicles, particularly on soils with the higher proportion of clay and silt particles, and with the low content of rock fragments, such as the Tunkhel and Bugant sites.

2.5 Acknowledgment

Thanks to all the Mongolian and Czech students that intensively assisted in soil sampling, sample preparation, and laboratory analysis, particularly Duulal Erdene, Namuuna Shinebayar, Angarag Zorigtbayar, Michal Mičulek and Amartuvshin Mashbat. We are grateful to the STREAM project team for establishing the experimental plots and conducting the project. Finally, we would like to thank our colleagues from MENDELU, namely Professor Douglas

Godbold, Ladislav Holík, Katka Havlíčková, and Jiří Volánek, for their support and professional work on soil preparation and analysis.

2.6 References

- Herzog, C., Peter, M., Pritsch, K., Günthardt-Goerg, M. S., & Egli, S. (2013). *Drought and air warming affects abundance and exoenzyme profiles of Cenococcum geophilum associated with Quercus robur, Q. petraea and Q. pubescens*. *Plant Biology*, 15, 230–237.
- IUSS Working Group WRB. (2015). *World Reference Base for Soil Resources 2014*. FAO.
- IUSS Working Group WRB. (2022). *World Reference Base for Soil Resources: International soil classification system for naming soils and creating legends for soil maps*. International Union of Soil Sciences.
- Rowley, M. C., Grand, S., & Verrecchia, É. P. (2018). Calcium-mediated stabilisation of soil organic carbon. *Biogeochemistry*, 137(1–2), 27–49. <https://doi.org/10.1007/s10533-017-0410-1>
- Trappe, J. M. (1964). *Mycorrhizal hosts and distribution of Cenococcum graniforme*. *Lloydia*, 27, 100–106.

**PEDOANTHRACOLOGICAL
SURVEY**

3 PEDOANTHROLOGICAL SURVEY: REFLECTION OF HISTORICAL FOREST DEVELOPMENT

Pavel Peška¹ and Jan Novák²

¹ Mendel University in Brno, Zemědělská 1, 613 00, Brno, Czech Republic

² Charles University, Opletalova 38, 110 00 Staré Město, Praha, Czech Republic

3.1 Introduction

Against the backdrop of climate change the knowledge of forest ecosystem evolution helps us to offer appropriate management leading to climate resilient forests. One of the methods to capture the long-term dynamics of forest ecosystems is analyses of macro-residues (pollen, charcoal) of native forest stands conserved in the soils (Figure 46).



Figure 46. Charcoal accumulated in soil.

Forest fires are a common phenomenon in Mongolian forests and in the taiga in general (Mühlenberg, 2012), and their consequences remain preserved in the soil in the form of charcoal macro-residues (Figure 47) for thousands of years (Ludemann, 2004). These charcoal residues are preserved in different layers of the soil profile and their microscopic identification allows the identification of species or genera of tree species (Feiss, 2017). This identification is based

on the ability of wood to retain its microscopic structure despite charring. It is also possible to date samples using the radiocarbon method, which provides a chronological series that can be linked to historical climatic data. The mass of preserved charcoal (anthracomass) then provides information on the frequency and intensity of historical forest fires (Davasse, 2008; Robin, 2013).

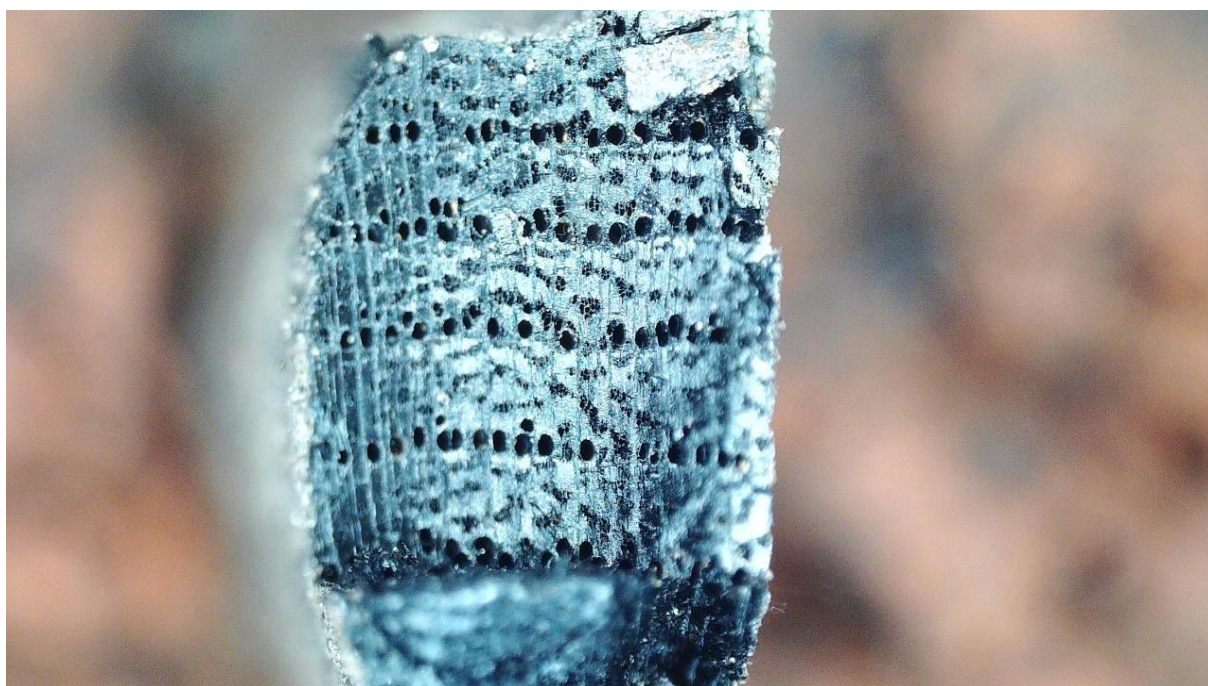


Figure 47. *Cross section of *Ulmus pumilla* charcoal piece.*

The results of this analysis have important applications in forest management and development planning. They can also be applied to the management of protected areas, where we often look for inspiration in natural or near-natural species composition. The knowledge gained through this method can provide valuable information for sustainable forest management and the protection of forest ecosystems in response to current and future challenges.

3.2 Methods

Samples were systematically collected in the vicinity of five STREAM demonstration plots, namely at Tunkhel, Javkhant, Bugant, Binder, and Bayan-Adarga sites. The soil profiles affected by pedoturbation, landslides, flood accumulations, and human activities were excluded. The plots where the slope gradient exceeds 10° were also excluded to eliminate the potential misinterpretation caused by diluvial processes (Novák, 2022).

The samples were taken from 10 cm wide layers from soil surface to parent rock or to the one metre depth. From each layer, one composite soil sample (1 m², ±10 kg) was collected. The wet sieving method was used (Figure 48, Figure 49, Figure 50) to separate charcoal from mineral soil (Carcaillet and Thinon, 1996; Robin et al., 2012). Charcoal pieces bigger than 1 mm were subsequently separated. The pieces smaller than 1 mm cannot be taxonomically classified (Robin, 2013).



Figure 48. *Charcoal separation using the wet sieving method.*



Figure 49. *Result of primary separation of the collected soil sample.*



Figure 50. Drying of samples collected at Bayan Adarga.

From each soil layer, 100 individual charcoal fragments were collected and microscopically determined in the laboratory of MENDELU (Talon, 2010). In the case that 100 charcoal fragments were not found in the layer, all the fragments were determined (Talon, 2010). The determination was carried out using the Olympus SZ 61 microscope with accessories (magnification 250x). In the case of very small fragments, the Keyence VHX - 5000 microscope, which allows magnification of up to 1000x, was used (Figure 51, Figure 52). The observation of microanatomical characteristics was crucial for the determination (Schweingruber, 1978). The genera *Larix sp.* and *Picea sp.* have very similar microanatomical structures, therefore, in the interpretation of the results, the two genera were merged into one common group (Saulnier et al., 2015). The anthracomass amounts for each genera/group (*Larix sp.*, *Pinus sp.*) were subsequently weighed. On the basis of this weight, the representation of woody species in each sampled layer was derived (Novák et al., 2022).



Figure 51. *Cross section of Pinus sylvestris charcoal.*

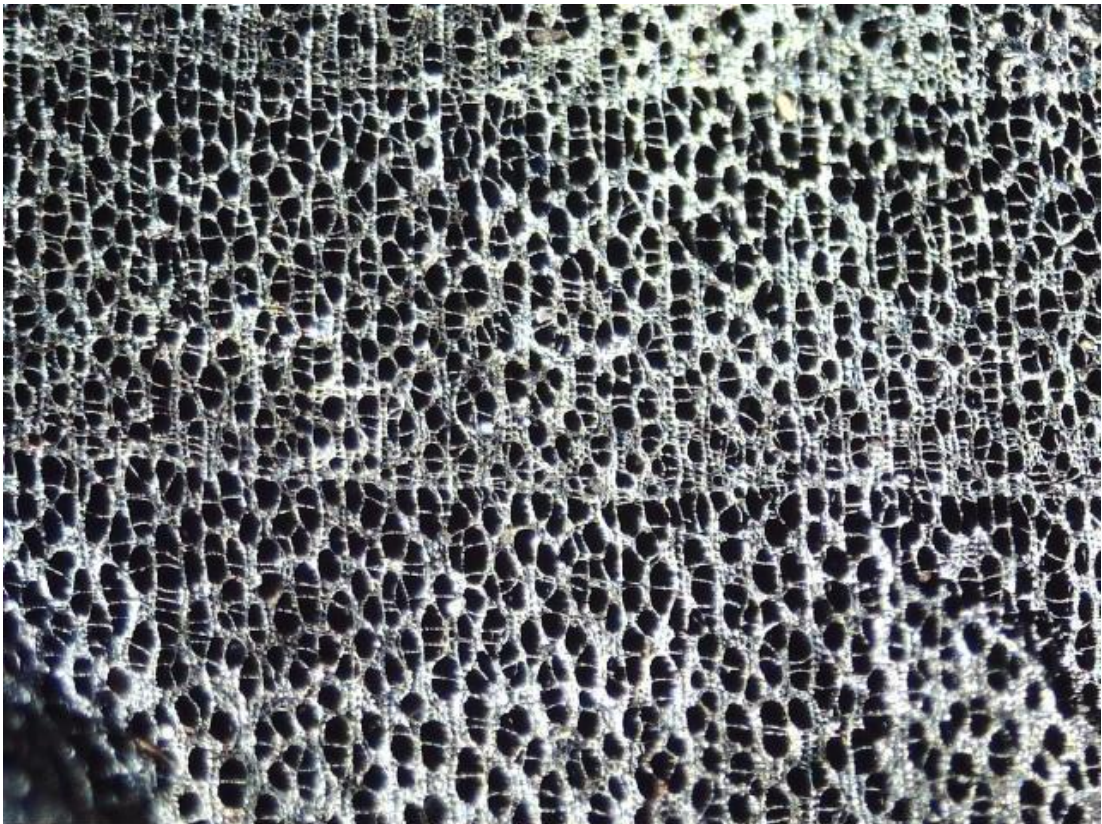


Figure 52. *Cross section of Populus tremula charcoal.*

Amount of anthracomass

The amount of separated anthracomass illustrates the intensity of a forest fire in each layer. However, on the basis of the amount of anthracnose, it is not possible to simply interpret the intensity of the forest fire that took place to the extent that it was a large-scale disturbance event, or whether it was only a small (Figure 53), sublevel forest fire that may not have significantly affected the upper storey of the stands at the time, causing large-scale deforestation (Talon, 2011). Although charcoal is very stable and is retained in the soil for thousands of years, it is also subject to decomposition and is broken down by various influences (e.g. root penetration, soil freezing, zoedaphone) and its quantity in the soil gradually decreases with increasing time (Bryanin et. at., 2018).



Figure 53. Pedoanthracological sampling at Bugant.

Radiocarbon dating

The age of individual charcoal fragments was determined by radiocarbon analysis, which was carried out by the radiocarbon laboratory of the Institute of Nuclear Physics of the Academy of Science of the Czech Republic (Kučera, 2022). The age determination was derived on the basis of the decay stage of radioactive carbon ^{14}C (Stuiver, 1977). The enclosed results of radiocarbon analyses are reported in BP format (i.e., "Before Present", by consensus considered to be the reference year 1950) (Bárta, 2007).

3.3 Results

Tunkhel

The result of the analysis of the Tunkhel site shows that there is a long-term stable representation of light taiga species (Figure 54; left side). The main factor of forest development at Tunkhel the predominant presence of coniferous species. The proportion of coniferous species reaches up to 70% of the total stand composition. However, in the youngest layer of the soil profile (0–10 cm), an increased representation of broadleaved trees was found, suggesting a possible impact of human activities on the change in the species composition of the forest. This trend is confirmed by the significant decrease in the abundance of *Larix sp.* in this layer, which may be due to harvesting of this tree species.

Analysis of the amount of anthracomass suggests a gradual increase in the intensity of forest fires over time. Figure 54 (right side) shows that human activity is having an increasing impact on the study site, which is reflected in higher amounts of anthracomass in the younger soil layers. A comparison of the amount of anthracomass with the species composition of the forest cover showed no significant correlation that would allow further conclusions to be drawn. No radiocarbon analyses have yet been done for this site.

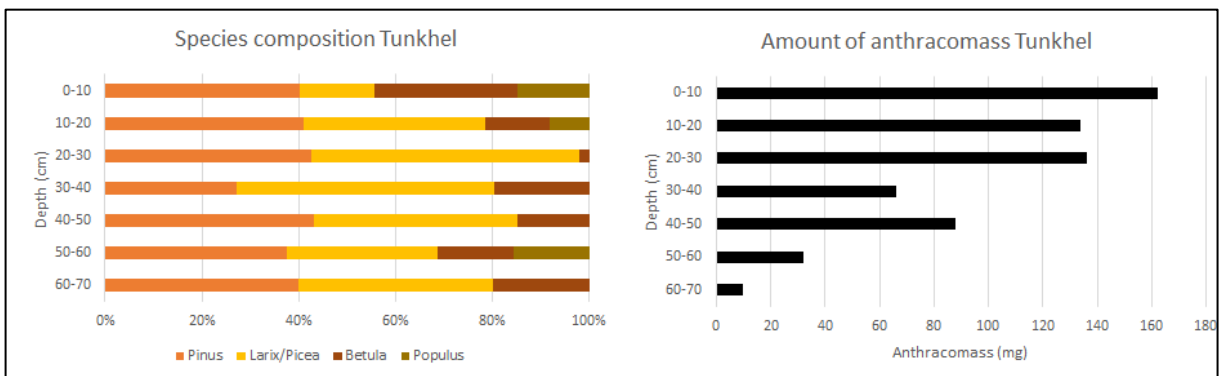


Figure 54. Results of the pedoanthracological analysis from the Tunkhel site.

Javkhlant

The results from the Javkhlant indicate the dynamic evolution of the area over time, which is reflected in the variability of species composition (Figure 55; left side). An interesting phenomenon is the representation of *Betula sp.* in soil layers at 20–30 cm and 30–40 cm depth. This indicates the probable existence of a more humid climate in the past, which allowed the distribution of this species. On the other hand, in the youngest layer (0–10 cm), charcoal pieces of *Caragana* and *Ulmus* species were detected, suggesting recent transition of natural ecosystem composition to species adapted to a drier climate. The recorded occurrence of *Pinus* species is relatively continuous. However, it is not possible to infer contemporary conditions based on the abundance of this tree species, as it is a species with a large ecological amplitude.

Analysis of anthracomass abundance indicates the alternation of forest-steppe and steppe periods in the area (Figure 55; right side). This hypothesis is supported by the low abundance or even complete absence of anthracomass. Radiocarbon dating of the carbon sample from this site determined its age at approximately 1000 years BP. This period corresponds to the beginning of the Medieval Climatic Optimum (Grove, 2004), characterized by a warm and stable climate (Sun, 2012). This favourable climatic epoch probably contributed to the development and expansion of the Mongol Empire in the following centuries.

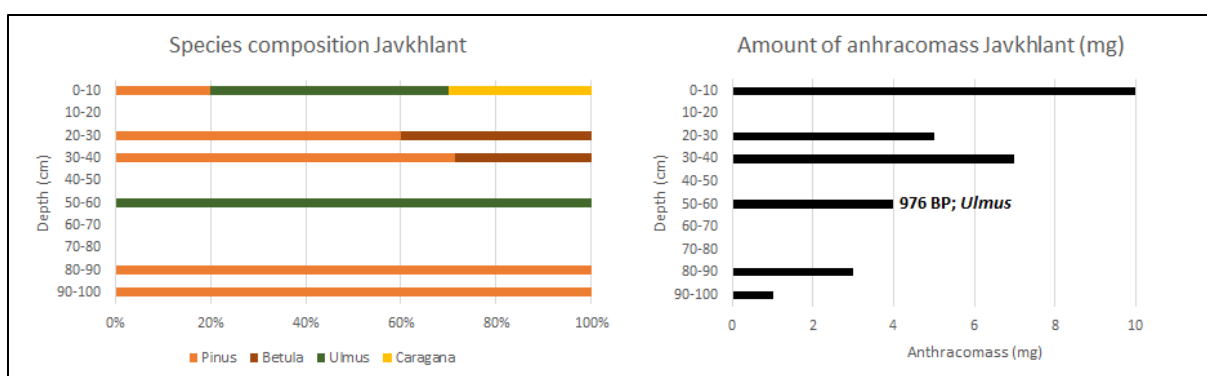


Figure 55. Results of the pedoanthracological analysis from Javkhlant.

Bugant

Research from the Bugant site shows long-term continuity in the species composition of the forest stand, but with some variability in the representation of individual species over time (Figure 56; left side). Two periods of fluctuating dominance between coniferous and deciduous

species were recorded. The recent dominance of broadleaf species is likely associated with a large-scale fire that occurred on the site about 212 years BP. This fire most likely destroyed almost pure coniferous forest and after this event, the site includes deciduous pioneer species that may have a successional, pioneer character, that still reverberates in the species composition today.

The analysis of anthracomass abundance indicates relative stability of the forest ecosystem, except for the 20–30 cm layer, where increased anthracomass abundance was observed, probably due to a large-scale fire (Figure 56; right side). Radiocarbon dating of the charcoal pieces showed a recent age in the 10–20 cm layer (approximately 200 years BP) and very old charcoal in the 40–50 cm layer (over 7000 years BP), which corresponds to the Holocene Climatic Optimum during which forest expansion occurred in the Central Asian region (An, 2008). The determined age of this charcoal is not chronologically related to the other dated samples and is likely a shift within the soil profile by pedoturbation. Dating of carbon in the 60–70 cm layer showed an age of 3735 years BP, which corresponds to the turn of two climatic periods – the ending Epi-Atlantic and the beginning of the drier and precipitation-poorer Subboreal.

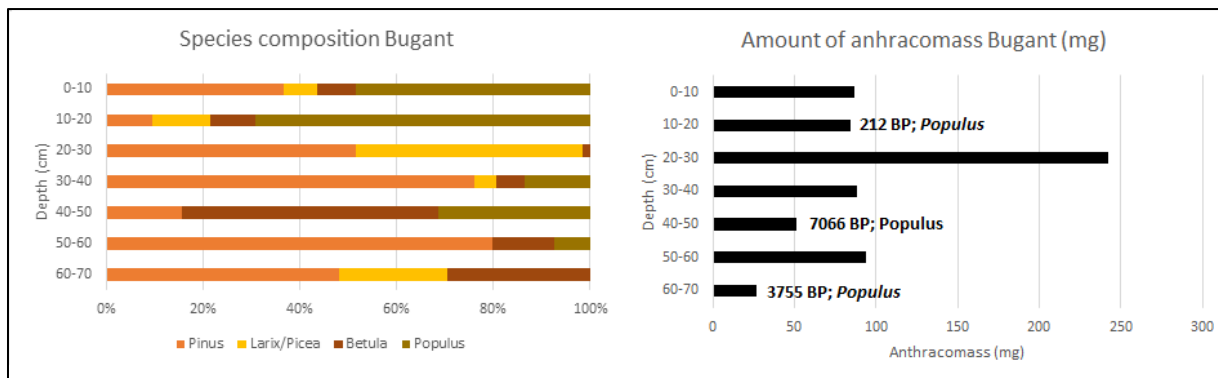


Figure 56. Results of the pedoanthracological analysis from Bugant.

Binder

Two pedoanthracological samplings were carried out at the Binder site to compare the development of two different sites in this area. One site was placed on a demonstration plot, while the other site was moved about 700 m east into the current steppe. This experiment was designed to evaluate whether the evolution of the two sites differed or whether the two sites showed a similar long-term trend.

This experiment allows for a deeper understanding of the vegetation dynamics in the Binder area and determination of whether it is more of a stable forest ecosystem or a steppe ecosystem. By comparison of the pedoanthracological results from both sites, the differences in species composition and the history of change at these sites are shown.

Binder – forest

The results from this forest site suggest that the last three sampled layers show establishment of light taiga species (Figure 57; left side). In the deeper layers, a more pronounced occurrence of *Caragana* species was observed, suggesting possible: i) historical human influence and likely grazing that could be limiting for forest development or ii) colonization of newly developed habitat on accumulated sands. This hypothesis is supported by the decrease in the amount of anthracomass separated with increasing depth of sampling (Figure 57; right side). The species composition graph at this site shows a long-term dominance of *Pinus* species, with an admixture of *Larix* and *Betula* species (Figure 57; left side).

In terms of the amount of separated anthracomass, there is a significant increase in charcoal in the three topmost layers at this site (Figure 57; right side). The amount of anthracomass decreases with decreasing depth, which could indicate that the forest stands at that time were very sparse due to grazing and were not accumulating enough woody material to burn or there was not enough wood because of early stage of habitat colonization. However, radiocarbon results are not yet available at this site to help better interpret the data. A large amount of charcoal was separated at this site, therefore, the graph shows the anthracnose mass on a logarithmic scale.

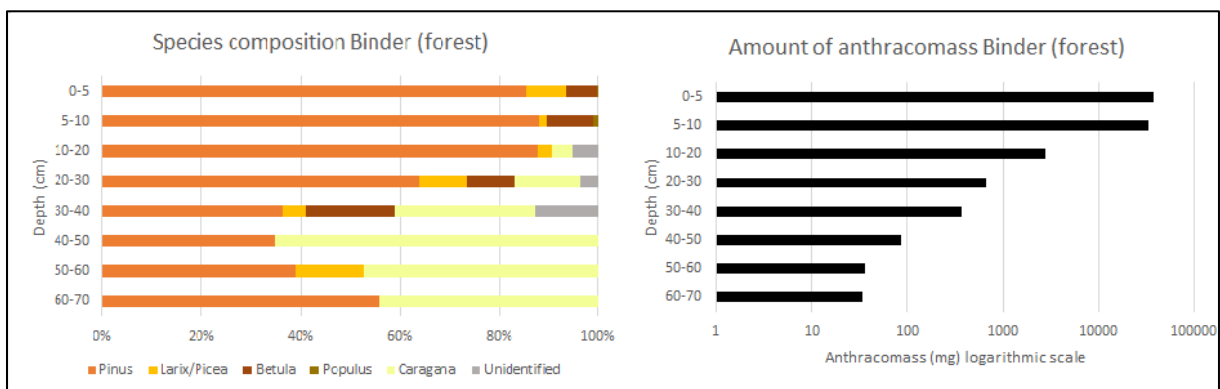


Figure 57. Results of the pedoanthracological analysis from Binder (forest).

Binder – steppe

The results of charcoal determination from the steppe site (Figure 58; left side) show that the reconstructed species composition contains at least partly the same species as the forest comparison plot (Figure 57; left side), but these results are based on very few charcoal determinations (Figure 58; right side). At this steppe site, a total of 10 charcoal specimens were determined in all sampling layers, with a total mass of 14 mg. These results may indicate heavy and continuous human influence in the steppe, or, more likely, that this is a stable steppe site.

The amount of anthracomass present in each layer (Figure 58; right side) is about several orders of magnitude lower than in the nearby forest control area (Figure 57; right side). In the case of the steppe site, only units of mg occur in the individual layers examined. A possible explanation for how these few pieces of charcoal got here is the influence of wind, which may have carried the small charcoal pieces and transported them to the present steppe. It is not possible to select the charcoal pieces from this steppe area and send them for radiocarbon analysis because they do not meet the minimum dimensions for this type of analysis.

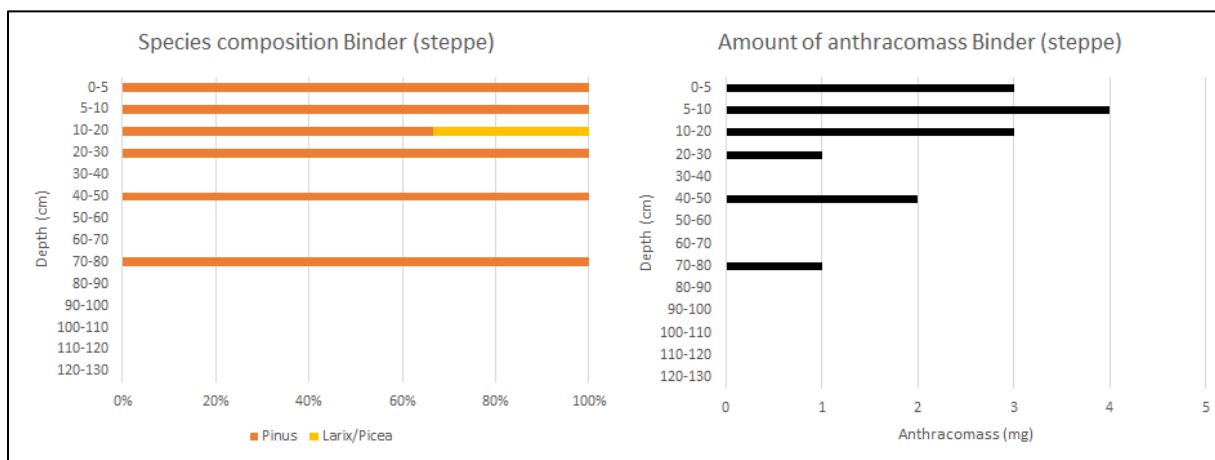


Figure 58. Results of the pedoanthracological analysis from Binder (steppe).

Bayan-Adarga

At this site, the sampling took place on the broader edge of a sparse pine stand, which gradually transitioned into a steppe. The results of the pedoanthracological analyses from this site show the long-term occurrence and dominance of *Pinus* species, with an admixture of mainly *Caragana* species and occasional, small representation of *Betula* species (Figure 59; left side).

The high abundance of *Caragana* species in the reconstructed species spectrum in recent history suggests that this site served as a long-standing buffer zone between the open forest and the steppe.

A similar trend can be observed in the results of the amount of anthracomass separated, which reaches the highest values in the topmost layers (Figure 59; right side). Therefore, it can be assumed that in historical epochs, there was not so much wood mass in this area that remained preserved in the soil in the form of charcoal. In other words, it is likely that there was a gradual spread of forest towards the steppe at this site. The results of the radiocarbon method are not yet available from this site to facilitate the interpretation of the data obtained.

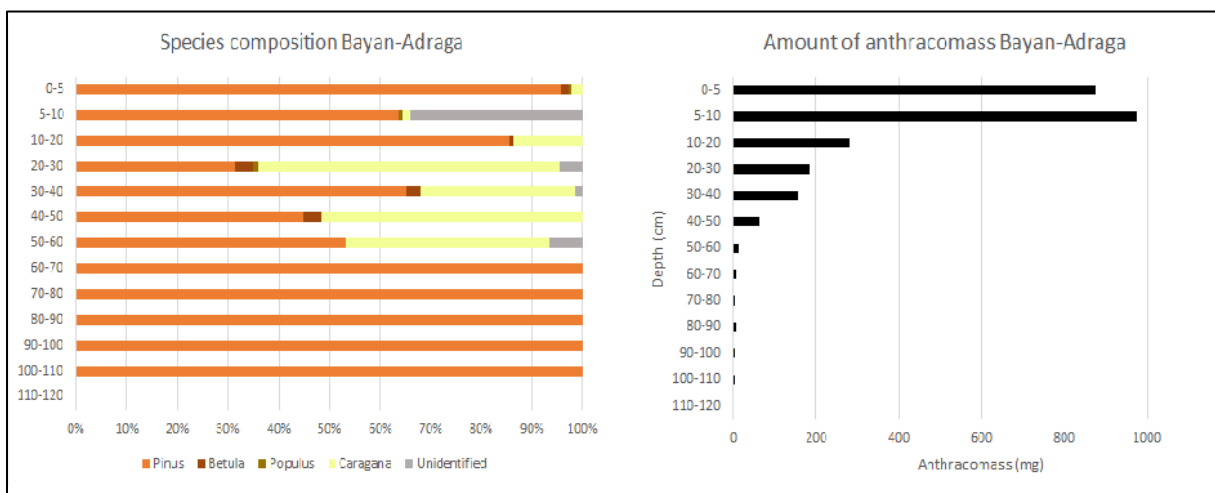


Figure 59. Results of the pedoanthracological analysis from the Bayan-Adarga site.

3.4 Summary

Within the framework of the STREAM project, a total of 6 soil profiles at the sites of Tunkhel, Javkhlant, Bugant, Binder and Bayan-Adarga were evaluated by pedoanthracological analysis. A total of more than 1700 charcoal pieces were identified to reconstruct the tree species composition. The selected charcoal fragments were sent for evaluation by the radiocarbon method to determine their age and to place them in historical climatic periods.

The results show that most of the sites currently have species composition similar to natural developmental potential. In the long-term historical development, we can observe fluctuations in the representation of individual species, which is probably the result of anthropogenic influence. At the Binder and Bayan-Adarga sites, it can be concluded that there is more of

a reduction in human influence on forests at present or improving environmental conditions in favour of forest growth. On the other hand, at the Bugant and Javkhlant sites, it can be assumed that the recent dynamic changes in species composition are due to human activities. This may not be a targeted impact on the study sites, it may be a secondary effect of grazing, browsing and forest exploitation. Based on the analyses carried out, the Tunkhel site appears to be stable in the long term in terms of species composition and representation of individual tree species.

3.5 Management recommendations

- 1) Based on previous research, it is advisable to prefer management with tree species that have been present throughout the Holocene in the study areas. This adaptation to historical climatic conditions indicates their potential for future environmental change.
- 2) Given the long-term natural existence of fires in the Mongolian environment, it is important to consider the role of deciduous tree species in minimizing their impact. These species have the ability to regulate and inhibit the spread of fire, which can contribute to the protection of forest ecosystems.
- 3) The sites of Tunkhel, Bugant and Binder (forests) have demonstrated the continuous existence of forest throughout the Holocene. This long-term presence of forest cover suggests the natural regeneration potential of these areas and supports a natural regeneration strategy for management interventions.
- 4) In contrast, the Javkhlant and Binder (steppe) sites appear to be forest-steppe to steppe areas where continuity of forest cover has not been established. When planning afforestation of these sites, it is therefore necessary to select tree species appropriate to these extreme conditions and to adapt the choice of species composition accordingly. However, first, it is necessary to think about whether to plant forests there at all, because they do not naturally belong there. Plantings in the number of several sparsely distributed individuals may be suitable.
- 5) It is important to note that the results of this report are based on a limited number of soil profiles from each site. For this reason, these results cannot be clearly applied to the wider region, and it is recommended to use them only as indicative guidelines for the specific surroundings of the study sites.

3.6 References

- An Cheng-Bang, A. C., Chen Fa-Hu, C. F., & Barton, L. (2008). *Holocene environmental changes in Mongolia: a review*.
- Barta, P., & Štolc, S. (2007). HBCO Correction: Its Impact on Archaeological Absolute Dating. *Radiocarbon*, 49(2), 465–472. <https://doi.org/10.1017/S0033822200042399>
- Bryanin, S., Abramova, E., & Makoto, K. (2018). Fire-derived charcoal might promote fine root decomposition in boreal forests. *Soil Biology and Biochemistry*, 116, 1–3.
- Carcaillet, C., & Thinon, M. (1996). Pedoanthracological contribution to the study of the evolution of the upper treeline in the Maurienne Valley (North French Alps): methodology and preliminary data. *Review of Palaeobotany and Palynology*, 91(1–4), 399–416.
- Feiss, T., Horen, H., Brasseur, B., Buridant, J., Gallet-Moron, E., & Decocq, G. (2017). Historical ecology of lowland forests: Does pedoanthracology support historical and archaeological data? *Quaternary International*, 457, 99–112.
- Grove, J. M. (2019). *The little ice age*. Routledge.
- Kučera, J., Maxeiner, S., & Müller, A. (2021). *A new AMS facility MILEA at the Nuclear Institute in Řež, Czech Republic*.
- Ludemann, T., Michiels, H.-G., & Nölken, W. (2004). Spatial patterns of past wood exploitation, natural wood supply and growth conditions: indications of natural tree species distribution by anthracological studies of charcoal-burning remains. *European Journal of Forest Research*, 123, 283–292.
- Mühlenberg, M., Appelfelder, J., Hoffmann, H., Ayush, E., & Wilson, K. J. (2012). Structure of the montane taiga forests of West Khentii, Northern Mongolia. *Journal of Forest Science*, 58(2), 45–56.
- Novák, J., Kusbach, A., Šebesta, J., & Rogers, P. C. (2022). Soil macrocharcoals reveal millennial-scale stability at the Pando aspen clonal colony, Utah, USA. *Forest Ecology and Management*, 521, 120436.
- Robin, V., Knapp, H., Bork, H.-R., & Nelle, O. (2013). Complementary use of pedoanthracology and peat macro-charcoal analysis for fire history assessment: illustration from Central Germany. *Quaternary International*, 289, 78–87.
- Robin, V., Rickert, B.-H., Nadeau, M.-J., & Nelle, O. (2012). Assessing Holocene vegetation and fire history by a multiproxy approach: The case of Stodthagen Forest (northern Germany). *The Holocene*, 22(3), 337–346. <https://doi.org/10.1177/0959683611423687>
- Robin, V., Talon, B., & Nelle, O. (2013). Pedoanthracological contribution to forest naturalness assessment. *Quaternary International*, 289, 5–15.
- Saulnier, M., Talon, B., & Edouard, J.-L. (2015). New pedoanthracological data for the long-term history of forest species at mid-high altitudes in the Queyras Valley (Inner Alps). *Quaternary International*, 366, 15–24.

- Schweingruber, F. H. (1978). Mikroskopische Holzanatomie (microscopic wood anatomy). *Eidgenössische Anstalt Für Das Forstliche Versuchswesen, Birmensdorf, Switzerland*.
- Sun, J (2012). Holocene climate in the Mongolian Plateau: a quantitative synthesis of paleoclimate data and climate simulations. *Quaternary International*. 278.
- Stuiver, M., & Polach, H. A. (1977). Discussion Reporting of ^{14}C Data. *Radiocarbon*, 19(3), 355–363. <https://doi.org/10.1017/S0033822200003672>
- Talon, B. (2010). Reconstruction of Holocene high-altitude vegetation cover in the French southern Alps: evidence from soil charcoal. *The Holocene*, 20(1), 35–44.

BOTANICAL SURVEY

4 BOTANICAL SURVEY

Jan Šebesta¹

¹ *Mendel University in Brno, Zemědělská 1, 613 00, Brno, Czech Republic*

4.1 Introduction

Vegetation is a major component of forest ecosystems; the herb layer averages more than 80% of the total plant species richness of a forest. The composition, diversity, and structure of vegetation are important factors for assessing the biological diversity of forest ecosystems. The central continental position of Mongolia, far from oceanic influences, defines its climate and under such conditions, the spectrum of natural climate zones is rather uniform, typically with climate extremes. The flora of Mongolia reflects these conditions and is comprised of native species of different origins including boreal, steppe, desert and mountainous elements of vegetation (Gunin et al., 1999). Overall, the species richness of vascular plants in Mongolia is not particularly high compared to other countries in Asia. The updated checklist of Mongolian flora comprises 3 041 native vascular plant taxa from 653 genera and 111 families (Baasanmunkh et al., 2022). Mongolia has the world's largest intact grasslands concerning its biodiversity, which has great importance for the preservation of native vascular plants.

While grassland vegetation is rather well explored, only few studies were focusing on forest flora. For example, Bazarrachaa et al. (2022) who worked in Bogd Khan Mountain, stated that the number of species recorded in the forest area is more than 50% of the total vascular flora recorded (species pool) in the area of their interest. In temperate and boreal forests, the tree layer frequently consists of a low number of tree species, while herb layer is a major component of forest vegetation diversity. It averages more than 80% of the total plant species richness (Gilliam, 2007). The study of forests as ecological communities stresses their species composition, with a focus on the number of species and their relative importance, two variables that determine species diversity. The composition, diversity, and structure of vegetation are key factors for assessing the biological diversity of forest ecosystems. Generally, boreal and temperate forests contain fewer vascular plant species per small area than grasslands occurring in the same region (Chytrý et al., 2012). This is probably why patterns of maximum species richness in boreal and temperate forests have not received much attention and remain poorly

studied. However, Chytrý et al. (2012) discovered forests with a rich herb layer in southern Siberia.

4.2 Methods

The field of vegetation science, which seeks to understand the patterns and processes of plant communities, has developed a diverse methodology to study vegetation dynamics in the field. The numerous field methods employed by vegetation scientists typically vary with vegetation type. For example, methods used in grasslands generally contrast sharply with those used in forests because of the differences in the physiognomy (i.e., size and height) of the dominant vegetation. Similarly, in studying the highly stratified (i.e., layered) vegetation of forest communities, scientists typically use different methods in the same study, with plots of varying size and shape to accommodate. Trees often are sampled by tallying species within relatively large plots (e.g., 400, 500, or even 1000 m²) of different shapes, including squares, rectangles, and circles; herbaceous layer species are often sampled by estimating density or cover within much smaller plots (most commonly 1 m²) of equally varying shapes. Other sampling methods avoid plots altogether, using line transects of varying lengths.

Thus, the study of vegetation at selected sites with different environmental conditions, under different treatments and different level of land-use will provide information on changes in other forest ecosystem variables (soil, microclimate, etc.). Ground vegetation is here defined as all terrestrial vascular plants: ferns, herbs, shrubs and trees.

Vegetation sampling was conducted in the summer of 2022 and 2023. Sampling plots were established at fenced and unfenced plots of all the sites, optionally with control to reflect the general design. All sample plots were maintained by GPS coordinates and layout. To sample forest vegetation, 15×15 m plots were used, moreover, one-three 1×1 m subplots were located in most of the big plots. In each plot, the total cover of herb, shrub and tree layers and the cover of each plant species within each layer were recorded, using the Braun-Blanquet abundance and dominance scale. Vertical layers of trees, shrubs and herbs were distinguished: tree layer – woody species higher than 5 m, shrub layer – woody species from 1.3 to 5 m, herb layer – woody saplings, considered as wood species regeneration, and herbs up to 1.3 m. Species were identified in the field when possible and samples of unknown species were collected and identified in the laboratory. The nomenclature of vascular plants follows Grubov et al. (2008).

4.3 Results

The pattern of vegetation highly depends on the type of forests and site conditions. Generally, hemiboreal coniferous forests of *Pinus sylvestris* and *Larix sibirica* predominate in the summit areas. However, birch (*Betula platyphylla*) and aspen (*Populus tremula*) forests often occur at previously disturbed sites, but they can also form natural forests in some places. The general macroclimatic pattern is modified by a local terrain topography causing substantial changes at a mesoclimatic level. This phenomenon of a local climate is distinctive on steep south-facing slopes with enormous temperature differences contrary to shady north-facing slopes with a low solar radiation. Besides, highlands of Bayan-Adarga and Umnudelger site gradually changes to forest-steppe steppe vegetation and lowlands of Javkhlant area consists of the steppe vegetation. Typically, species richness along a huge longitudinal and altitudinal gradient is very high.

Tunkhel

Light taiga sparse forest near GIZ cabin on northern slopes is represented by the Siberian larch (*Larix sibirica*) and birch (*Betula platyphylla*). The forest vegetation faces the disturbance by man and livestock, especially on the transition of meadow and forest stands. Some parts were affected by fire and other parts were recently managed. In some places, the shrubs are well-developed but, in some places, they are absent. The shrub vegetation is composed of *Rosa acicularis*, *Padus asiatica*, *Ribes rubrum* and small trees of *Populus tremula*, *Betula platyphyllos*, *Larix sibirica*. The underground vegetation is very diverse and contains various tall perennial and biennial forbs: *Geranium pseudosibiricum*, *Fragaria orientalis*, *Thalictrum petaloideum*, *Lamium album*, *Urtica angustifolia*, *Ranunculus monophyllus*, *Iris ruthenica*, *Aegopodium alpestre*, *Sanguisorba officinalis*, *Vicia baikalensis*, *V. amoena*, *Epilobium angustifolium*, *Cacalia hastata*, *Polemonium racemosum*, *Moehringia laterifolia*, *Trolius asiaticus*, *Pleurospermum uralense*, *Rubus saxatile* etc.; and grasses and sedges: *Poa sibirica*, *Trisetum sibiricum*, *Carex appendiculata*, *C. falcata*, *C. lanceolata*. These forests belong to the *Geranio-pseudosibirici-Laricetum sibirica* forest.

Javkhlant

The low-productivity steppes dominated by the tussock-forming short grasses. The cover of vegetation is quite variable, ranging from 30 to 80%. Common species of the herb layer consist of species adapted to grazing pressure, disturbance and intensive solar radiation. The matrix comprises of *Carex duriuscula*, hard and durable sedge of low growth. Other dominant species consist of grasses *Elymus sibirica*, *Poa pratensis*, *Achnatheron splendens* and the dicot herbs *Plantago major*, *Potentilla tanacetifolia*, *P. acaulis*, *Rumex pulchellus*, *Artemisia spp.*, *Heteropappus hispidus*, *Schizonepeta annua* etc. Some of the dominant plants are nutrient demanding – *Chenopodium album*, *Medicago lupulina*, *Taraxacum spp.* and *Urtica cannabina* which is another consequence of grazing. Besides, some of the species are halophytes (salt meadow plants) e.g. *Potentilla anserina*, *Glaux maritima* and *Saussurea davurica*, saline grasslands are quite common in the surrounding habitats. After all, the diversity is still high. Probably the bunchy hard grass as *Achnatheron splendens* creates micro-habitats where some species find their niche. Besides, even small difference in geomorphology like the terrain depression hosts other types of species: *Schizonepeta annua*, *Potentilla bifurca*, *Iris lactea* and others.

Bugant

Light taiga forest near the creek consists of birch (*Betula platyphylla*) and pine (*Pinus sylvestris*), aspen (*Populus tremula*) is rarely found there. Other wood species also appear at the location, especially shrubs *Spiraea aquifolia*, *Rosa acicularis* and *Padus asiatica*. The understorey vegetation covers 50–70 % of soil surface, the grazing is limited and occasional there. The vegetation is dominantly composed of *Carex lanceolata*, *Iris ruthenica* and *Maianthemum bifolium*. Yet, many other species occur there, of which are more abundant *Vicia baikalensis*, *Vicia amoena*, *Viola biflora*, *Fragaria orientalis*, *Aegopodium alpestre*, *Anemone crinita*, *Trollius asiaticus*, *Geranium pseudosibiricum*, *Filipendula palmata* and *Poa sibirica*. However, montane and acidophilous species are also common *Vaccinium vitis-idaea*, *Ledum palustre*, *Pyrola incarnata* and *Trientalis europaea*. Among rare species, it is necessary to highlight the orchids *Cypripedium calceolus* and *C. guttatum*.

Umnudelger

Light taiga young forest stands are significantly influenced by pasture of livestock (grazing and trampling) and partly by fire. Hence, these forests are in some places very dense, and in other places sparse with open gaps. The forests are dominantly represented by the Siberian larch (*Larix sibirica*). We focused on the comparison of species composition in forests with different types of management and we plan to compare the data soon. In the dense forest stand, the vegetation is composed of *Thalictrum petaloideum*, *Geranium pseudosibiricum*, *Campanula glomerata*, *Sanguisorba officinalis*, *Urtica cannabina*, *Carex argunensis*, *C. lanceolata*, *Sedum aizoon*, *Chrysanthemum zawadski* etc. Further, we established the fenced areas for tree seedlings protection. Here, we found mostly dense understory vegetation with heliophilous species, as *Potentilla anserina*, *Stellera chamaejasme*, *Agropyron cristatum*, *Agrostis mongolica*, *Galium verum*, *Medicago ruthenica*, *Angelica tenuifolia* etc.

Binder

Pine (*Pinus sylvestris*) and larch (*Larix sibirica*) forests cover the slopes of the river Orkhon terrace. Woody species *Rosa dahurica* and *Potentilla fruticosa* are sub-dominant at some places. Diverse understorey vegetation grows on the forest and non-forest edges. The tree seedlings have difficulty competing with tall and dense vegetation there. Based on the frequent fire scars on the trees, it can be assumed that regeneration is inhibited by the fire here. The understorey vegetation covers 30–75% of soil surface, the grazing is quite common. The vegetation is dominantly composed of *Carex lanceolata*, *Agrostis mongolica*, *Calamagrostis obtusata*, *Leontopodiu leotopidoides*, *Veronica incana*, *Vicia cracca*, *Stellera chamaejasme*, *Solidago dahurica*, *Clematis hexapetala*, *Galium verum*, *Helictotrichon schellianum* etc.

Bayan-Adarga

Aspen (*Populus tremula*) is a typical tree for open landscapes of former fireplaces, and it is one of the dominant tree species here. Aspen populations form single living organisms called clones where “trees” are genetically identical and linked by expansive root systems. We found woody shrub species *Rosa dahurica*, *Spiraea aquifolia* and *Cotoneaster mongolica*. The vegetation is

dominantly composed of *Carex argunensis*, *Bromus inermis*, *Vicia amoena* and *Helictotrichon schelianum*. However, many other species occur there, as *Clematis hexapetala*, *Lilium pumilum*, *Astragalus adsurgens*, *Youngia tenuifolia*, *Leuzea uniflora*, *Galium verum*, *Dracocephalum ruysianum* etc.

4.4 References

- Baasanmunkh, S., Urgamal, M., Oyuntsetseg, B., Sukhorukov, A.P., Tsegmed, Z., Son, D.C., Erst, A., Oyundelger, K., Kechaykin, A.A., Norris, J. and Kosachev, P., 2022. *Flora of Mongolia: annotated checklist of native vascular plants*. *PhytoKeys*, 192, p.63. <https://doi.org/10.3897/phytokeys.192.79702>.
- Bazarragchaa, B., Kim, H.S., Batdelger, G., Batkhoo, M., Lee, S.M., Yang, S., Peak, W.K. and Lee, J., 2022. Forest vegetation structure of the Bogd Khan Mountain: A strictly protected area in Mongolia. *Journal of Asia-Pacific Biodiversity*, 15(2), pp.267-279. <https://doi.org/10.1016/j.japb.2022.04.001>.
- Chytrý, M., Ermakov, N., Danihelka, J., Hajek, M., Hájková, P., Horsák, M., Kočí, M., Kubešová, S., Lustyk, P., Otýpková, Z. and Pelánková, B., 2012. High species richness in hemiboreal forests of the northern Russian Altai, southern Siberia. *Journal of Vegetation Science*, 23(4), pp.605-616. <https://doi.org/10.1111/j.1654-1103.2011.01383.x>.
- Gilliam, F.S., 2007. The ecological significance of the herbaceous layer in temperate forest ecosystems. *BioScience*, 57(10), pp.845-858. <https://doi.org/10.1641/B571007>.
- Grubov V.I., 2008. *Key to the vascular plants of Mongolia*. Ulaanbaatar, Mongolia, Gan Print.
- Gunin, P.D., Vostokova, E.A., Dorofeyuk, N.I., Tarasov, P.E. and Black, C.C. eds., 1999. *Vegetation Dynamics of Mongolia*. Boston, London Kluwer Academics.

**LEPIDOPTERA
EVALUATION**

5 LEPIDOPTERA EVALUATION: A REFLECTION OF BIODIVERSITY

Vladimír Hula¹

¹ Mendel University in Brno, Zemědělská 1, 613 00, Brno, Czech Republic

5.1 Introduction

The fauna of butterflies and moths of Mongolia has been extensively studied within the last decades (Tshikolovets et al., 2009). Most studies focus on biodiversity hotspots in the west of the country, mainly in the Altai Ridge and surrounding regions. Forest habitats north of Ulaanbaatar are only scarcely explored and especially eastern localities are almost unknown and promising from a faunistic point of view.

The conservation of butterflies and moths in Mongolia is not performed independently but only as part of international law (CITES) and as part of landscape protection (National Parks, reserves, etc.). Any special conservation management is planned in Mongolia. There is even no Red List of butterflies. The main threats in Mongolia are almost the same as those in the rest of that part of the World – overgrazing, mining, and global climate change.

Several species of *Lepidoptera* are regarded as forests pests. Namely *Erannis defoliaria* (Clerck, 1759), *Lymantria dispar* (Linnaeus, 1758), *Dendrolimus superans sibiricus* (Tschetverikov, 1908) or *Coleophora laricella* (Hübner, 1817). All these species are becoming more and more important together with intensifying climate change (and with more and more extreme events – droughts and more frequent fire events). All these species have more and more often defoliating impacts on target tree species. And it leads to the use of pesticides which were not used here before (insecticides against caterpillars).

On the basis of this, we can say that that fauna of forests of Mongolia is facing quite a big change, which was not present here in recent history. It is highly questionable how these changes happen and how the fauna reflects it. For that reason, we established transects for butterflies and points for collecting moths. Unfortunately, one visit is not enough for such a study, so the author of this report hopes that the study will continue. The results are promising.

5.2 Methods

Methods must be split according to the activity. Butterflies were collected during the daytime, moths at night. The STREAM sites were visited by the author during June and at the beginning of July 2023. Some material was also obtained in the autumn of 2023 by Jan Šebesta.

Butterflies

All sites were explored to understand the whole habitat. To collect all species flying around, entomological nets were used. The collecting place selection was always done according to the conditions – to cover the highest possible species richness. The locality was walked through in all directions and all environmental characteristics were noted. As there was only one visit, final places have not been selected yet.

Moths

Moths were collected in a different way. Also, in this case, the main focus was put on high species richness, so traps were always set on places, where specialists were expected. This leads to different results from each locality. But on the other hand, it should lead to novelties, which was the motivation of collecting during the first visit. The trap that was used was a bucket funnel trap with UV LED lighting (Figure 60) from InLamp company (263 nm UV light). Chloroform was used as a killing agent in a small evaporation dish. Material was obtained each night and collected early morning to prevent destruction by wind (and other factors). Immediately after collecting, the material was stored on cotton layers and frozen after transfer. Part of the material was mounted. The material was identified on the basis of various available literature.



Figure 60. *Light trap in operation.*

5.3 Results and discussion

The results are still very preliminary and are based mainly on field observations. The main observation on butterflies is that the richest fauna is living on the edge of forest and meadows, an ecotone (Figure 61). Even in dark taiga forest, butterflies always occur in natural clearings, on steep slopes or in river valleys. Dark taiga was not evaluated due to bad weather conditions, so all observations are from “cultivated” forests. Surprisingly, in Mongolia very common species are those which are highly protected in Europe: *Coenonympha hero* (extinct in many countries, preferring open forest structures), *C. oedippus* (extinct in many countries, preferring damp meadows within forests) and *Lopinga achine* (needs light in forests). All these species were almost everywhere – the first two in meadows, the last one even in “dark” pine forest. A similar situation was with *Lycaena helle* (Figure 62; almost extinct in many countries, needs damp meadows with *Bistorta major*) and all *Euphydryas* species (open forests specialist). It is obvious that such structured forests that we can find in Mongolia are very valuable for hosting a very rich fauna of butterflies and we can learn a lot there. We can apply habitat information

from there in Central Europe to the creation of typical habitats within conservation management.



Figure 61. *Typical non-forest habitat within forest. Such places host very valuable fauna.*

It is obvious that the main factor is the connectivity of different parts of the forests – it means that Mongolian forests are usually not like forests in Europe. Due to catastrophic events (fire, snow, drought), forests are always with very fine open structure which leads to favourable conditions supporting butterflies. The same applies to species specialists like steppe butterflies. Steppes as structures within a larger complex of forests also host a very specific fauna. These places were usually occupied by steppe species (*Plebejus* spp., *Muschampia cribrellum*, *Neolycaena* spp.) or meadow species if mesophilic (*Colias heos*, *Melitaea* spp., *Polyommatus amandus* etc.) and we can assume that these places are/were not isolated by forests all the time based on their presence. These places were probably connected during the postglacial period (probably due to events like forest fires or insect outbreaks) and host a rather interesting fauna. As mentioned above, such refugees helped typical meadow or forest meadow fauna survive during forest optimal periods. Nowadays, the situation is a bit different due to intensive pressure

of livestock grazing. This phenomenon leads to the connectivity of these places and makes them connected with other localities again. It is possible to say that for many Lepidoptera species livestock make the countryside even more suitable than it was before. But this is true only for highly afforested regions where grazing pressure is just moderate. With increasing grazing pressure, the diversity of butterflies and moths is also decreasing.

It is very complicated to discuss some results for butterflies and moths if the results are not finished yet. Even the systematic position of many collected butterflies and moths needs to be revised, using modern approaches within the field. Also, alpha-biodiversity of Mongolian forests is generally unknown. There are only a few publications dealing with this topic, but only scattered and based on the same effort as this one. For real results fauna needs to be observed more properly using the same design.



Figure 62. *Lycaena helle* is an example of butterfly, which is almost extinct in Europe due to the destruction of its habitat, but which is still quite common in Mongolia.

5.4 References

Tshikolovets V., Yakovlev R., & Bálint Z. (2009). *The butterflies of Mongolia*. Tshikolovets publishing.

Title: Environmental research, monitoring and evaluation: Results of the STREAM project

Editors: David Juříčka and Václav Pecina

Authors: David Juříčka, Martin Valtera, Burenjargal Otgonsuren, Pavel Peška, Jan Novák, Jan Šebesta, Vladimír Hula

Pages: 110

Title: Environmental research, monitoring and evaluation:
Results of the STREAM project

Editors: David Juříčka and Václav Pecina

Publisher: Mendel University in Brno, Zemědělská 1, 613 00 Brno

Website: <https://mendelu.cz/en/>

More information:

<https://forest4mongolia.mendelu.cz/en/>

<https://www.facebook.com/forest4mongolia>